

MATHEMATICAL ANALYSIS AND SIMULATION OF CROP MICROMETEOROLOGY

aan mijn vrouw en dochter

CENTRALE LANDBOUWCATALOGUS



0000 0030 4952

Promotoren : dr. ir. C.T. de Wit, buitengewoon hoogleraar in de
theoretische teeltkunde

dr. ir. L. Wartena, hoogleraar in de landbouwweerkunde en
de omgevingsnatuurkunde

Co-promotor: dr. ir. J. Goudriaan, wetenschappelijk hoofdmedewerker,
vakgroep theoretische teeltkunde

NN08201, 993

Chen Jialin

MATHEMATICAL ANALYSIS AND SIMULATION OF CROP MICROMETEOROLOGY

Proefschrift

ter verkrijging van de graad van
doctor in de landbouwwetenschappen,
op gezag van de rector magnificus,
dr. C.C. Oosterlee,
in het openbaar te verdedigen
op woensdag 26 september 1984
des namiddags te vier uur in de aula
van de Landbouwhogeschool te Wageningen

ISBN: 211498-03

PROPOSITIONS

1. The validity of the reciprocity relation between a direct light source and the reflected (or transmitted) radiance from vegetation is based on the reversibility of each radiation path contributing to the reflected (or transmitted) radiation vector. This reversibility is generally true for reflection whereas for transmission a vertically uniform canopy and a black soil surface are required.

This dissertation, Chapter 2.

2. The Kubelka-Munk equations in vector-matrix form can describe the directional transfer of radiation in a canopy with non-horizontal, non-Lambertian leaves, and the reflectance pattern of a canopy can be obtained from the analytical solution to these equations.

This dissertation, Chapter 3.

3. To study transpiration from a multi-layer canopy, flux densities of enthalpy and saturation heat are to be preferred to those of sensible and latent heat.

This dissertation, Chapter 4.

4. In term of flux densities of enthalpy and saturation heat, the well known Penman's formulae can be expressed in a unified form applicable to both single- and multi-layer crop canopies.

This dissertation, Chapter 4.

5. In Monteith's extrapolation method, the profile of dew-point temperature is to be preferred to that of vapour pressure.

This dissertation, Chapter 6.

6. Experiments have confirmed that the canopy resistance is approximately equal to a bulk stomatal resistance calculated as all component leaf stomatal resistances acting in parallel. This assertion is correct, however, only for a dense canopy with a dry soil surface.

This dissertation, Chapter 7.

BIBLIOTHEEK
DER
LANDBOUWHOOGESCHOOL
WAGENINGEN

7. The conclusion of Idso that the stomatal conductance is proportional to the net radiation absorbed under conditions of potential evaporation is invalid, since in his argument he ignored the possibility that the stomatal resistance varies with the vapour pressure deficit.

Idso, S.B., Agric. Meteorol., 29, 213-217 (1983).

8. The concept of centripetal force should not be used in textbooks of physics in secondary schools, because it suggests that the centripetal force might be an additional force to the existing forces exerted on a moving object. The concept of centripetal acceleration suffices to characterize the curvilinear movement of an object.
9. Feedback as a physical concept may be bypassed in mathematics to simplify solution procedures.
10. Modern cybernetics will provide a good framework for further development of the traditional chinese theory of medicine, because both disciplines have similar basic ideas while the former is more systematic and better developed.
11. It has been observed (Wang W., Institute of Health, Beijing, China) that tobacco smoke reduces considerably the basic metabolic rate in mice. Since this may positively affect longevity it should be investigated in a respiratory chamber whether this also holds for human beings.
12. Chinese kitchen makes busy cooks and lazy eaters.

Chen Jialin

Wageningen, 26 September, 1984

Contents

List of Symbols

1	Introduction	1
1.1	Improving models by using more adequate mathematical methods	1
1.2	The outline of the work	1
2	The reciprocity relation for reflection and transmission of radiation by crops and other plane-parallel scattering media	3
2.1	Introduction	3
2.2	Proof based on Goudriaan's model	4
2.2.1	Reciprocity relation and the symmetry of the matrices	4
2.2.2	Reversibility of the radiation paths through the canopy	7
2.3	Proof of the general case	11
2.4	Discussion and conclusions	15
3	Kubelka-Munk equations in vector-matrix forms and the solution for bidirectional vegetative canopy reflectance	17
3.1	Introduction	17
3.2	Vector-matrix representation of radiation and its interaction with a leaf or a canopy	19
3.3	The Kubelka-Munk equations in vector-matrix forms	20
3.4	Including azimuthal variations	24
3.5	Calculation of the matrices M^* , F^* , and B^* and the normalization	25
3.6	Techniques of reducing execution time for a leaf canopy without azimuthal preference	27
3.7	Approximation method	30
3.8	Some illustrative results	32
3.9	Discussion	33
3.9.1	Non-Lambertian scatterers	33
3.9.2	Applicability to the atmosphere and clouds	33
3.9.3	Superposition of several heterogeneous layers	34

4	Uncoupled multi-layer model for the transfer of sensible and latent heat flux densities from vegetation	35
4.1	Introduction	35
4.2	Coupled multi-layer model	36
4.3	Uncoupling	39
4.4	Uncoupled electrical analogues for H and J	41
4.5	Solutions for the total flux densities H_1 and J_1 above a canopy	42
4.6	An equivalent expression for Penman's formulas	45
4.7	Physical significance of J	46
4.8	Discussion and conclusions	47
5	A crop micrometeorology simulation program in BASIC on microcomputers	49
5.1	Introduction	49
5.2	Description of the simulation model	50
5.2.1	Basic equations for profile calculation	50
5.2.2	Distinguishing sunlit and shaded leaves	53
5.2.3	Heat flux density into the soil surface	55
5.2.4	Parameter evaluation	56
5.3	Simulation program	57
5.3.1	Some remarks	57
5.3.2	Results	59
5.4	Discussion	59
6	A graphical extrapolation method to determine canopy resistance	62
6.1	Introduction	62
6.2	Monteith' extrapolation method	63
6.3	Graphical extrapolation method to determine r_c	65
6.4	The effect of choosing different r_{ex} on r_c	67
6.5	Discussion	69

7	Canopy resistance and excess resistance derived from a multi-layer micrometeorological model	70
7.1	Introduction	70
7.2	Formulas linking r_c and r_{ex} to the parameters in multi-layer models	72
7.3	Behaviour of the canopy resistance r_c	74
7.4	Behaviour of the excess resistance r_{ex}	78
7.4.1	Estimation of R_g	79
7.4.2	Behaviour of r_{ex} and B^{-1} for a wet canopy	81
7.4.3	Behaviour of r_{ex} and B^{-1} for a dry canopy	83
7.5	Discussion	85
8	General discussion and suggestions	87
	Appendix	91
A-1	List of the simulation program developed in Chapter 5	91
A-2	List of the symbols in the program	97
	Summary	102
	Samenvatting	106
	Acknowledgements	111
	References	112
	Curriculum vitae	116

List of Symbols

Symbol	Description	Dimension
α	incident angle to the normal of a leaf	rad
α'	exitant angle to the normal of a leaf	rad
A_j	determinants defined in Eqs.(4.28-31)	-
b_j	parameters defined in Eq.(4.26)	$J\ m^{-2}\ s^{-1}$
$b_{j,k}$	same as b_j while irradiation levels are distinguished	$J\ m^{-2}\ s^{-1}$
B	back scattering matrix of a canopy layer	-
B^*	same as B while azimuthal variations are included	-
B^{-1}	dimensionless excess resistance	-
$B(i)$	zonal reflectance of a canopy layer	-
$B_u(i)$	zonal reflectance of a Lambertian reflector	-
c	sum of the leaf reflection and transmission coefficients	-
c_d	leaf drag coefficient	-
C_j	cumulative sensible heat flux density above layer j	$J\ m^{-2}\ s^{-1}$
C'_j	sensible heat source from layer j	$J\ m^{-2}\ s^{-1}$
d	zero plane displacement	m
\underline{d}	known incoming downward radiation vector	$J\ m^{-2}\ s^{-1}$
d_1	half of the thickness of the top soil layer	m
$\delta_{i'i}$	Kronecker delta	-
$d(i,j)$	intensity of incident light from direction (i,j)	$J\ m^{-2}\ s^{-1}$
D_0	vapour pressure deficit of the air at reference height	mbar
D_j	vapour pressure deficit of the air at layer j	mbar
$e_{a,0}$	vapour pressure of the air at reference height	mbar
$e_{a,j}$	vapour pressure of the air at layer j	mbar
$e(0)_1, e(0)_2$	surface vapour pressure obtained by extrapolation	mbar
$f(i_L)$	leaf inclination distribution function	-
F	forward scattering matrix of a canopy layer	-
F^*	same as F while azimuthal variations are included	-
g_j	reciprocal of r_j	$m\ s^{-1}$
G	heat flux density into the soil surface	$J\ m^{-2}\ s^{-1}$

G^0	first guess of G in an iteration method	$J m^{-2} s^{-1}$
G'	required increment for the next guess of G	$J m^{-2} s^{-1}$
G_j	sum of g_i ($i=j$ to n)	$m s^{-1}$
H_j	cumulative enthalpy flux density above layer j	$J m^{-2} s^{-1}$
H'_j	enthalpy source from layer j	$J m^{-2} s^{-1}$
i	inclination of the incident direction	rad
i'	inclination of the exitant direction	rad
I	identity matrix	-
J_j	cumulative saturation heat flux density above layer j	$J m^{-2} s^{-1}$
J'_j	saturation heat source from layer j	$J m^{-2} s^{-1}$
k	von Karman's constant	-
k'	heat conductivity in soil	$J m^{-1} s^{-1} K^{-1}$
K_H	constant turbulent exchange coefficient within a canopy	$m^2 s^{-1}$
l_c	total leaf area index of a canopy	-
L	Monin-Obukhov length	m
LAI	leaf area index	$m^2 m^{-2}$
m	parameter for wind profile within a canopy	-
M	interception matrix	-
M^*	same as M while azimuthal variations are included	-
$M_i(i)$	probability of interception for inclination i	-
n	total number of layers of the models	-
$o(i, i_L)$	projection of the leaves with inclination i_L on inclination i	-
$O(i)$	projection of the leaves in one layer on inclination i	-
p_j	fraction of the energy gain in layer j	-
P	zonal transmission radiance matrix of a canopy	-
Q	zonal reflection radiance matrix of a canopy	-
r	hemispherical reflection coefficient of a leaf	-
$r(i', j', i, j)$	bidirectional reflectance of a leaf	sr^{-1}
r_a, r_b	component resistances of the canopy resistance	$s m^{-1}$
$r_{b,v}$	surface boundary-layer resistance to vapour transfer	$s m^{-1}$
r_c	canopy resistance	$s m^{-1}$
r_{ex}	excess resistance	$s m^{-1}$

$r_{H,j}$	surface boundary-layer resistance of layer j to heat transfer	$s\ m^{-1}$
$r_{H,j,k}$	same as $r_{H,j}$ while irradiation levels are distinguished	$s\ m^{-1}$
r_{HT}	bulk leaf surface boundary-layer resistance to heat transfer	$s\ m^{-1}$
r_j	sum of $r_{H,j}$ and $r_{s,j}$	$s\ m^{-1}$
$r_{j,k}$	same as r_j while irradiation levels are distinguished	$s\ m^{-1}$
r_s	hemispherical reflection coefficient of the soil surface	-
$r_{s,j}$	difference between $r_{v,j}$ and $r_{H,j}$	$s\ m^{-1}$
$r_{s,j,k}$	same as $r_{s,j}$ while irradiation levels are distinguished	$s\ m^{-1}$
r_{ST}	bulk stomatal resistance of a canopy	$s\ m^{-1}$
$r_{v,j}$	leaf resistance of layer j to vapour transfer	$s\ m^{-1}$
\underline{r}	reflected radiance vector at the top of a canopy	$J\ m^{-2}\ sr^{-1}\ s^{-1}$
R	reflectance matrix of a canopy layer	-
R^*	same as R while azimuthal variations are included	-
R_a	turbulent resistance defined in Eq.(7.31)	$s\ m^{-1}$
R_{zon}	zonal reflectance matrix of a canopy	-
R_c^*	reflectance matrix of a canopy including azimuthal variations	-
R_g	load resistance of the potential source at reference height	$s\ m^{-1}$
R_i	reflectance matrix of a canopy with an infinite LAI	-
R_j	turbulent resistance between layers j and j-1	$s\ m^{-1}$
R_m	turbulent resistance to momentum transfer between reference height and the equivalent surface for momentum absorption	$s\ m^{-1}$
R_p	turbulent resistance between the top and bottom of a canopy	$s\ m^{-1}$
R_s	reflectance matrix of the soil surface	-
s	leaf area index in each canopy layer	-
s_{Td}	slope of the dew point temperature profile	K^{-1}
S_j	net energy gain of layer j	$J\ m^{-2}\ s^{-1}$

S_L^*	sum of B^* and F^*	-
t	hemispherical transmission coefficient of a leaf	-
$t(i',j',i,j)$	bidirectional transmittance of a leaf	sr^{-1}
\underline{t}	transmitted radiance vector through the bottom of a canopy	$J m^{-2} sr^{-1} s^{-1}$
T	transmittance matrix of a canopy layer	-
T^*	same as T while azimuthal variations are included	-
$T_{a,0}$	temperature of the air at reference height	K
$T_{a,j}$	temperature of the air at layer j	K
T_{zon}	zonal transmittance matrix of a canopy	-
T_c^*	transmittance matrix of a canopy including azimuthal variations	-
$T_{L,j}$	leaf (or soil surface) temperature of layer j	K
T_p	a properly chosen temperature for evaluating the slope of the saturation vapour pressure curve	K
T_s^*	required soil surface temperature	K
$T_{s,a}$	soil surface temperature calculated in above-ground part	K
$T_{s,u}$	soil surface temperature calculated in under-ground part	K
$T_{s,1}$	temperature of the top soil layer	K
T_d	dew point temperature	K
$T_{e,a,j}$	equivalent temperature of the air at layer j	K
$T(0)_1, T(0)_2$	surface temperature obtained by extrapolation	K
$u(z)$	wind velocity at height z	$m s^{-1}$
u_*	friction velocity	$m s^{-1}$
\underline{u}	sum of the downward and upward radiation vectors	$J m^{-2} s^{-1}$
\underline{v}	difference between the downward and upward radiation vectors	$J m^{-2} s^{-1}$
w_i	angular width of the inclination interval	rad
w_j	angular width of the azimuth interval	rad
w_L	mean width of the leaves	m
w_s	mean diameter of the soil clods	m
x_{ij}	downward radiation tensor	$J m^{-2}$
\underline{x}	downward radiation vector	$J m^{-2} s^{-1}$
\underline{x}^*	same as \underline{x} while azimuthal variations are included	$J m^{-2} s^{-1}$
\underline{y}	upward radiation vector	$J m^{-2} s^{-1}$

z	height above the ground	m
z_0	roughness length	m
z_c	crop height	m
z_H	location of the equivalent surface for heat and vapour	m
z_r	reference height	m
α	constant defined in Eq.(4.20)	-
β	Bowen ratio	-
γ	psychrometric constant	mbar K ⁻¹
Δ	slope to the vapour saturation curve	mbar K ⁻¹
λE_j	cumulative latent heat flux density above layer j	J m ⁻² s ⁻¹
$\lambda E'_j$	latent heat source from layer j	J m ⁻² s ⁻¹
ρc_p	volumetric heat capacity of air	J m ⁻³ K ⁻¹

1 Introduction

1.1 Improving models by using more adequate mathematical methods

Crop micrometeorology has developed rapidly over the last 35 years. Many measurements of the profiles of wind, radiation, temperature, humidity and carbon dioxide above and within crop canopies have been published (Monsi and Saeki, 1953; Inoue, 1963; Lemon, 1963; Long et al., 1964; Begg et al., 1964; Brown and Covey, 1966; Denmead, 1969; Lemon and Wright, 1969; van Laar et al., 1977). In the meantime, various simulation models have been developed. Single layer models (Penman, 1948; Lemon, 1960; Monteith, 1963) have been widely used because of their simplicity; multi-layer models (de Wit, 1965; Cowen, 1968; Waggoner and Reifsnyder, 1968; Goudriaan and Waggoner, 1972; Perrier, 1976; Shuttleworth, 1976; Goudriaan, 1977) are preferred by crop micrometeorologists, because they simulate the profiles concerned. The multi-layer models have become more and more complicated, as the regime of radiation, wind, temperature and humidity within crop canopies have been simulated in greater detail.

The multi-layer models are fairly successful; Goudriaan's (1977) model is the outstanding one. One of the major problems, however, is that the model is not easily graspable and the computation is tedious and time consuming. There is a great need for simple programs that can handle the crop micrometeorology. The execution time of a simulation program can be reduced by: (a) making more simplified assumptions about the mechanism of the involved physical and physiological processes; (b) improving programming techniques; and (c) using more adequate mathematical methods. Usually, making more simplified assumptions reduces the applicability of the model, and improving programming techniques can hardly reduce the execution time by one order of magnitude. Using more adequate mathematical methods, however, can greatly reduce the execution time but not the applicability of the model. In the mean time, the lucidity of the models will be improved, which helps to deepen the understanding of the behaviour of the studied systems. This dissertation presents means of improving the model of the radiation transfer in a crop canopy and the model of the sensible and latent heat transfer from or to vegetation, by applying more adequate mathematical methods.

1.2 The outline of the work

This dissertation contains three parts. The first part, Chapters 2 and 3, is concerned with the radiation regime. For the transfer of the total downward and upward short-wave radiation within a canopy with horizontal, Lambertian leaves, the Kubelka-Munk equations have already been developed and solved. When leaves are non-horizontal, Kubelka-Munk equations can not be applied. Suits (1972) considered a simplified canopy with vertical and horizontal leaves only, and found the analytical solution of the radiation profile within the canopy. Goudriaan (1977) specified the radiation with different inclinations, using nine intensities from nine contiguous zones spanning a whole hemisphere; this model allows any leaf inclination distribution, and thus is more realistic. Goudriaan derived a set of equations for the radiation components at each level within the canopy and solved the equations by iteration. Chapters 2 and 3 will show that Goudriaan's equations can be expressed more lucidly in terms of vector-matrix notation. Then the reciprocity relation is proven (Chapter 2) and the generalized Kubelka-Munk equations are derived (Chapter 3). The bidirectional reflectance pattern of a canopy can be obtained in a greatly reduced execution time.

The second part of this dissertation, Chapters 4 and 5, deals with the transfer of sensible and latent heat from or to a multi-layer canopy - a major problem of crop micrometeorology. Although many models have been successful in calculating sensible and latent heat flux densities from a canopy, most of them rely on a mainframe computer. For practical use, a simulation program which can be executed on a microcomputer is needed. This can be achieved by uncoupling the equations for sensible and latent heat flux densities in terms of enthalpy and saturation heat flux densities (Chapter 4). A crop micrometeorology simulation program in BASIC is then developed (Chapter 5); this can be executed on a microcomputer.

The third part of this dissertation discusses the relationship between single-layer and multi-layer models. The single-layer model is still widely used because of its simplicity, but the values of the two basic parameters, the canopy resistance and the excess resistance, are not easily obtainable. In Chapter 6, a new extrapolation method is developed, which shows the canopy resistance and excess resistance graphically. Chapter 7, discusses methods of determining these two resistances in terms of the parameters of a multi-layer model.

2 The Reciprocity Relation for Reflection and Transmission of Radiation by Crops and Other Plane-Parallel Scattering Media (published in Remote Sensing of Environment 13: 475-486 (1983))

Abstract

A mathematical proof of the reciprocity relation for reflection and transmission of radiation by plane-parallel scattering media like crop canopies is presented. First, the proof is based on Goudriaan's model for crop canopies, and then the proof is generalized. Matrix methods are used, leading to the tensors in the general case. The conditions for the validity of the reciprocity relation are discussed.

2.1 Introduction

Using model calculations, Goudriaan (1977) discovered a reciprocity relation for reflection and transmission by crop surfaces in which the radiance of a scattering surface at inclination i' , with direct light incident from i , is equal to the radiance at inclination i with direct light incident from i' , provided that the flux densities at the horizontal plane through the reflector are the same in both cases. This result was obtained by computer experimentation, but a mathematical proof was not found. The same result for reflection was obtained by Chance and Cantu (1975) and Chance and LeMaster (1977) for the Suits (1972) model, and an analytical proof was given for an infinite leaf area index. Bunnik (1978) proved this relation analytically for a one-layer Suits model with a definite leaf area index. Although the model of Suits yields a good approximation of the light climate of a crop canopy, it only distinguishes, in principle, horizontal and vertical leaf elements, while Goudriaan's model allows any leaf inclination distribution. For a mathematical proof of the relation, therefore, Goudriaan's model is more suitable.

The reciprocity relation for reflection and transmission is a physical law, it claims an interchange property between a direct light source, the sun, for instance, and an airborne or spaceborne sensor, so that it is closely related to the remote sensing. In this Chapter a mathematical proof is presented, initially based on Goudriaan's model using matrix notation and then generalized using tensor notation. It will be seen in Chapter 3 that the tensor notation thus developed is a useful tool for describing radiation transfer in a scattering medium.

2.2 Proof based on Goudriaan's model

2.2.1 Reciprocity relation and the symmetry of the matrices

In the AGR model (Allen, Gayle and Richardson, 1970) and Suits model, radiation is divided into two kinds, direct and diffuse. Each of the three fluxes, direct, downward diffuse and upward diffuse, has a separate equation to describe its transfer and the boundary conditions are given for each component. In contrast, there is no special concern for direct or diffuse fluxes in Goudriaan's model. The radiation at any level in the canopy is divided into downward and upward fluxes, each being divided into nine intensities in nine contiguous zones in a hemisphere. Therefore, Goudriaan's model provides more detailed information about radiation distribution within a canopy.

The finite difference equations describing the transfer of radiation in these nine directions were derived by Goudriaan (1977):

$$x(i', j+1) = M_t(i')x(i', j) + 0.5cB(i') \sum_{i=1}^9 M_i(i)(x(i, j) + y(i, j+1)), \quad (2.1a)$$

$$y(i', j) = M_t(i')y(i', j+1) + 0.5cB(i') \sum_{i=1}^9 M_i(i)(x(i, j) + y(i, j+1)), \quad (2.1b)$$

where $x(i', j)$ and $y(i', j)$ are the flux densities of, respectively, the downward and upward radiation at layer j and c is the sum of the reflection and transmission coefficients of the leaves. $M_t(i')$ and $M_i(i)$ are, respectively, the probabilities of penetration and interception of the radiation with inclination i' (or i) when passing through one layer. They are given by

$$M_t(i') = 1 - M_i(i'), \quad M_i(i) = sO(i)/\sin(i), \quad (2.2)$$

where s is the leaf area index of the layer and $O(i)$ is the projection of the leaves onto inclination i :

$$O(i) = \sum_{i_L=1}^9 f(i_L) o(i, i_L) \quad (2.2a)$$

in which $f(i_L)$ is the leaf inclination distribution and $o(i, i_L)$ is the projection onto inclination i of the leaves with inclination i_L . $B(i')$ is the zonal distribution of radiation scattered by the layer into direction i' . If the

leaves are assumed to be Lambertian scatterers, it can be determined from

$$B(i') = B_u(i')M_i(i')/s, \quad (2.2b)$$

where $B_u(i')$ is the zonal distribution of radiation reflected by a Lambertian reflector and is equal to

$$B_u(i') = 2w_i \sin(i') \cos(i') \quad (2.2c)$$

in which w_i is the interval of the inclination angle, being $\pi/18$ in the model where a hemisphere is divided into nine zones. The canopy with $LAI=l_c$ is divided into $n-1$ layers, each with an LAI of $s=l_c/(n-1)$.

There are two boundary conditions. One is the nine incident radiation intensities from nine specified zones on the top of the canopy, and the other is the reflectance of the soil surface. The radiation intensities are denoted by the intensities at a horizontal plane. A pure direct light source is denoted thus by a set of nine figures of which eight are zero. Any combination of the direct light source and the sky light can be represented by different combinations of these nine figures. The soil surface is regarded as a Lambertian reflector in the model, so that the distribution of the reflected radiation in nine zones can be described by B_u in Eq. (2.2c). When these two boundary conditions are given, an iteration method, developed by Goudriaan, gives all profiles of the downward and upward flux densities in nine zones.

By computer calculation, Goudriaan (1977) found the following results for the reciprocity relation under pure direct incoming radiation:

1. It holds for reflected radiance at the top of the canopy with any reflection coefficient of the soil surface.
2. It holds for transmitted radiance through the bottom of the canopy only when the reflection coefficient of the soil surface is zero.
3. It cannot be invalidated by changing the leaf inclination distribution or the reflection or transmission coefficients of the leaves.

The mathematical proof of these results and the essential features of the model leading to these results were not found.

Goudriaan's model, however, can be represented equivalently and more lucidly, if the matrix notation is adopted. After some manipulations Eqs. (2.1a) and (2.1b) can be written as a set of vector equations:

$$\underline{x}(j+1) = \underline{T}x(j) + \underline{R}y(j+1), \quad \underline{y}(j) = \underline{T}y(j+1) + \underline{R}x(j), \quad (2.3)$$

where vectors \underline{x} and \underline{y} are called the downward and upward radiation vectors, respectively, with their components $x(i)$ and $y(i)$ being the flux densities of the corresponding radiation at a horizontal plane; T and R are the zonal transmittance and reflectance matrices of one layer with the components

$$R(i', i) = 0.5cB(i')M_i(i) = c.s.(\pi/18)\cos(i')O(i')O(i)/\sin(i), \quad (2.4a)$$

$$T(i', i) = M_t(i')d_{i', i} + R(i', i) = (1-sO(i')/\sin(i'))d_{i', i} + R(i', i). \quad (2.4b)$$

$R(i', i)$ and $T(i', i)$ represent the bidirectional reflectance and transmittance of one layer with respect to incident direction i and exitant direction i' , respectively, and $d_{i', i}$ is unity when $i'=i$, and zero otherwise. The boundary conditions can also be written in a concise form:

$$\underline{x}(1) = \underline{d}, \quad \underline{y}(n) = \underline{R}_s \underline{x}(n), \quad (2.5)$$

where \underline{d} is a known incoming downward radiation vector and \underline{R}_s the zonal reflectance matrix of the soil surface. If the soil surface is assumed to be Lambertian, the components of \underline{R}_s depend only on the exitant direction:

$$R_s(i', i) = r_s B_u(i') = r_s (\pi/18) 2 \sin(i') \cos(i') \quad (2.4c)$$

where r_s is the hemispherical reflection coefficient of the soil surface.

Given the boundary conditions, Eqs.(2.3) can be solved so that the upward radiation vector reflected by the canopy $\underline{y}(1)$ and the downward radiation vector transmitted through the canopy to the soil surface, $\underline{x}(n)$, can be obtained. The radiance vectors, \underline{r} and \underline{t} , reflected by and transmitted through the canopy, are given by

$$\underline{r} = \underline{H} \underline{y}(1), \quad \underline{t} = \underline{H} \underline{x}(n), \quad (2.6)$$

where H is a diagonal matrix with diagonal components

$$H(i', i') = 1/(2\pi(\pi/18)\sin(i')\cos(i')). \quad (2.7)$$

The vectors \underline{r} and \underline{t} can also be written in forms directly related to the known incoming radiation vector \underline{d} :

$$\underline{r} = Q\underline{d}, \quad \underline{t} = P\underline{d}, \quad (2.8)$$

where Q and P can be called the zonal reflection and transmission radiance matrices of the canopy, respectively.

The mathematical meaning of the reciprocity relation is easily seen using the matrix notation. Pure direct incident radiation is denoted, under vector notation, by a vector with only one non-zero component corresponding to the incident direction. For example,

$$\underline{d} = (0, \dots, 0, a, 0, \dots, 0)^t, \quad (2.9)$$

where a is the flux density at a horizontal plane from direction i and t denotes the transposition. The component of reflected radiance vector in direction i' is

$$r(i') = Q(i', i)a. \quad (2.10a)$$

If direct incident light comes from direction i' with flux density b , the component of the reflected radiance vector in direction i is

$$r(i) = Q(i, i')b. \quad (2.10b)$$

The reciprocity relation states that if $a=b$, then $r(i)=r(i')$. It means, therefore, that the matrix Q should be a symmetrical one. Conversely, if Q is a symmetrical matrix, the reciprocity relation holds. The same argument can be followed for transmittance and the transmission radiance matrix P . Therefore, the zonal reflection and transmission radiance matrices of a canopy being symmetric is a sufficient and necessary condition for the reciprocity relation. To prove this relation, it must be proven that the zonal reflection and transmission radiance matrices are symmetric.

2.2.2 Reversibility of the radiation paths through the canopy

One way to prove Q and P are symmetric is to solve Eqs.(2.3) under the boundary conditions (Eqs.(2.5)). There is an easier way to do it, however. As an illustration, a canopy with three layers and an underlying soil surface are shown in Fig.2.1(a). The zonal transmittance and reflectance matrices of the layer j are denoted by T_j and R_j , respectively. In general, T_j and R_j can be different for different layers.

Suppose that an incident light vector \underline{d} falls upon the first layer. After the interaction with the first layer, it is partly reflected forming vector $R_1 \underline{d}$, and partly transmitted forming vector $T_1 \underline{d}$. If the whole canopy consists of only one layer, the total reflected radiation vector is $R_1 \underline{d}$, and $T_1 \underline{d}$ is the transmitted one. But if more layers are taken into account, $R_1 \underline{d}$ is only one component of the reflected radiation vector, and $T_1 \underline{d}$ is not a component of transmitted radiation yet; it has to interact with other layers before it emerges from the canopy, forming either a component of the reflected radiation vector or of the transmitted one.

Many paths along which a reflected component can be established are possible. In Fig.2.1(a) one of them, with a component reflected radiation vector \underline{a}_k , is illustrated. It should be noted that the arrows, representing radiation vectors in Fig.2.1(a), are not the conventional vectors in a three-dimensional space, so that the inclinations of these arrows have no actual meaning. It follows from Fig.2.1(a) that

$$\underline{a}_k = (T_1 T_2 T_3 R_3 R_2 R_3 T_2 T_1) \underline{d}. \quad (2.11)$$

According to Eqs.(2.6) the corresponding radiance vector \underline{r}_k is

$$\underline{r}_k = H \underline{a}_k = (H T_1 T_2 T_3 R_3 R_2 R_3 T_2 T_1) \underline{d} = Q_k \underline{d}. \quad (2.12)$$

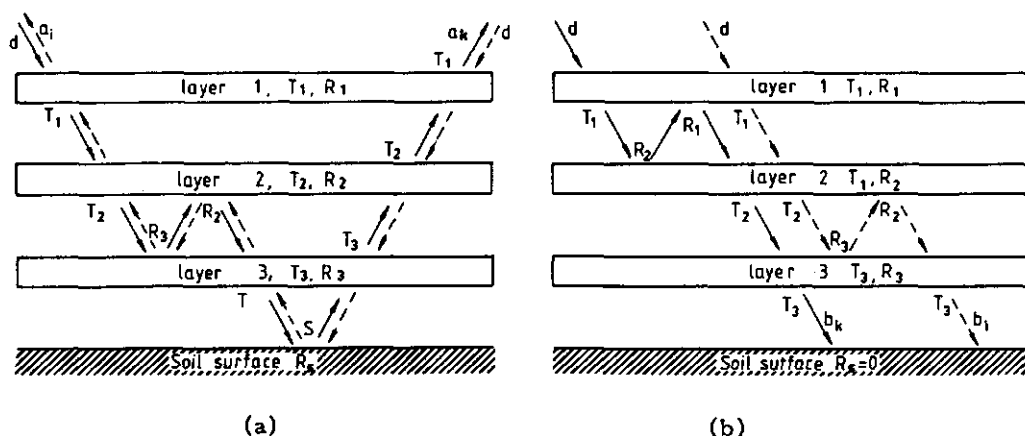


Fig.2.1. (a) One possible path giving one of the reflected components \underline{a}_k (in solid lines) and the corresponding reversed path giving \underline{a}_i (in broken lines). (b) The pair of the corresponding paths for transmission.

It can be seen now that for each of these possible paths a reverse path exists, along which another component is formed, denoted by \underline{a}_i , and illustrated in Fig.2.1(a) by the arrows with the broken lines. The resulting radiance vector is

$$\underline{r}_i = \underline{H}\underline{a}_i = (\underline{H}\underline{T}_1\underline{T}_2\underline{R}_3\underline{R}_2\underline{T}_3\underline{R}_s\underline{T}_3\underline{T}_2\underline{T}_1)\underline{d} = \underline{Q}_i\underline{d}. \quad (2.13)$$

The sum of these two components is

$$\underline{r}_j = \underline{r}_k + \underline{r}_i = (\underline{Q}_k + \underline{Q}_i)\underline{d} = \underline{Q}_j\underline{d}. \quad (2.14)$$

It can be proven now that \underline{Q}_j is a symmetrical matrix. It follows from Eqs.(2.4a, b and c) that the matrices \underline{R} , \underline{T} , and \underline{R}_s are asymmetric. However, by defining

$$\underline{C} = \underline{H}\underline{R}, \quad \underline{D} = \underline{H}\underline{T}, \quad \underline{W} = \underline{H}\underline{R}_s, \quad (2.15)$$

it can be proven that \underline{C} , \underline{D} , and \underline{W} are symmetric, since their components are

$$\underline{C}(i', i) = (cs/2\pi)(O(i')/\sin(i'))(O(i)/\sin(i)) = \underline{C}(i, i'), \quad (2.16a)$$

$$\begin{aligned} \underline{D}(i', i) &= (1 - sO(i')/\sin(i')) / (2\pi(\pi/18)\sin(i')\cos(i')) d_{i', i} + \underline{C}(i', i) \\ &= \underline{D}(i, i') \end{aligned} \quad (2.16b)$$

$$\underline{W}(i', i) = r_s/\pi = \underline{W}(i, i'). \quad (2.16c)$$

The matrices \underline{Q}_k and \underline{Q}_i in Eqs.(2.12) and (2.13) now can be rewritten as

$$\underline{Q}_k = \underline{D}_1\underline{H}^{-1}\underline{D}_2\underline{H}^{-1}\underline{D}_3\underline{H}^{-1}\underline{W}\underline{H}^{-1}\underline{D}_3\underline{H}^{-1}\underline{C}_2\underline{H}^{-1}\underline{C}_3\underline{H}^{-1}\underline{D}_2\underline{H}^{-1}\underline{D}_1\underline{H}^{-1}, \quad (2.17a)$$

$$\underline{Q}_i = \underline{D}_1\underline{H}^{-1}\underline{D}_2\underline{H}^{-1}\underline{C}_3\underline{H}^{-1}\underline{C}_2\underline{H}^{-1}\underline{D}_3\underline{H}^{-1}\underline{W}\underline{H}^{-1}\underline{D}_3\underline{H}^{-1}\underline{D}_2\underline{H}^{-1}\underline{D}_1\underline{H}^{-1}, \quad (2.17b)$$

where $\underline{D}_j = \underline{H}\underline{T}_j$, $\underline{C}_j = \underline{H}\underline{R}_j$ ($j=1$ to 3), and \underline{H}^{-1} is the inverse of \underline{H} . \underline{H}^{-1} is symmetric too, since \underline{H} is a diagonal matrix.

Although \underline{D}_j , \underline{C}_j , and \underline{H}^{-1} are all symmetric, \underline{Q}_k and \underline{Q}_i are not necessarily symmetric, because the product of two symmetrical matrices is usually asymmetric. But it can be easily verified by using Eqs.(2.17a and b) that the transposition of matrix \underline{Q}_k is equal to \underline{Q}_i , and $\underline{Q}_i^t = \underline{Q}_k$, consequently. The sum of \underline{Q}_k and \underline{Q}_i , \underline{Q}_j , therefore, is symmetric, since

$$\underline{Q}_j^t = (\underline{Q}_k + \underline{Q}_i)^t = \underline{Q}_k^t + \underline{Q}_i^t = \underline{Q}_i + \underline{Q}_k = \underline{Q}_j. \quad (2.18)$$

The total reflected radiance vector is composed of an infinite number of such pairs of vectors (divided by 2). For each of them the transformation matrix Q_j is symmetric, so that the resulting zonal reflection radiance matrix of the canopy Q is also symmetric.

For transmission, the conditions under which the reciprocity relation is valid are more restricted. Goudriaan (1977) found that the necessary condition is the "black" soil surface, as previously mentioned. But there is another restriction that the zonal transmittance and reflectance matrices of the different layers, T_j and R_j , should all be the same. Under these two restrictions, the same reasoning can be followed to prove that the zonal transmission radiance matrix of the canopy P is symmetric. The illustration is shown in Fig.2.1(b), while the argument is omitted.

If these two restrictions are removed, no corresponding "reverse" path can be found for each path along which a component transmission radiance vector is established. This argument, however, cannot serve as a mathematical proof that these two restrictions are two necessary conditions. The reason is simple; the sum of several asymmetrical matrices is not necessarily asymmetric. However, it can be shown that the reciprocity relation for transmission fails for a simple canopy with two layers with different T and R , even though the soil surface is black.

Suppose that the first layer is composed of black leaves with a spherical leaf inclination distribution, while the second is composed of horizontal leaves with equal transmission and reflection coefficients. The leaf area indices of the two layers are s_1 and s_2 , respectively, and s_1 is much smaller than unity while $s_2=1$. T_1 , R_1 , T_2 , and R_2 can be obtained from Eqs. (2.4a, b), and (2.2a, b, c). Noting that $O(i)=0.5$ for the spherical leaf inclination distribution and $O(i)=\sin(i)$ for horizontal leaves,

$$R_1(i', i) = 0, \quad (2.19)$$

$$T_1(i', i) = M_t(i', i)d_{i', i} = (1 - 0.5s_1/\sin(i')), \quad (2.20)$$

$$T_2(i', i) = R_2(i', i) = c(\pi/18)\cos(i')\sin(i'). \quad (2.21)$$

Since $R_1=0$, there is no multi-scattering between two layers, so that the zonal transmission radiance matrix of the canopy P simply equals HT_2T_1 :

$$P(i', i) = (c/2\pi)(1 - 0.5s_1/\sin(i')). \quad (2.22)$$

It can be seen that P is asymmetric.

2.3 Proof of the general case

In Goudriaan's model only zonal intensities of radiation are treated. The variations in azimuthal direction were completely ignored, so that radiation could be represented by vectors and the transmission and reflection of a layer as well as the whole canopy could be represented by matrices. The reciprocity relation proven above thus should be called, more precisely, the zonal reciprocity relation.

In the general case, the light incident, reflected or transmitted should be denoted by a tensor of order 2, $x_{i,j}$, its component $x(i,j)$ represents the flux density at a horizontal plane in the direction (i,j) , where i denotes the inclination and j the azimuth of the light. The reflection and transmission of a layer as well as a canopy should be denoted by tensors of order 4, $r_{i'j'ij}$ and $t_{i'j'ij}$, respectively. The reciprocity relation now requires that the reflection radiance tensor $q_{i'j'ij}$ and the transmission radiance tensor $p_{i'j'ij}$ of the canopy be symmetric in the sense that i' is interchangeable with i and j' with j . The reasoning for proving the reciprocity relation in this case is the same as that presented above, except that vectors and matrices are replaced by the corresponding tensors of order 2 or 4.

It can be seen that according to the preceding arguments, the proof of the reciprocity relation for a canopy requires that the reflection and transmission radiance matrices, or tensors, of the single layer are symmetric. Furthermore, it can be assumed that the layers are so thin that the multiple scattering within one layer can be neglected, so that the reflectance and transmittance tensors of a layer can be considered as the sum of these tensors of the corresponding components. Therefore, what must be proven is that the reflection and transmission radiance tensors of a horizontal layer containing only one scattering element, for example, a leaf, are symmetric.

Consider first a horizontal leaf element with a surface area s . Suppose that the leaf element is illuminated by a light source from direction (i,j) ; the flux density of the incoming light at the leaf surface is denoted by $d(i,j)$. The total flux reflected by the leaf is thus equal to $d(i,j)rs$. The distribution of the reflected radiation in different directions is determined by a so-called bidirectional reflection distribution function, which depends, generally speaking, not only on the exitant direction, but also on the direc-

tion of the incident illuminating light. Under tensor notation, the bidirectional reflection of the leaf can be fully described by the reflection radiance tensor of the leaf $r_{i'j'i,j}$. A component of this tensor, $r(i',j',i,j)$ represents the reflected radiance in the direction (i',j') of incident radiation with unit flux density, from the direction (i,j) . Here i' and j' denote the inclination and the azimuth of the exitant direction, respectively, and i and j denote those of the incident direction. The dimension of $r(i',j',i,j)$ thus is sr^{-1} .

The reflection radiance tensor of a given leaf can be determined by experiments, while the components $r(i',j',i,j)$ can be obtained by calculation for two extreme cases. For a Lambertian reflector, the reflected radiance is independent of the incident as well as the exitant direction, so that it can be readily obtained:

$$r(i',j',i,j) = r/\pi. \quad (2.23)$$

For a pure specular reflector, such as a mirror, the radiance is zero in all directions except in the direction of the reflected radiation. Under tensor notation, the whole hemisphere is divided into a definite number of discrete solid angles, and the radiance in these single solid angles is assumed uniform, so that, even in the solid angle in which the reflected radiation from a point light source lies, the radiance still has a definite value:

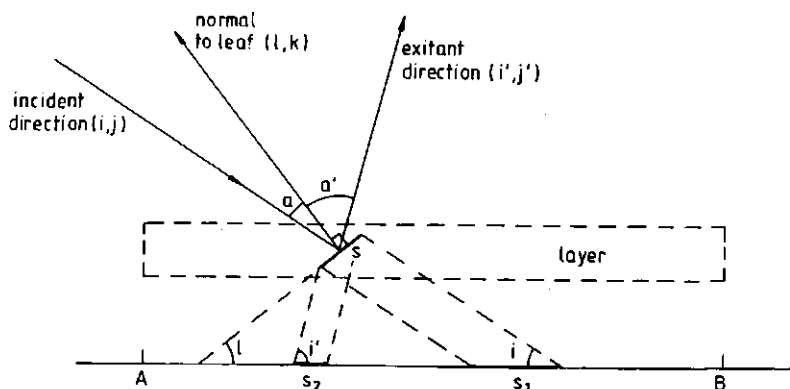


Fig.2.2. The bidirectional reflected radiance of a layer containing one inclined leaf element. For meaning of symbols see the text.

$$\begin{aligned}
 r(i', j', i, j) &= r / (\cos(i') w_i, w_j) \text{ when } i' = i \text{ and } |j' - j| = \pi, \\
 b(i', j', i, j) &= 0 \quad \text{otherwise.}
 \end{aligned}
 \tag{2.24}$$

It can be seen that in both cases the reflection radiance tensors are symmetric. This means the reciprocity relation holds. It is reasonable to assume that, at least as a first approximation, a real leaf is a combination of Lambertian reflector and specular reflector, so that the reflection radiance tensor of the leaf can be expected to be symmetric. The measurements of bidirectional reflection for healthy green soybean and maize leaves (Breece and Holmes, 1971) showed that the reflection radiance tensors are indeed symmetric. Therefore, the reciprocity relation is valid for a single horizontal leaf element. The transmission radiance tensor $t_{ij'ij}$ of a leaf can be defined in the same way, and the experiments done by Breece and Holmes (1971) showed that it is also symmetric.

Now consider the general case shown in Fig.2.2 in which a horizontal layer contains only one inclined leaf element. The inclination and the azimuth of the leaf are denoted by i_L and j_L , respectively. The surface area of the element, which has a relative value with respect to the unit horizontal plane AB, is denoted by s , and s is much smaller than unity. The task is to prove the reflection radiance tensor of the horizontal layer is symmetric. Denote again the flux density of the incident light at the plane AB by $d(i, j)$. The flux density at the leaf surface is then

$$F = (s_1/s) d(i, j), \tag{2.25}$$

where s_1 is the projection of s in the direction (i, j) onto the horizontal plane AB,

$$s_1 = s |\cos(a) / \sin(i)|, \tag{2.25a}$$

and a is the angle between the incident light and the normal to the leaf:

$$\begin{aligned}
 \cos(a) &= \cos(i) \cos(j) \sin(i_L) \cos(j_L) + \cos(i) \sin(j) \sin(i_L) \sin(j_L) \\
 &\quad + \sin(i) \cos(i_L).
 \end{aligned}
 \tag{2.25b}$$

The radiance of the points on the leaf surface in direction (i', j') is

$$g(i', j') = e(i_1', j_1', i_1, j_1) |\cos(a) / \sin(i)| d(i, j), \tag{2.25c}$$

where $g(i',j')$ is the radiance of the leaf surface in direction (i',j') under the illumination from direction (i,j) ; i_1' , j_1' , i_1 , and j_1 are the corresponding inclination and azimuth of the incident and exitant direction in the coordinate system fixed on the leaf element, and $e(i_1',j_1',i_1,j_1)$ is equal to $r(i_1',j_1',i_1,j_1)$ when $\cos(a)\cos(a')$ is larger than zero, and to $t(i_1',j_1',i_1,j_1)$, when $\cos(a)\cos(a')$ is smaller than or equal to zero.

The average radiance over the horizontal layer should be calculated as a weighted sum of the radiance in the area s_2 , shown in Fig.2.2, and that in the rest part of the plane AB, where s_2 is the projection of s from direction (i,j) onto the plane AB,

$$s_2 = s |\cos(a')/\sin(i')| \quad (2.25d)$$

in which a' is the angle between the exitant direction and the normal to the leaf:

$$\begin{aligned} \cos(a') = & \cos(i')\cos(j')\sin(i_L)\cos(j_L) + \cos(i')\sin(j')\sin(i_L)\sin(j_L) \\ & + \sin(i')\cos(i_L). \end{aligned} \quad (2.25e)$$

Thus,

$$\begin{aligned} n(i',j') = & s_2 g(i',j') + (1-s_2) \cdot 0 \\ = & se(i_1',j_1',i_1,j_1) |\cos(a')/\sin(i')| |\cos(a)/\sin(i)| d(i,j) \\ = & q(i',j',i,j) d(i,j), \end{aligned} \quad (2.25f)$$

where $n(i',j')$ is the radiance of the layer in direction (i',j') and $q(i',j',i,j)$ is the component of the reflection radiance tensor of the layer. The tensor e in Eq.(2.25f) is symmetric in the sense that i_1' is interchangeable with i_1 , and j_1' with j_1 , but the two coordinate systems fixed on the leaf and on the horizontal plane AB are related by

$$i_1' = u_1(i',j'), \quad i_1 = u_2(i,j), \quad j_1' = v_1(i',j'), \quad j_1 = v_2(i,j). \quad (2.26)$$

When the position of the leaf element is determined, the functions u_1 and v_1 are the same as the function u_2 and v_2 , respectively, so that the tensor e is symmetric also in the sense that i' is interchangeable with i and j' with j . Inspecting Eq.(2.25f) shows that the reflection radiance tensor $q_{i'j'ij}$ of the plane AB is symmetric.

The same argument can be followed to prove the transmission radiance tensor of a layer $P_{i'j'ij}$ is also symmetric.

2.4 Discussion and conclusions

For bidirectional reflection and transmission problems, tensor analysis is a powerful tool. It can be applied to a single leaf as well as to a horizontally homogeneous plane-parallel scattering medium, such as a crop canopy. In fact, in the continuous case, the upward and downward radiation are denoted by continuous functions of two variables, the inclination i and the azimuth j . The bidirectional reflectance and transmittance contain four variables, i' , j' , i , and j . When the hemisphere is divided into a number of contiguous sectors, it is a natural development to represent the radiation by a tensor of order 2, and the bidirectional reflection and transmission by tensors of order 4.

Using tensor representation, the equations describing radiation transfer within the scattering medium as well as the boundary conditions become much more concise and straightforward. Any combination of the direct solar radiation and the diffuse radiation under a clear or an overcast sky and their variations in the hemisphere are easily represented by a single known incoming radiation tensor.

Under tensor notation, the meaning of the reciprocity relation becomes clearer. It is simply related to the symmetry of the reflection or transmission radiance tensors of the scattering medium.

In this Chapter, for a horizontal homogeneous scattering medium, it is proven mathematically that:

1. For reflection, a reciprocity relation holds for a pure direct light source, regardless of whether soil surface is black or not.
2. For transmission, the reciprocity relation holds for a vertically uniform scattering medium with a black soil surface.

The proof is given for any leaf inclination distribution function. The only assumption is that the reflection and transmission radiance tensors of the single leaves are symmetric. The reflection radiance tensors for both sides of the leaves are not necessarily the same. This requirement is a relaxation to the conditions for the reciprocity relation, because both the Suits model and Goudriaan's model assume that the leaves are Lambertian scatterers. This relaxation is important in practice, because, for the leaves of many crops, the off-normal incident reflectance shows considerable specular contributions, as found experimentally for leaves of soybean and maize by Breece and Holmes (1971). Their data strongly supported the assumption

about the symmetry of the reflection and transmission radiance tensors of single leaves, but further confirmation is still needed for various kinds of crops.

It was noticed by Chance and LeMaster (1977), Bunnik (1978), and Goudriaan (1977) that the reciprocity relation breaks down for a mixture of both direct and diffuse light. Using tensor notation, the failure can be easily explained. Diffuse sky light is denoted under tensor notation by a radiation tensor in which all components are usually non-zero. The reflected radiance in directions (i_1', j_1') and (i_2', j_2') are calculated as

$$n(i_1', j_1') = \sum_{i,j} q(i_1', j_1', i, j) d(i, j), \quad (2.27a)$$

$$n(i_2', j_2') = \sum_{i,j} q(i_2', j_2', i, j) d(i, j), \quad (2.27b)$$

where $n(i_1', j_1')$ and $n(i_2', j_2')$ are the reflected radiance in the corresponding directions. The symmetry of the tensor $q_{ij'ij}$ cannot ensure that $q(i_1', j_1', i, j)$ and $q(i_2', j_2', i, j)$ are the same, so that $n(i_1', j_1')$ is not equal to $n(i_2', j_2')$ generally.

When the incident radiation is a mixture of both direct and diffuse light, the resulting radiance is the sum of the direct and diffuse light radiances, because the radiation transfer is a linear process. It can be seen that the reciprocity relation fails in the case when the relative contribution of the diffuse sky light is not negligibly small.

The reciprocity relation imposes a constraint on the radiance distribution of reflected radiation. This constraint can be used in remote sensing either to reduce the number of necessary measurements or to improve the accuracy of the results when the redundant measurements are done.

A special application of the possibility to reduce the number of measurements was given by Goudriaan (1977). It was proven that the dependence of the hemispherical reflection coefficient of a surface on the inclination of the incoming direct light is the same as the dependence of the radiance on the exitant inclination, under a uniformly overcast sky. Therefore, measurement of one of them provides the information about the other.

3 Kubelka-Munk Equations in Vector-Matrix Forms and the Solution for Bidirectional Vegetative Canopy Reflectance (submitted to Applied Optics)

Abstract

The radiation from different directions can be specified by upward and downward radiation vectors, and the interactions of the radiation with a leaf or with a vegetative canopy can be specified by matrices. The Kubelka-Munk (1931) equations, which are applicable only to a canopy with horizontal and Lambertian leaves, can then be extended to describe the directional transfer of radiation in a canopy with non-horizontal, non-Lambertian leaves. In the extended Kubelka-Munk equations, variables are upward and downward radiation vectors, and the coefficients are matrices. The solutions are found, from which the bidirectional vegetative canopy reflectance, including azimuthal variations, can be obtained. Simplified and approximate methods are presented for a canopy with leaves without azimuthal preference in order to reduce the execution time.

3.1 Introduction

The transfer of radiation through a turbid medium, such as the atmosphere or clouds has been of interest for some time. Recent developments in remote sensing techniques require calculation of bidirectional reflectance patterns of various vegetative canopies. Although the integral equations of Chandrasekhar (1950) have been established for more than thirty years, the semi-analytic solution is possible only for the simplest phase functions such as that of Rayleigh scatter. For cases of Mie scatter, even numerical solution is difficult (Paltridge and Platt, 1976).

The interaction of short-wave sun radiation with vegetative canopies has an additional complexity because the scattering elements are now mainly leaves, which are planar, so the bidirectional reflectance of a leaf depends not only on the angle between the incident and exitant directions but also on the orientation of the leaf. In the simplest case, all the leaves of a horizontally homogeneous canopy are assumed to be Lambertian scatterers and orientate horizontally, the directional distribution of radiation within and above the canopy is then a known function. The radiation transfer in such a canopy can therefore be fully described by the vertical variation of

the total downward and upward radiation intensities. The Kubelka-Munk equations address this situation. When two boundary conditions - incident radiation above the canopy and the reflectance of the underlying soil surface - are given, the Kubelka-Munk equations can be solved for profiles of the total downward and upward radiation intensities within the canopy, thus the reflectance of the canopy can also be obtained.

If a canopy consists of non-horizontal leaves, it is no longer a Lambertian reflector as a whole, even though all the leaves are Lambertian scatterers (Goudriaan, 1977). The simple form of the Kubelka-Munk equations cannot be applied, because the directional reflection and transmission of the radiation have to be taken into account. If azimuthal variations of the radiation is ignored and only the change of the radiation in zenith (or inclination) is considered, the radiation from all directions in a hemisphere can be specified by the radiation intensities from several discretized and contiguous zones which span the whole hemisphere (Goudriaan, 1977). Goudriaan (1977) further divided the whole canopy into several layers and derived a set of equations for these unknown upward and downward radiation components. He solved these equations by iteration. Cooper et al. (1982) applied the adding method, developed by van de Hulst (1963) under vector-matrix notation, and solved the same transfer problem without referring to the equations. Neither method, however, is feasible for including the azimuthal variations, because of the prohibitively long execution time.

It was shown in Chapter 2 that in vector-matrix notation, the equations for radiation transfer derived by Goudriaan (1977) can be written as difference equations in vector-matrix forms. In this Chapter it is shown that these difference equations can be derived directly under vector-matrix notation and transformed into differential equations, which are, in fact, extended Kubelka-Munk equations (where the variables are downward and upward radiation vectors and the coefficients are matrices). These equations can then be solved using standard matrix algebra methods. The directional reflectance into different zones of a hemisphere can be directly obtained from the solutions. It is shown in this Chapter further that the equations and the solutions are also able to account for azimuthal variations, but although analytical solutions are available the resolution in azimuth is restricted by the execution time. A special method is then developed to reduce the execution time for leaf canopies without obvious azimuthal preference, which is the case for most crop canopies (de Wit,

1965). A few illustrative examples are presented to show the feasibility of the theory, while comparison of the results with experimental data is left for future work.

3.2 Vector-matrix representation of radiation and its interaction with a leaf or a canopy

For the transfer of radiation in a horizontally homogeneous vegetative canopy, it is convenient to divide the radiation into downward and upward components x and y from and into an upper-hemisphere, respectively. The direction from a hemisphere is determined by two variables, inclination i (or zenith) and azimuth j , so that x and y are continuous functions of i and j . If a whole hemisphere is subdivided into several contiguous sectors each with a solid angle $\cos(i)w_iw_j$, where w_i and w_j are, respectively, the inclination and azimuth widths of the sector, and if within each sector the radiance is assumed the same, x and y can be represented by tensors of order two (matrices). The bidirectional reflectance and transmittance of a leaf or a horizontally homogeneous canopy layer can be specified by tensors of order four (Chapter 2). An illustration is given in Fig.3.1. Two sectors, A and A' with solid angles $\cos(i)w_iw_j$ and $\cos(i')w_{i'}w_{j'}$, respectively, are shown. The radiation flux densities from all sectors in the hemisphere constitute a downward radiation tensor. In Fig.3.1 one component of the

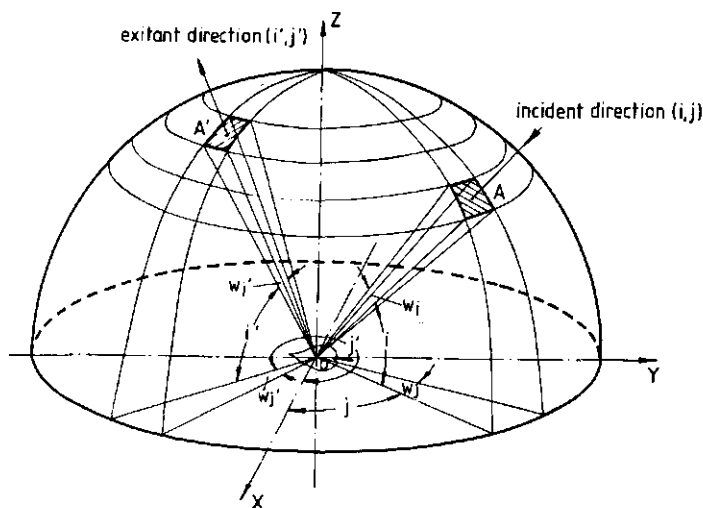


Fig.3.1. The vector-matrix representation of the radiation and its interaction with a horizontal leaf.

downward radiation tensor from the direction specified by (i,j) is incident on a horizontal leaf. The leaf reflects radiation into all the sectors in the hemisphere, these reflected radiation components constitute an upward radiation tensor. In the figure one of these components in the direction specified by (i',j') is shown. For these two fixed incident and exitant directions, the bidirectional reflectance of the leaf is denoted by $r(i',j',i,j)$. These bidirectional reflectance coefficients for all different values of i', j', i , and j , constitute the reflectance tensor of the leaf, which is of order four.

If the azimuthal variation of the radiation is ignored, the sectors shown in Fig.3.1 with the same inclinations can be combined into horizontal zones, and the radiation intensities from the relevant sectors can be summed up to form a total intensity of the zones, then the downward and upward radiation can be specified by vectors (tensors of order one), and the bidirectional reflectance and transmittance by matrices (tensors of order two). This situation will be examined first. The radiation flux densities in this Chapter, following Goudriaan's usage (1977), refer to those at a horizontal plane.

3.3 The Kubelka-Munk equations in vector-matrix forms

Divide a vegetative canopy into several layers, each having a leaf area index s . Denote the downward and upward radiation vectors above layer j by \underline{x}_j and \underline{y}_j , respectively (Fig.3.2). As a downward radiation vector, say \underline{x}_j , interacts with the layer j , both upward and downward radiation vectors are generated. If there are no other layers above and below the layer j , the generated downward radiation vector \underline{x}_{j+1} is $T\underline{x}_j$ and the upward one \underline{y}_j is $R\underline{x}_j$, where T and R are, respectively, the transmittance and reflectance matrices of the layer. If the leaf area index, s , of the layer is very small, the multiple scattering between the leaves within the layer can be ignored. The interception fractions of the radiation from different directions are determined by the projections of the total leaf area in the layer onto the relevant directions and can be denoted by sM , where M is the interception matrix and is diagonal. The penetration fraction then is $I-sM$, where I is the identity matrix. The radiation intercepted by the leaves will be scattered either back or forward, and this interaction can be specified by the back-scattering matrix B and the forward-scattering matrix F . The transmittance and reflectance matrices T and R then can be obtained as:

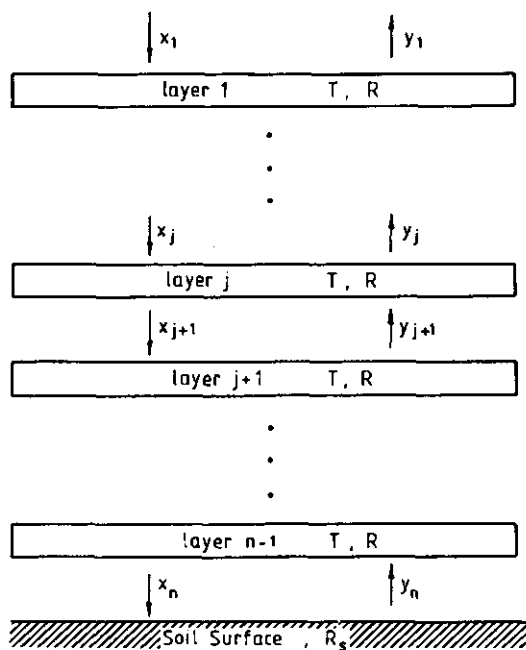


Fig.3.2. Downward and upward radiation vectors at different layers. For meaning of symbols see the text.

$$T = I - sM + sF, \quad R = sB. \quad (3.1)$$

When there are other layers above and below the layer j , the radiation reflected by the layers $j-1$ and $j+1$ have to be taken into account. By referring to Fig.3.2, the following equations can be obtained:

$$\underline{x}_{j+1} = T\underline{x}_j + R\underline{y}_{j+1}, \quad \underline{y}_j = T\underline{y}_{j+1} + R\underline{x}_j. \quad (3.2)$$

Substituting Eqs.(3.1) into (3.2) and rearranging gives:

$$(\underline{x}_{j+1} - \underline{x}_j)/s = -(M-F)\underline{x}_j + B\underline{y}_{j+1}, \quad (\underline{y}_{j+1} - \underline{y}_j)/s = (M-F)\underline{y}_{j+1} - B\underline{x}_j. \quad (3.3)$$

As s tends to zero, Eqs.(3.3) become differential equations:

$$d\underline{x}/dl = -(M-F)\underline{x} + B\underline{y}, \quad d\underline{y}/dl = -B\underline{x} + (M-F)\underline{y}, \quad (3.4)$$

where l is the cumulative leaf area index reckoned from the top of the canopy. The boundary conditions are:

$$\underline{x}(0) = \underline{x}_0, \quad \underline{y}(l_c) = R_s \underline{x}(l_c), \quad (3.5)$$

where l_c is the total leaf area index of the canopy, \underline{x}_0 a known downward radiation vector on the top of the canopy, and R_s is the reflectance matrix of the soil surface.

Compared with the Kubelka-Munk equations (Allen and Richardson, 1968):

$$dx/dl = -(1-t)x + ry, \quad dy/dl = -rx + (1-t)y, \quad (3.6)$$

where t and r are, respectively, the transmission and reflection coefficients of the leaves, it can be seen that Eqs.(3.4) are an extended version of the Kubelka-Munk equations. The variables are now the downward and upward radiation vectors, and the coefficients are the interception matrix M , forward scattering matrix F , and back scattering matrix B in place of the scalars 1 , t , and r , respectively.

By introducing two new variables

$$\underline{u}(l) = \underline{x}(l) + \underline{y}(l), \quad \underline{v}(l) = \underline{x}(l) - \underline{y}(l), \quad (3.7)$$

Eqs.(3.4) can be written as:

$$d\underline{u}/dl = -(M-F+B)\underline{v}, \quad d\underline{v}/dl = -(M-F-B)\underline{u}. \quad (3.8)$$

From Eqs.(3.8):

$$d^2\underline{v}/dl^2 = (M-F-B)(M-F+B)\underline{v} = Q\underline{v}. \quad (3.9)$$

To solve Eq.(3.9) the matrix Q must first be transformed into a diagonal matrix. Computation shows that Q can be diagonalized and is positive definite, so Q can be written as:

$$Q = VP^2V^{-1}, \quad (3.10)$$

where the matrices P and V can be obtained by using standard software. In terms of Eq.(3.10), Q^n and $Q^{1/2}$ can be obtained as $Q^n = V(P^2)^nV^{-1}$ and $Q^{1/2} = VPV^{-1}$. A matrix exponential function of the independent variable l , $\exp(Q^{1/2}l)$, can then be obtained as $V\exp(Pl)V^{-1}$. Because P is a diagonal matrix, there is no difficulty in calculating $\exp(Pl)$. It can be verified by substitution that

$$\underline{v}_1(1) = \text{Vexp}(P1)V^{-1}2\underline{c}, \quad \underline{v}_2(1) = \text{Vexp}(-P1)V^{-1}2\underline{d}, \quad (3.11)$$

are two solutions of Eq.(3.9). The general solution can be obtained as:

$$\underline{v}(1) = \text{Vexp}(P1)V^{-1}2\underline{c} + \text{Vexp}(-P1)V^{-1}2\underline{d}, \quad (3.12)$$

where \underline{c} and \underline{d} are two arbitrary vectors, and \underline{u} can be found from Eqs.(3.8):

$$\underline{u}(1) = -(M-F-B)^{-1}VPV^{-1}(\text{Vexp}(P1)V^{-1}2\underline{c} - \text{Vexp}(-P1)V^{-1}2\underline{d}). \quad (3.13)$$

Since $VPV^{-1} = (VP^2V^{-1})(VP^{-1}V^{-1}) = (M-F-B)(M-F+B)VP^{-1}V^{-1}$, Eq.(3.13) can be rewritten as

$$\underline{u} = -(M-F+B)VP^{-1}V^{-1}(\text{Vexp}(P1)V^{-1}2\underline{c} - \text{Vexp}(-P1)V^{-1}2\underline{d}). \quad (3.14)$$

This procedure removes an inversion operation, which is more time-consuming than multiplication, particularly when the matrices are large.

It follows from Eqs.(3.7), (3.12) and (3.14) that

$$\underline{x}(1) = -R_1E(1)J\underline{c} + E(-1)J\underline{d}, \quad \underline{y}(1) = -E(1)J\underline{c} + R_1E(-1)J\underline{d}, \quad (3.15)$$

where

$$R_1 = HJ^{-1}, \quad H = (M-F+B)VP^{-1}V^{-1} - I, \quad J = (M-F+B)VP^{-1}V^{-1} + I, \quad (3.16)$$

and $E(1)$ is a matrix function of 1 defined as

$$E(1) = (JV)\exp(P1)(JV)^{-1}. \quad (3.17)$$

The two constant vectors \underline{c} and \underline{d} can be determined by the boundary conditions (Eqs.(3.5)) as:

$$\underline{c} = -J^{-1}(I + CR_1)^{-1}C\underline{x}_0, \quad \underline{d} = J^{-1}(I - R_1(I + CR_1)^{-1}C)\underline{x}_0, \quad (3.18)$$

where the matrix C is defined as:

$$C = E(-1_c)GE(-1_c) \quad \text{with } G = (R_sR_1 - I)^{-1}(R_1 - R_s). \quad (3.19)$$

Substituting Eqs.(3.18) into (3.15) yields:

$$\underline{x}(1) = (R_1 D(1) + A(-1)) \underline{x}_0, \quad \underline{y}(1) = (D(1) + R_1 A(-1)) \underline{x}_0 \quad (3.20)$$

where

$$D(1) = E(1)(I + CR_1)^{-1}C, \quad A(-1) = E(-1)(I - R_1(I + CR_1)^{-1}C). \quad (3.21)$$

The zonal transmittance matrix, T_{zon} , and the zonal reflectance matrix, R_{zon} , of the whole canopy can be obtained from Eqs.(3.20) by substituting l_c or zero, respectively, for l :

$$T_{zon} = R_1 E(l_c)(I + CR_1)^{-1}C + E(-l_c)(I - R_1(I + CR_1)^{-1}C) \quad (3.22)$$

$$R_{zon} = R_1 + (I - R_1^2)(I + CR_1)^{-1}C. \quad (3.23)$$

As l_c tends to infinity, $E(-l_c)$ and then C tend to zero, so R_{zon} tends to R_1 . R_1 is thus the zonal reflectance matrix of a canopy with an infinite leaf area index.

3.4 Including azimuthal variations

In the general case, if azimuthal variations of the radiations are also of interest, radiation must be represented by a tensor of order two. But the radiation tensor of order two can be represented by an extended vector, if all the components are arranged in one column:

$$\underline{x}^* = (\underline{x}_1, \underline{x}_2, \dots, \underline{x}_m)^t, \quad (3.24)$$

where \underline{x}_j ($j=1$ to m) is the radiation vector for a fixed azimuth j , m is the total number of the intervals in the azimuth, and t denotes transposition.

The forward scattering matrix F , for instance, should also be extended to form the matrix F^* :

$$F^* = \begin{pmatrix} F_{11} & F_{12} & \dots & F_{1m} \\ F_{21} & F_{22} & \dots & F_{2m} \\ \vdots & \vdots & & \vdots \\ \vdots & \vdots & & \vdots \\ F_{m1} & F_{m2} & \dots & F_{mm} \end{pmatrix}, \quad (3.25)$$

where F_{jj} ($j, j'=1$ to m) is the forward scattering matrix for the incident radiation vector \underline{x}_j and the exitant radiation vector $\underline{x}_{j'}$. The upward radiation vector, \underline{y} , and the matrices I , M , and B should also be extended in the same way. The Kubelka-Munk equations in vector-matrix forms (Eqs.(3.4)), the solutions (Eqs.(3.20)), and the directional transmittance and reflectance of the whole canopy (Eqs.(3.22) and (3.23)) can then be used to determine the azimuthal variations.

3.5 Calculation of the matrices M^* , F^* , and B^* and the normalization

The coefficients in the generalized Kubelka-Munk equations (Eqs.(3.4)), the matrices M , F and B (or their extended forms M^* , F^* , and B^*) must be determined. These basic matrices can be obtained from those of the single leaves and the leaf angular distribution. The back and forward scattering matrices of a horizontal layer containing only one Lambertian leaf with inclination i_L and azimuth j_L can be determined as (Chapter 2):

$$B_L^*(i', j', i, j) = s(q/\pi) \cos(i') w_{i, w_j} |\cos(a') \cos(a)| \sin^{-1}(i), \quad (3.26)$$

$$F_L^*(i', j', i, j) = s(q'/\pi) \cos(i') w_{i, w_j} |\cos(a') \cos(a)| \sin^{-1}(i). \quad (3.27)$$

Here s is the leaf area index, a is the angle between the incident radiation and the normal of the leaf, and a' is that for exitant radiation:

$$\begin{aligned} \cos(a) &= \cos(i) \cos(j) \sin(i_L) \cos(j_L) \\ &+ \cos(i) \sin(j) \sin(i_L) \sin(j_L) + \sin(i) \cos(i_L), \end{aligned} \quad (3.28)$$

$$\begin{aligned} \cos(a') &= \cos(i') \cos(j') \sin(i_L) \cos(j_L) \\ &+ \cos(i') \sin(j') \sin(i_L) \sin(j_L) + \sin(i') \cos(i_L), \end{aligned} \quad (3.29)$$

and $q=r$, $q'=t$, when $\cos(a)\cos(a') \geq 0$; $q=t$, $q'=r$, when $\cos(a)\cos(a') < 0$. The notation of $\sin(i)$ and $\cos(i)$ means that the sine and cosine functions for the angle interval i are calculated using a representative angle, e.g. the value in the middle of the interval.

Summing all the back and forward scattering matrices of the leaves with different orientations, weighted by angular distribution, yields the corresponding matrices B^* and F^* . The diagonal components of the interception matrix M^* can be calculated as:

$$M^*(i, j, i, j) = O(i, j) / \sin(i), \quad (3.30)$$

where $O(i, j)$ is the projection of the leaves in a layer with a unit leaf area index onto the direction (i, j) .

Because of the discretization the sum of the all components of F^* and B^* is usually not exactly equal to $s(t+r)$ multiplied by the incident radiation. This means that the conservation of the radiation energy is violated. When the value of $t+r$ is high, the multiple scattering between layers plays an important role. The non-conservation of energy in the matrices F^* and B^* will be greatly amplified in the end results. Thus the normalization procedure is not trivial, as noticed by Goudriaan (1977).

Denote the sum of F_L^* and B_L^* as S_L^* . Now

$$S_L^*(i', j', i, j) = s((t+r)/\pi) \cos(i') w_{i'} w_j |\cos(a') \cos(a)| \sin^{-1}(i). \quad (3.31)$$

Consider the horizontal leaf first. According to Eqs.(3.28) and (3.29), $\cos(a) = \sin(i)$ and $\cos(a') = \sin(i')$ in this case, so Eq.(3.31) becomes:

$$S_L^*(i', j', i, j) = s((t+r)/\pi) \cos(i') w_{i'} w_j \sin(i') \quad (3.32)$$

The normalization condition requires that the sum of $S_L^*(i', j', i, j)$, with respect to i' and j' over the whole upper-hemisphere, be exactly equal to $s(t+r)$. After summing $S_L^*(i', j', i, j)$ over the azimuth, this requirement becomes that the sum of $2\sin(i') \cos(i') w_{i'}$ over all inclination intervals should be exactly equal to unity. This is true, however, only as $w_{i'}$ tends to zero, when the summation becomes an integral of $2\sin(t) \cos(t) dt$ from $t=0$ to $\pi/2$. But if $w_{i'}$ is replaced by $\sin(w_{i'})$ (the difference between them tends to zero as $w_{i'}$ tends zero), it can be proven that the normalization condition is fulfilled. In fact, the integral of $2\sin(t) \cos(t) dt$ from the lower boundary b_1 to the upper boundary b_2 of the interval $w_{i'}$, is equal to $2\sin((b_1+b_2)/2) \cos((b_1+b_2)/2) \sin(b_2-b_1)$. This expression can be written as $2\sin(i') \cos(i') \sin(w_{i'})$, if the middle point of the interval $w_{i'}$ is used to calculate $\sin(i')$ and $\cos(i')$. Since the sum of $2\sin(i') \cos(i') \sin(w_{i'})$ over the all intervals is the integral of $2\sin(t) \cos(t) dt$ from $t=0$ to $\pi/2$, which equals unity, the normalization condition will be fulfilled for a horizontal leaf, if $w_{i'}$ in Eqs.(3.26) and (3.27) is replaced by $\sin(w_{i'})$. For an inclined leaf the normalization condition can be fulfilled by adjusting $\cos(a')$ according to the following equation:

$$(1/\pi) \sum_{i'=1}^n \sum_{j'=1}^m \cos(i') \sin(w_{i'}) w_{j'} |\cos(a')| = 1. \quad (3.33)$$

The value of $\cos(a')$ thus obtained is used also for $\cos(a)$, which ensures the validity of the reciprocity relation (Chapter 2).

3.6 Techniques of reducing execution time for a leaf canopy without azimuthal preference

As the basic matrices M^* , F^* , B^* , and the boundary condition R_s^* have been determined, the bidirectional reflectance pattern of a canopy can be calculated by the analytical solution Eq.(3.23). It can be seen that multiplication, inversion and similarity transformation of matrices are involved. The execution time is approximately proportional to the cube of the dimensions of the matrices. If each inclination interval is taken as 10 degrees, the matrices involved in calculating zonal reflectance of the canopy have dimensions 9×9 . For accounting for the azimuthal variations, if the azimuth interval is also taken as 10 degrees, the relevant extended matrices will have dimensions of 324×324 . The execution time for calculating the bidirectional reflectance patterns of the canopy will be prohibitively long even though the analytical solution is available. It is desirable, therefore, to develop techniques to reduce the execution time. This is possible for a leaf canopy without obvious azimuthal preference, as is the case for most crops (de Wit, 1965).

For such a canopy, because of the azimuthal symmetry the interception matrix M^* is independent of the azimuth, and the azimuthal dependence of the back and forward scattering matrices F^* and B^* is related only to the difference between the azimuths of incident and exitant directions. Therefore, among the component matrices of an extended matrix only m matrices are distinct. The matrix F^* (Eq.(3.25)), e.g. has only m distinct matrices $F_{j'j}$. Hence, Eq.(3.25) becomes:

$$F^* = \begin{vmatrix} F_1 & F_2 & F_3 & \dots & F_m \\ F_2 & F_1 & F_2 & \dots & F_{m-1} \\ F_3 & F_2 & F_1 & \dots & F_{m-2} \\ \cdot & \cdot & \cdot & & \cdot \\ \cdot & \cdot & \cdot & & \cdot \\ \cdot & \cdot & \cdot & & \cdot \\ F_m & F_{m-1} & F_{m-2} & \dots & F_1 \end{vmatrix}, \quad (3.34)$$

where F_k ($k=1$ to m) equals $F_{|j-j'|+1}$, so that $k=1$ means that the azimuths of the incident and exitant direction are coincident. Moreover, if m is taken as an even number, and $m/2$ is denoted by m' , only $m'+1$ matrices among F_k 's are distinct, because $F_{m'+1+k} = F_{m'+1-k}$ ($k=1$ to $m'-1$). Hence, the matrix F^* can be represented as:

$$F^* = \begin{pmatrix} F_1 & F_2 & \dots & F_{m'} & F_{m'+1} & F_{m'} & \dots & F_2 \\ \vdots & \vdots & & \vdots & \vdots & \vdots & & \vdots \\ \vdots & \vdots & & \vdots & \vdots & \vdots & & \vdots \\ F_{m'} & F_{m'-1} & \dots & F_1 & F_2 & F_3 & \dots & F_{m'+1} \\ F_{m'+1} & F_{m'} & \dots & F_2 & F_1 & F_2 & \dots & F_{m'} \\ \vdots & \vdots & & \vdots & \vdots & \vdots & & \vdots \\ \vdots & \vdots & & \vdots & \vdots & \vdots & & \vdots \\ F_2 & F_3 & \dots & F_{m'+1} & F_{m'} & F_{m'-1} & \dots & F_1 \end{pmatrix}. \quad (3.35)$$

When the matrices F_1 to $F_{m'+1}$ are known, the matrix F^* is determined, so F_1 to $F_{m'+1}$ are called elementary matrices of F^* . It can be proven that the product of two such matrices A^* and B^* , C^* , retains the same property as A^* and B^* , and the elementary matrices of C^* , C_k , can be obtained directly from the elementary matrices of A^* and B^* , A_j and B_j , by:

$$C_k = A_1 B_k + \sum_{j=2}^{m'} A_j (B_{|k-j|+1} + B_{m'+1-|m'+2-k-j|}) + A_{m'+1} B_{m'+2-k} \quad (3.36)$$

A diagram shown in Fig.3.3 is designed for $m=6$ to derive Eq.(3.36). The elementary matrices of A^* and B^* are arranged counterclockwise along two circles as $A_1 A_2 A_3 A_4 A_3 A_2$ and $B_1 B_2 B_3 B_4 B_3 B_2$. The elementary matrices of the product, C_k , are the sum of the products of A_k and B_k on the same positions in the circles. For C_1 , the matrices A 's and B 's with the same subscripts just on the same positions. For C_2 the A -circle is fixed, while the B -circle is turned clockwise one step; for C_3 , two steps and so on. It is clear that Eq.(3.36) greatly reduces storage as well as the computing time.

Unfortunately, no simple method is found to invert such matrices directly from their elementary matrices. But there exists a method to reduce the dimension by a factor of two. Inspecting Eq.(3.35) shows that the equivalent matrix F^* contains only two different blocks P and Q as:

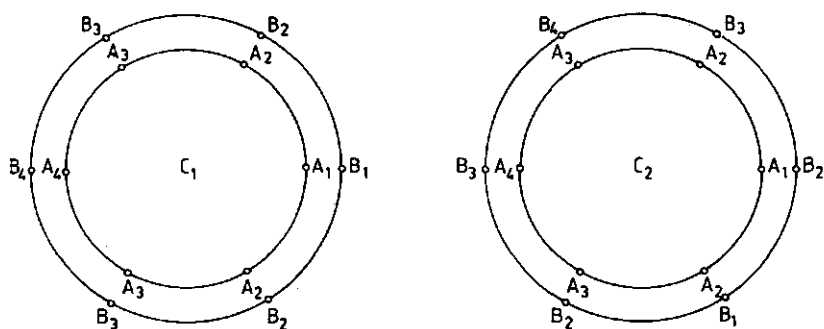


Fig.3.3. The component matrices C_1 and C_2 of the product of A and B.

$$F^* = \begin{vmatrix} P & Q \\ Q & P \end{vmatrix}, \quad (3.37)$$

so that the inverse can be determined by

$$(F^*)^{-1} = \begin{vmatrix} S & G \\ G & S \end{vmatrix}, \quad (3.38)$$

where

$$S = (P - QP^{-1}Q)^{-1}, \quad G = -P^{-1}QS. \quad (3.39)$$

For similarity transformation of matrix Q^* to a diagonal matrix, the same method can be applied. By denoting Q^* in the block form

$$Q^* = \begin{vmatrix} A & B \\ B & A \end{vmatrix}, \quad (3.40)$$

Q^* can be rewritten as

$$Q^* = \frac{1}{2} \begin{vmatrix} I & I \\ -I & I \end{vmatrix} \begin{vmatrix} A-B & 0 \\ 0 & A+B \end{vmatrix} \begin{vmatrix} I & -I \\ I & I \end{vmatrix}. \quad (3.41)$$

Computation shows that $A-B$ and $A+B$ can be transformed into diagonal matrices S and G :

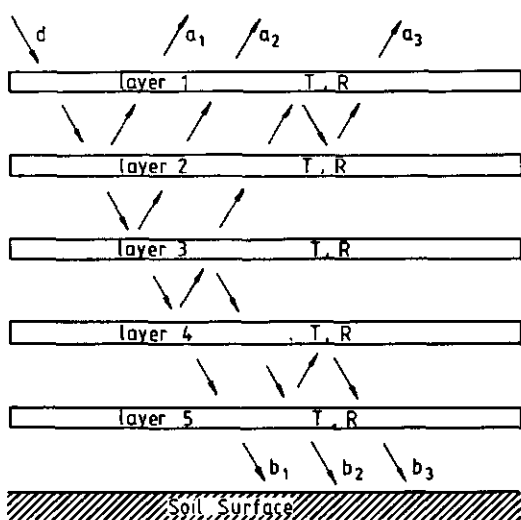


Fig.3.4. Components of the reflected and transmitted radiation vectors with different paths.

$$A - B = VSV^{-1}, \quad A + B = UGU^{-1}, \quad (3.42)$$

Q^* can thus be expressed as:

$$Q^* = \frac{1}{2} \begin{bmatrix} V & U \\ -V & U \end{bmatrix} \begin{bmatrix} S & 0 \\ 0 & G \end{bmatrix} \begin{bmatrix} V^{-1} & -V^{-1} \\ U^{-1} & U^{-1} \end{bmatrix}. \quad (3.43)$$

The validity of Eq.(3.43) can be verified directly by multiplications.

3.7 Approximation method

Although techniques have been developed to reduce the execution time, the resolution in azimuth is still restricted. It was shown in Chapter 2 that the reflected and transmitted radiation vectors of a canopy are composed of an infinite number of component vectors. An illustration is shown in Fig.3.4. A radiation vector \underline{d} is incident upon the top of the canopy. The radiation vector \underline{a}_1 is obtained by the interaction of \underline{d} with layers 1 and 2: $\underline{a}_1 = TRT\underline{d}$, as shown in the figure. The radiation vectors \underline{a}_2 and \underline{a}_3 can be obtained similarly. An infinite number of the component radiation vectors such as \underline{a}_1 , \underline{a}_2 , and \underline{a}_3 constitute a reflected radiation vector from the top of the canopy. The transmitted radiation vector through the bottom of the canopy is, similarly, composed of an infinite number of the compo-

nent radiation vectors such as \underline{b}_1 , \underline{b}_2 , and \underline{b}_3 . It can be seen from Fig.3.4 that for establishing either a reflected or a transmitted component radiation vector, there must be an odd number of reflections by the layers. For a leaf canopy without azimuthal preference, the back and forward scattering matrices are composed of the elementary matrices as mentioned above. The formula determining the product of two such kind of matrices (Eq.(3.36)) ensures that the more the interaction of the radiation vector with the layers takes place, the more the variations of the radiation intensity with azimuth will be smoothed. In fact, little variation is left after three-fold interactions. For practical purposes, it is sufficient to consider only the single reflection from different layers to find the contribution to the azimuthal variation of the reflected radiation vectors.

Consider an infinitesimal layer with leaf area index dl at the depth l . Assume the azimuth of the incident radiation to be zero. The component reflectance matrix, dR^* , formed by single reflection from the layer dl with no interaction with the other layers can be calculated as:

$$dR^*(i', j', i, 0) = e^{-M(i', i')l} e^{-M(i, i)l} B^*(i', j', i, 0) dl, \quad (3.44)$$

where M is the elementary matrix of the interception matrix M^* . The total contribution of all the layers can be obtained by integration:

$$R^*(i', j', i, 0) = B^*(i', j', i, 0) (1 - e^{-(M(i', i') + M(i, i))l_c}) / (M(i', i') + M(i, i)). \quad (3.45)$$

Meanwhile, the total zonal reflectance matrix R_{zon} of the canopy can be easily calculated using the analytical solution Eq.(3.24). The difference between $R_{zon}(i', i)$ and the sum of $R^*(i', j', i, 0)$ ($j'=1$ to m) can be considered evenly distributed over azimuth. The elementary matrices of the reflectance matrix of the canopy thus can be obtained:

$$R_c^*(i', j', i, 0) = R^*(i', j', i, 0) + (R_{zon}(i', i) - \sum_{j'=1}^m R^*(i', j', i, 0)) / m. \quad (3.46)$$

The transmittance matrix of the canopy can be treated similarly, except that a directly transmitted part should be added:

$$T^*(i', j', i, 0) = F^*(i', j', i, 0) (e^{-M(i', i')l_c} - e^{-M(i, i)l_c}) / (M(i, i) - M(i', i')) + d_{i', i} e^{-M(i, i)l_c} \quad (3.47)$$

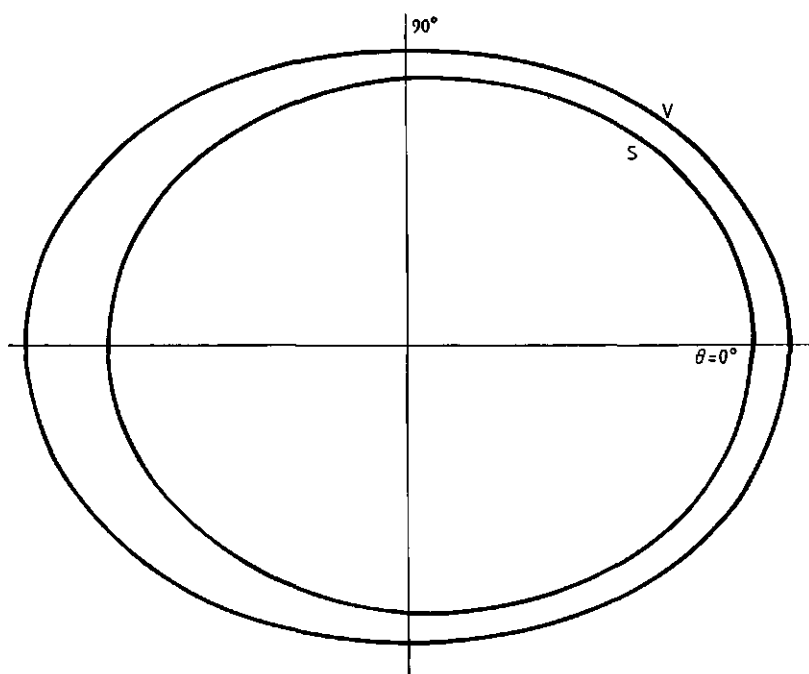


Fig.3.5. Azimuthal variations of reflection radiance from a canopy with spherical inclination distribution (S) and with vertical leaves (V). The inclination for incident and exitant directions are 25 degrees.

where $d_{i'i}$ is equal to unity when $i=i'$, and zero otherwise. The transmittance matrix of the canopy is:

$$T_c^*(i', j', i, 0) = T^*(i', j', i, 0) + (T_{zon}(i', i) - \sum_{j'=1}^m T^*(i', j', i, 0)) / m \quad (3.48)$$

where T_{zon} is the total zonal transmittance matrix.

3.8 Some illustrative results

It is not the purpose of this Chapter to calculate and discuss the reflectance and transmittance matrices for various kinds of crop canopies, although the method developed is aimed primarily at practical applications.

For total zonal reflectance and transmittance, the results are almost exactly the same as those obtained by Goudriaan (1977), while the execution time is greatly reduced (about 1 second on the computer DEC10). The approximate method is used to calculate the detailed azimuthal variations of the reflected radiance, as shown in Fig.3.5. The results are given for vertical leaves and for the leaves with a spherical inclination distribution. The inclinations for incident and exitant directions are 25 degrees. The azimuthal angle interval is 10 degrees, so high resolution is ensured. The execution time is about 10 seconds. The azimuthal variations shown in Fig.3.5 refer to a canopy with $t=r=0.4$. Because of the multiple scattering between the layers they are less variable than the results obtained by Ross (1981) for a 'mean leaf'.

3.9 Discussion

3.9.1 Non-Lambertian scatterers

That leaves are Lambertian scatterers is an oversimplified assumption. It is adopted in this Chapter merely for convenience of explaining the method. Under vector-matrix notation, it is no longer a restriction. The reflectance and transmittance matrices of a given leaf can be measured experimentally (Breece and Holmes, 1971). The basic back and forward scattering matrices of a canopy can be calculated by the formulas given in Chapter 2, and the rest of the procedure remains the same.

3.9.2 Applicability to the atmosphere and clouds

Although the differential equations and the methods to solve the equations in this Chapter are developed with special attention to crop canopies, it can be obviously applied to the radiation transfer through the atmosphere or through clouds. The only difference lies in the way of calculating the basic back and forward scattering matrices. In this case, they can be calculated from the phase function of the constituent scattering substances, such as gas molecules, particles or water droplets, and the knowledge of their size distribution functions. The cumulative leaf area index, of course, should be replaced by the optical depth used conventionally.

3.9.3 Superposition of several heterogeneous layers

Sometimes, the scattering medium cannot be represented by one layer with uniform properties. For instance, a mature rice or wheat crop canopy is better represented by two layers, one corresponding to the ears, and the other to the leaves. For remote sensing, between the crop canopy and the sensors, there is a layer of air, which also scatters radiation. This effect must be included if a more accurate result is demanded. The method developed in this Chapter can be readily adapted to these cases. The calculation should be started from the lowest layer, and the reflectance matrix of the underlying surface, the soil surface, say, is taken as the boundary condition. The solution of the reflectance matrix of the lowest layer thus obtained can be employed as the boundary condition for the second layer, and so on.

4 Uncoupled Multi-Layer Model for the Transfer of Sensible and Latent Heat Flux Densities from Vegetation

(accepted by Boundary-Layer Meteorology)

Abstract

The sensible heat flux density C and the latent heat flux density λE are coupled in the case of a multi-layer model of vegetation. Therefore two linearly independent combinations of C and λE , the enthalpy flux density H and the saturation heat flux density J , are introduced. Two electrical analogues, for H and J , are designed. They are equivalent to the resistance scheme for C and λE , but uncoupled. Penman's formulas for C and λE , which are applicable only to single-layer models, can be expressed equivalently in terms of H and J . This version of Penman's formulas can be extended easily to multi-layer canopies.

4.1 Introduction

Transpiration from a crop stand has been and is still being extensively studied, both experimentally and theoretically, because of its importance to agriculture as well as to meteorology. As to the theoretical work, there are two different approaches: single-layer models and multi-layer models. Both are well developed. For single-layer models, Penman's (1948) formulas are the most frequently used equations for determining sensible and latent heat flux densities from an evaporating surface, based on the energy balance approach. The energy balance method can also be used in the multilayer models. The unknown variables are the temperatures and humidities of each layer, and the sensible and latent heat flux densities at different levels within the canopy. Unfortunately, the equations for sensible and latent heat flux densities are coupled, so that explicit expressions for canopy latent and sensible heat flux densities have not been developed.

Although single-layer models may not be adequate for many cases, they have been widely used because of their simplicity. Multi-layer models should be more useful if analytical solutions can be offered for their steady-state flux densities. Shuttleworth (1976) derived a so-called combination equation in an attempt to obtain a unified model for single- and multi-layer ones.

In this Chapter the multi-layer model developed by Goudriaan and Waggoner (1972) is examined. Then two linearly independent combinations of sensible and latent heat flux densities are introduced. Using the enthalpy flux density H and the saturation heat flux density J as two new variables, the equations are uncoupled. Two electrical analogues for H and J are designed. Based on the uncoupled electrical analogues, analytical solutions can be found.

4.2 Coupled multi-layer model

Agrometeorologists are interested not only in the sensible and latent heat flux densities above a crop canopy, but also in the profiles of temperature and humidity within the canopy. To simulate these profiles, single-layer models are no longer applicable. One has to divide the whole canopy into several layers, and define the leaf temperature, air temperature and humidity, and the sensible and latent heat flux densities in each layer as state variables.

Because the heat capacity of the air in the free space within the canopy and that of the leaves are rather small, for a mean state over a relatively long period, one hour say, the heat storage term can be ignored in the energy balance equation. For every layer, therefore, the net radiation absorbed can be considered to be equal to the sum of the sensible and latent heat flux densities. These energy balance equations together with the relationships between flux densities and relevant driving forces, using the analogy of the electrical circuit theory, constitute a closed set of equations for all unknown variables. This method was used by Waggoner et al. (1969) and Goudriaan and Waggoner (1972). The electrical analogue shown in Fig.4.1 is based on these two papers, but the notations for the variables and the symbols for the potential and current sources are adapted to standard usage.

The driving force (potential source) above the canopy for sensible heat flux density is $\rho c_p T_{a,0}$, in which ρc_p is the volumetric heat capacity of air, $T_{a,0}$ is the air temperature at the reference height. The driving force above the canopy for latent heat flux density is $(\rho c_p / \gamma) e_{a,0}$, where γ is the psychrometric constant and $e_{a,0}$ is the water vapour pressure of the air at the reference height. In addition to these two potential sources, there is a current source for each layer. This is the net radiation absorbed within

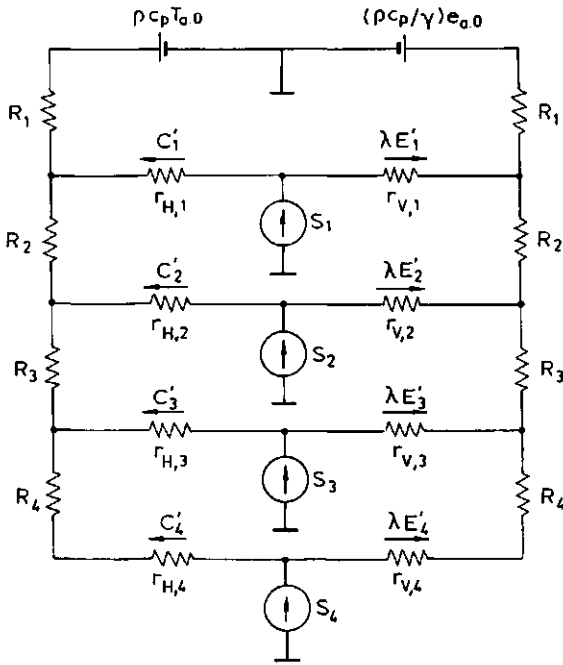


Fig. 4.1. Electrical analogue for sensible and latent heat flux densities. For meaning of symbols, see the text.

the layer, denoted as S_i , where i specifies the layer index. The sensible and latent heat flux densities supplied by the layer i are denoted by C_i' and $\lambda E_i'$, respectively. The corresponding resistances are specified by $r_{H,i}$ and $r_{V,i}$. The resistances in the vertical direction due to turbulent exchange are represented by the R_i 's, which are assumed to be the same for both the sensible and latent heat transfers. Based on this electrical analogue, the following equations can be obtained:

$$C_i' + \lambda E_i' = S_i, \quad (4.1)$$

$$C_i' = \rho c_p (T_{L,i} - T_{a,i}) / r_{H,i}, \quad (4.2)$$

$$\lambda E_i' = (\rho c_p / \gamma) (e_s(T_{L,i}) - e_{a,i}) / r_{V,i}, \quad (4.3)$$

$$e_s(T_{L,i}) = e_s(T_{a,i}) + \Delta(T_{L,i} - T_{a,i}). \quad (4.4)$$

Eq.(4.1) is the energy balance equation. Eqs.(4.2) and (4.3) are the analogues of the Ohm's law for the sources of the sensible and latent heat flux densities. The sensible heat flux density originates from the leaf

surfaces, so that the leaf temperature $T_{L,i}$ is introduced. $T_{a,i}$ is the temperature of the air surrounding the leaves. $r_{H,i}$ consists of only the leaf boundary-layer resistance for heat transfer. The latent heat flux density originates from the substomatal cavities. The air within the cavities is assumed to be saturated by water vapour, so that the vapour pressure there can be determined as the saturated vapour pressure at the corresponding leaf temperature $e_s(T_{L,i})$. The variable $e_{a,i}$ is the vapour pressure of the air surrounding the leaves. The resistance for the vapour transfer from the substomatal cavities to the surrounding free space within the canopy, $r_{V,i}$, is composed of two parts: the stomatal resistance and the leaf boundary-layer resistance.

Due to the different diffusion coefficients of vapour and heat in air, the leaf boundary-layer resistance for latent heat is slightly different from $r_{H,i}$. It is often convenient to define the stomatal resistance r_s as

$$r_s = r_V - r_H. \quad (4.5)$$

Eq.(4.4) is the linearized saturated vapour pressure versus temperature curve, which is in fact more or less exponential, and Δ is its slope determined at a proper temperature, T_p . To complete the system of equations, Ohm's law can be applied in the vertical direction:

$$\sum_{j=n}^i C_j' = \rho c_p (T_{a,i-1} - T_{a,i}) / R_i \quad (i=1 \text{ to } n) \quad (4.6)$$

$$\sum_{j=n}^i \lambda E_j' = (\rho c_p / \gamma) (e_{a,i-1} - e_{a,i}) / R_i \quad (i=1 \text{ to } n) \quad (4.7)$$

where n specifies the total number of the layers.

The driving forces in the vertical direction for sensible and latent heat flux densities are, respectively, the differences in $\rho c_p T_a$ and $\rho c_p e_a / \gamma$ between layers. The flux densities through R_i are composed of all sources from layers i to n , so the summation is carried out on the left-hand sides of Eqs.(4.6) and (4.7).

Eqs.(4.1) through (4.4), (4.6) and (4.7) constitute a closed set of equations. Being coupled they have to be solved simultaneously. A matrix method was developed by Waggoner et al. (1969). Although sophisticated software for solving matrix problems are available, explicit analytical

solutions are needed to simplify the application of this theory and to provide a more direct physical insight into canopy behaviour. The idea is to make the equations uncoupled by introducing two linearly independent combinations of C and λE .

4.3 Uncoupling

One of the two required combinations of C and λE is straightforward. It follows from Eq.(4.1) that if a new variable H , called the enthalpy flux density, is defined as:

$$H = C + \lambda E. \quad (4.8)$$

The source for H from layer i , following Eq.(4.1), can be written as:

$$H_i' = S_i'. \quad (4.9)$$

Because the net radiation absorbed within each layer is a known variable, H_i can be obtained immediately.

The driving force for the enthalpy flux density in the vertical direction is the difference in $\rho c_p (T_a + e_a / \gamma)$ between layers, a combination of the driving forces for sensible and latent heat flux densities, following the definition of H . The term $T_a + e_a / \gamma$ is often called the equivalent temperature of air, denoted by Te_a :

$$Te_a = T_a + e_a / \gamma. \quad (4.10)$$

The problem is to find another combination. It follows from Eqs.(4.1) through (4.4) that C_i' and $\lambda E_i'$ can be rewritten as:

$$C_i' = (\gamma r_{V,i} S_i - \rho c_p D_i) / (\Delta r_{H,i} + \gamma r_{V,i}) \quad (4.11)$$

$$\lambda E_i' = (\Delta r_{H,i} S_i + \rho c_p D_i) / (\Delta r_{H,i} + \gamma r_{V,i}) \quad (4.12)$$

where D_i is the water vapour pressure deficit of the air in layer i :

$$D_i = e_s(T_{a,i}) - e_{a,i}. \quad (4.13)$$

To find the other combination, it can be noticed that Eqs.(4.11) and (4.12) only contain one property of the air in the form of the vapour pressure deficit, D_i . Therefore the flux density driven by the difference

in D between layers, should be the desired combination of the sensible and latent heat flux densities. The saturated vapour pressure at air temperature, $e_s(T_a)$ can be expressed as:

$$e_s(T_a) = e_s(T_p) + \Delta(T_a - T_p) \quad (4.14)$$

where T_p is the properly chosen temperature for evaluating Δ , as mentioned before. Eq.(4.13) can be rewritten as:

$$D_i = \Delta T_{a,i} - e_{a,i} + e_s(T_p) - \Delta T_p. \quad (4.15)$$

By taking the difference of D_i between layers $i-1$ and i , the constant $e_s(T_p) - \Delta T_p$ in Eq.(4.15) is eliminated. A subsequent multiplication of both sides with $(\rho c_p / \Delta) / R_i$ yields:

$$\begin{aligned} (\rho c_p / \Delta)(D_{i-1} - D_i) / R_i &= \rho c_p (T_{a,i-1} - T_{a,i}) / R_i \\ &\quad - (\gamma / \Delta)(\rho c_p / \gamma)(e_{a,i-1} - e_{a,i}) / R_i \end{aligned} \quad (4.16)$$

Referring to Eqs.(4.6) and (4.7) shows that the right-hand side of Eq.(4.16) can be written as $C_i - (\gamma / \Delta) \lambda E_i$. C_i and λE_i denote the cumulative sensible and latent heat flux densities above layer i , which are the sums of the relevant sources from layers i through n as expressed on the left-hand side of Eqs.(4.6) and (4.7). The left-hand side of Eq.(4.16) represents a new cumulative flux density denoted now by J_i :

$$J_i = \sum_{j=i}^n J_j' = (\rho c_p / \Delta)(D_{i-1} - D_i) / R_i \quad (4.17)$$

where J_j' is the source term from layer j . Therefore the desired combination of the sensible and latent heat flux densities is:

$$J = C - (\gamma / \Delta) \lambda E \quad (4.18)$$

which is valid for both J_i and J_i' .

It follows from Eqs.(4.11), (4.12) and (4.18) that the source J_i' is:

$$J_i' = \frac{-(\rho c_p / \Delta) D_i}{(r_{H,i} + \alpha r_{s,i})} + \frac{S_i}{(1 + r_{H,i} / \alpha r_{s,i})}, \quad (4.19)$$

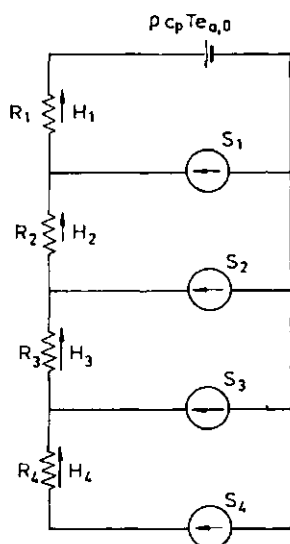


Fig.4.2. Electrical analogue for enthalpy flux density H .

where r_s is the stomatal resistance defined by Eq.(4.5), and α is defined as:

$$\alpha = \gamma / (\gamma + \Delta) \quad (4.20)$$

4.4 Uncoupled electrical analogues for H and J

For the required electrical analogue for H , a potential source above the canopy can be specified as $\rho c_p T_{e,a,0}$, in which $T_{e,a,0}$ is the equivalent temperature of the air at the reference height. The current sources are given by Eq.(4.9) for each layer. The electrical analogue is simple, as is shown in Fig.4.2. The meaning of the symbols is the same as those in Fig.4.1. Now H_i specifies the cumulative flux density above layer i , which is the sum of the sources H_i from layers i through n . H_i is positive upwards. The change of usage is necessary for obtaining a simpler form of solution later. It is obvious that the H_i 's are determined only by the current sources and independent of the potential source.

Similar to the electrical analogue for the enthalpy flux density H , a potential source above the canopy for J can be specified as $(\rho c_p / \Delta) D_0$, in which D_0 is the vapour pressure deficit of the air at the reference height.

The role of the current sources requires more consideration. First, a diagram can be designed for a single layer. Inspection of Eq.(4.19) indi-

cates that J_i' is composed of two parts. The first term on the right-hand side of Eq.(4.19) is due to the potential source $(\rho c_p / \Delta) D_i$. The diagram can be easily designed, as is shown in Fig.4.3(a). The second term on the right-hand side of Eq.(4.19) is caused by the current source S_i (for the soil surface the heat flux into the soil G should be subtracted from S_i). The diagram obtained is shown in Fig.4.3(b).

The diagrams in Figs.4.3(a) and 4.3(b) can be combined, according to the superposition theorem in electrical theory, as shown in Fig.4.3(c). The electrical analogue for the whole canopy can be obtained, based on that for the single layers (Fig.4.4).

4.5 Solutions for the total flux densities H_1 and J_1 above a canopy

The total flux density H_1 above the canopy is simply:

$$H_1 = \sum_{j=1}^n S_j, \quad (4.21)$$

while that of J_1 has to be determined from Fig.4.4. For simplicity, only four layers are assumed, but the solutions can be easily extended to the general case. Under the notations presently used, J_i is now cumulative to each layer i , hence $J_i' = J_i - J_{i+1}$, and Eq.(4.19) becomes:

$$r_i (J_i - J_{i+1}) = -(\rho c_p / \Delta) D_i + \alpha r_{s,i} S_i \quad (i=1 \text{ to } 4), \quad (4.22)$$

where J_5 is defined as to be zero, and r_i is defined as:

$$r_i = r_{H,i} + \alpha r_{s,i}. \quad (4.23)$$

The other four equations can be obtained for each R_i in the vertical direction:

$$R_i J_i = (\rho c_p / \Delta) (D_i - D_{i-1}) \quad (i=1 \text{ to } 4). \quad (4.24)$$

Eqs.(4.22) and (4.24) represent eight equations for eight unknown variables: J_i and D_i ($i=1$ to 4), so that this is a closed system.

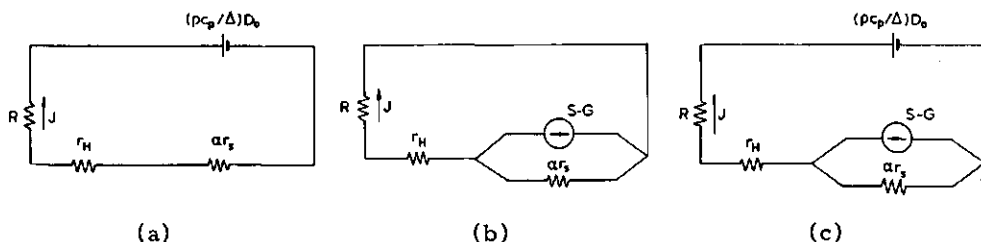


Fig.4.3. Electrical analogues for J for one layer. (a) For the potential source; (b) for the current source; (c) combined.

Substituting Eq.(4.22) into Eq.(4.24) and rearranging gives four equations for the J_i ($i=1$ to 4):

$$(1+R_1/r_1)J_1 - J_2 = b_1 \quad (4.25a)$$

$$(R_1/r_2)J_1 + (1+R_2/r_2)J_2 - J_3 = b_2 \quad (4.25b)$$

$$(R_1/r_3)J_1 + (R_2/r_3)J_2 + (1+R_3/r_3)J_3 - J_4 = b_3 \quad (4.25c)$$

$$(R_1/r_4)J_1 + (R_2/r_4)J_2 + (R_3/r_4)J_3 + (1+R_4/r_4)J_4 = b_4 \quad (4.25d)$$

where

$$b_i = (-(\rho c_p/\Delta)D_0 + \alpha r_{s,i} S_i)/r_i. \quad (4.26)$$

J_1 can be solved by using Cramer's rule:

$$J_1 = \frac{\begin{vmatrix} b_1 & -1 & 0 & 0 \\ b_2 & 1+R_2/r_2 & -1 & 0 \\ b_3 & R_2/r_3 & 1+R_3/r_3 & -1 \\ b_4 & R_2/r_4 & R_3/r_4 & 1+R_4/r_4 \end{vmatrix}}{\begin{vmatrix} 1+R_1/r_1 & -1 & 0 & 0 \\ R_1/r_2 & 1+R_2/r_2 & -1 & 0 \\ R_1/r_3 & R_2/r_3 & 1+R_3/r_3 & -1 \\ R_1/r_4 & R_2/r_4 & R_3/r_4 & 1+R_4/r_4 \end{vmatrix}}. \quad (4.27)$$

By denoting the determinant in the denominator in Eq.(4.27) as A_0 , and defining the sub-determinants as:

$$A_1 = \begin{vmatrix} 1+R_2/r_2 & -1 & 0 \\ R_2/r_3 & 1+R_3/r_3 & -1 \\ R_2/r_4 & R_3/r_4 & 1+R_4/r_4 \end{vmatrix} \quad (4.28)$$

$$A_2 = \begin{vmatrix} 1+R_3/r_3 & -1 \\ R_3/r_4 & 1+R_4/r_4 \end{vmatrix} \quad (4.29)$$

$$A_3 = 1 + R_4/r_4 \quad (4.30)$$

$$A_4 = 1, \quad (4.31)$$

Eq.(4.27) can be written in a concise form by unfolding the numerator according to the column b_i :

$$J_1 = \sum_{j=1}^n (A_j/A_0) b_j = \sum_{j=1}^n (A_j/A_0) (-(\rho c_p/\Delta) D_0/r_j + (\alpha r_{s,j}/r_j) S_j). \quad (4.32)$$

A recurrent relation for A_i can be found. Unfolding A_1 , for instance, according to the first column gives:

$$A_1 = (1+R_2/r_2)A_2 + (R_2/r_3)A_3 + (R_2/r_4)A_4 = A_2 + R_2 \sum_{j=2}^n (A_j/r_j). \quad (4.33)$$

It can be proven that Eq.(4.33) is valid for each A_i :

$$A_i = A_{i+1} + R_{i+1} \sum_{j=i+1}^n (A_j/r_j) \quad (i=0 \text{ to } n-1). \quad (4.34)$$

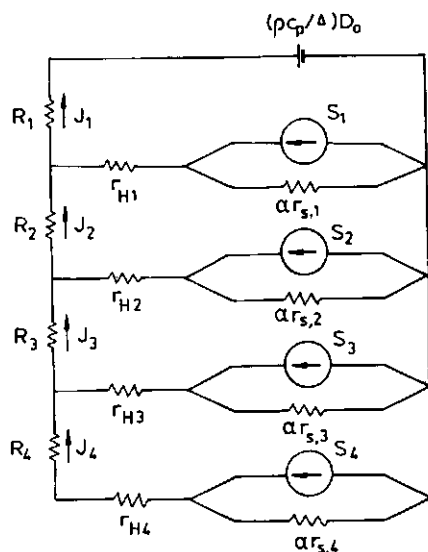


Fig.4.4. Electrical analogue for saturation heat flux density J .

The profiles of J can also be obtained, as well as those of air temperature, vapour pressure and leaf temperature. Because these profiles are calculated from the explicit expressions, the computing time is greatly reduced, so that the calculation can be executed on a microcomputer. This subject will be discussed in Chapter 5.

4.6 An equivalent expression for Penman's formulas

As mentioned above, the Penman's formulas are often used for calculating the sensible and latent heat flux densities from an evaporating surface:

$$C = \frac{\gamma^*(S-G) - \rho_c D_0 / (R+r_H)}{\Delta + \gamma^*} \quad (4.35)$$

$$\lambda E = \frac{\Delta(S-G) + \rho_c D_0 / (R+r_H)}{\Delta + \gamma^*} \quad (4.36)$$

where G is the heat flux density into the soil, γ^* is the apparent psychrometric constant, defined as:

$$\gamma^* = \gamma(R + r_V) / (R + r_H). \quad (4.37)$$

The problem is that no equivalent expressions exist for C and λE in the multi-layer model. By using the definitions of H and J, Eqs.(4.8) and (4.17), however, Penman's formulas can also be expressed in terms of H and J:

$$H = S - G \quad (4.38)$$

$$J = \frac{\alpha r_s (S-G) - (\rho_c / \Delta) D_0}{R + r_H + \alpha r_s}. \quad (4.39)$$

These equivalent expressions for Penman's formulas are in fact only special forms of Eqs.(4.21) and (4.32) as can be seen as follows.

For the single-layer model, $n=1$, S_j becomes $S-G$, A_1 becomes unity, and $A_0=1/R/(r_H+\alpha r_s)$, so that Eq.(4.32) becomes the same as Eq.(4.39). In fact, C and λE can be expressed in terms of H and J:

$$C = \alpha H + (1 - \alpha)J, \quad (4.40)$$

$$\lambda E = (1 - \alpha)(H - J). \quad (4.41)$$

The familiar Penman equations (4.35) and (4.36) are obtained by substituting Eqs.(4.38) and (4.39) into (4.40) and (4.41) and simplifying. The equivalent Penman's formulas in terms of H and J, Eqs.(4.38) and (4.39) are preferable, because for both single- and multi-layer models, the same formulas can be used.

In fact, Eqs.(4.21) and (4.32) provide a bridge between the single- and multi-layer models, from which several conclusions, particularly for the canopy resistance r_c , can be drawn. This subject will be discussed in Chapter 7.

4.7 Physical significance of J

The flux densities H and J were introduced during the mathematical process of uncoupling. But it can be seen that they have clear physical meanings. The physical meaning of H is obvious, viz., the total heat or enthalpy flux density. On the contrary, the physical meaning of J is not immediately clear and is exposed now.

The Bowen ratio β is defined as the ratio of sensible to latent heat flux densities. It can be expressed in terms of H and J:

$$\beta = C/\lambda E = ((\gamma/\Delta)H + J)/(H - J). \quad (4.42)$$

This equation shows a unique relationship exists between β and J, as long as H is fixed. The larger the J, the larger the Bowen ratio will be. It can be seen that $\beta = \gamma/\Delta$ when $J=0$, $\beta < \gamma/\Delta$ when $J<0$, and $\beta > \gamma/\Delta$ when $J>0$, in which the value of γ/Δ is often called the critical value of the Bowen ratio (Monteith, 1973). Likewise $J=0$ can also be called a critical value.

According to the preceding derivation, the flux density J is driven by the gradient of D. Therefore when J equals zero, the gradient of vapour pressure deficit is zero, and vice versa. In this case, λE is equal to $(1-\alpha)H$ or

$$\lambda E = (1-\alpha)(S-G) \quad (4.43)$$

which is often called the equilibrium evaporation rate (Priestley and Taylor, 1972).

In addition to the three classical flux densities of enthalpy, sensible heat and latent heat, it is proper to emphasize the role of J , as a fourth flux density. Together with the driving forces (gradients) they are:

Driving force (gradient):	Flux density:
temperature T	sensible heat C
vapour pressure e	latent heat λE
equivalent temperature T_e	enthalpy H
vapour pressure deficit D	saturation heat J .

Noting the important role of the vapour pressure deficit in evapotranspiration and the clear physical meaning of the related flux density J , it can be realized that J is not merely a mathematical device. It seems proper to give it a name. Here J is called the saturation heat flux density.

4.8 Discussion and conclusions

The saturation heat flux density J is equivalent to $\psi_2 = -\Delta C + \gamma \lambda E$, derived by McNaughton (1976) in his two-dimensional and single-layer model for evaporation and advection. Perrier (1976) has also derived a second-order differential equation for the so-called saturation temperature deficit $Y = T - T_d$, where T_d is the dew-point temperature. Both their derivations are based on a continuous model in vertical direction rather than on a discrete multi-layer model. Because the resulting second order differential equation cannot be solved analytically and a numerical solution based on a difference method has to be used, it is more straightforward to derive the equations for J directly from a multi-layer model. Based on these equations for the discrete model, the electrical analogue, which gives a clearer picture, can be easily designed.

In this Chapter, the quantity J is introduced based on the linearized saturated vapour pressure versus temperature curve. This is only an approximation. Inspection of the saturated vapour pressure curve shows that, within a 10°C temperature interval, the error caused by the linearization is rather small. Calculations show that for the intervals of 10-20, 20-30 and 30-40 $^\circ\text{C}$, the largest relative errors are, respectively, 4.3, 3.0 and 1.8%, Δ being evaluated at the mid-points of the intervals. For a larger interval of 15-35 $^\circ\text{C}$, however, the relative error reaches 13.5%. This

temperature interval is determined in practice by the difference between the highest leaf temperature and the lowest air temperature following Eq.(4.4). Under most field conditions, this temperature difference is expected not to exceed 10°C , so that the linearization of the saturated vapour pressure curve is feasible.

The substitution of D/Δ by the saturation temperature deficit Y extends unnecessarily the temperature interval. The lowest air temperature now is replaced by the lowest dew-point temperature. The extension depends on the value of D , or more precisely, on the relative humidity h . Calculations show that as a rule of thumb, $h=0.5$ is equivalent to $Y=10^{\circ}\text{C}$. Thus the substitution of D/Δ by Y introduces an additional error, which becomes substantial when h is small.

The other basic assumption related to the substitution of H and J for C and λE , viz., the similarity between the exchange coefficients of heat and water vapour. This is a rather good approximation, the conditions for its validity having been extensively studied (Monteith, 1973). Obviously, it does not hold for the transfer process in the soil. When the substitution is applied to the canopy, the heat flux density into the soil at the soil surface, G , should be known. If G is unknown and is an output of the simulation program as in Goudriaan's model (1977), an iteration method has to be used.

The treatment in this Chapter is different from that by Shuttleworth (1976). He derived his combination equation based on the redefinition of the relevant resistances, e.g. r_H and r_V . The introduction of H and J retains all the resistances in an ordinary sense, and the electrical analogues thus developed use the concepts of the potential and current sources in a standard way.

Based on these considerations, the following conclusions can be drawn:

- a) To study transpiration from a canopy, flux densities of enthalpy H and saturation heat J are preferred to flux densities of sensible heat C and latent heat λE , because the resulting equations are uncoupled.
- b) The flux density J is uniquely related to the Bowen ratio at each value of H . The equilibrium evaporation rate occurs when $J=0$.
- c) The electrical analogues for H and J provide a method to calculate the flux densities; the method is applicable to both single- and multi-layer models. In the case of single-layer models, the derived formulas for H and J are another version of the familiar Penman formulas for C and λE .

5 A Crop Micrometeorology Simulation Program in BASIC on Microcomputers (submitted to Agricultural Meteorology)

Abstract

Based on two uncoupled electrical analogues for enthalpy and saturation heat flux densities H and J , and the appropriate recurrent formulas, a simulation program in BASIC is developed. The formulae needed for describing radiation characteristics, aerodynamic and plant-physiological resistances are taken from the simulation model MICROWEATHER (Goudriaan, 1977), so that the present program gives the same detailed description of the micrometeorological situation in the crop. It treats direct and diffuse, visible and near-infrared radiation separately, distinguishes between sunlit and shaded leaves for calculating net photosynthesis rate, calculates stomatal resistance according to both irradiation and plant water status, and gives profiles of air and leaf temperature, air humidity, sensible and latent heat flux densities. It can, however, be executed on a microcomputer, because of the steady-state approach based on uncoupled equations. The output of the program is compared with that of MICROWEATHER.

5.1 Introduction

During the past two decades, crop micrometeorologists have developed various simulation models to calculate the regime of wind, radiation, temperature and humidity within a crop canopy. Roughly speaking, two kinds of techniques have been used. One is to trace the time course of the relevant variables by integration (Goudriaan, 1977); the other is to calculate steady-state values of these variables (Waggoner and Reifsnyder, 1968; Goudriaan and Waggoner, 1972; Perrier, 1976; Shuttleworth, 1976). Apparently, the former gives a more detailed description, while the latter needs less computation. Both approaches are fairly successful. The remaining problem is that they rely on mainframe computers because of their complexity and the lack of analytical solutions to the equations involved. The everincreasing popularization of microcomputers, however, demands a model which can handle the crop micrometeorology on a microcomputer.

In terms of a mathematical uncoupling technique two uncoupled electrical analogues for enthalpy and saturation heat were developed in Chapter 4 to replace the coupled one for sensible and latent heat. The time-consuming

matrix inversion used in the coupled model (Waggoner et al., 1969) is thus no longer necessary. The derived recurrent formula for solving the equations further simplifies the computation, so it has become possible to construct a simulation program which can be executed on a microcomputer.

In this Chapter, the formulas required for calculating the profiles of potentials and fluxes are derived. A method of treating sunlit and shaded leaves separately is presented. A simulation program is written in BASIC and its output is compared with that of Goudriaan's model MICROWEATHER.

5.2 Description of the simulation model

5.2.1 Basic equations for profile calculation

The definition of the enthalpy and saturation heat flux densities, H and J , are (Chapter 4):

$$H = C + \lambda E, \quad J = C - (\gamma/\Delta)\lambda E, \quad (5.1)$$

where γ is the psychrometric constant, Δ the slope of the saturation vapour pressure curve, and C and λE are sensible and latent heat flux densities, respectively. The following equations are equivalent:

$$C = \alpha H + (1 - \alpha)J, \quad \lambda E = (1 - \alpha)(H - J), \quad (5.2)$$

where α is defined as:

$$\alpha = \gamma / (\gamma + \Delta). \quad (5.3)$$

Two uncoupled electrical analogues for H and J are presented, respectively, in Figs.5.1(a) and 5.1(b). The relevant profiles are calculated according to the following procedures.

(a) H profile

$$H_i = \sum_{j=n}^i H_j' \quad (5.4)$$

where H_i is the cumulative enthalpy flux density above layer i , and H_j' is the enthalpy source for layer j . $H_j' = S_j - F_j$ for the canopy ($j=1$ to $n-1$) and $H_n' = S_n - G$ for the soil surface, in which S_j and F_j are the net radiation absorbed and net energy consumption rate by photosynthesis in layer j , G

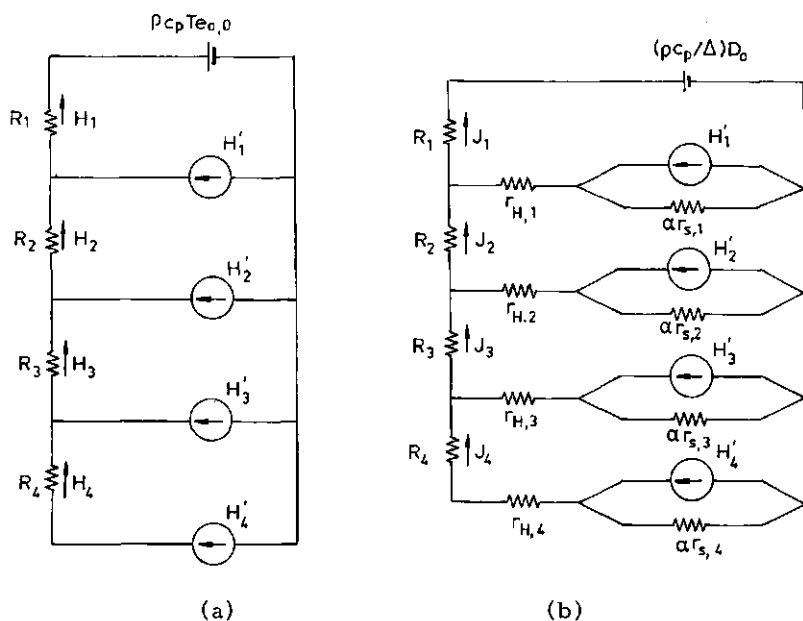


Fig.5.1. Electrical analogues for (a) enthalpy and (b) saturation heat.

the heat flux density penetrating into the soil surface, and n the total number of layers, including the soil surface.

(b) J profile

The total flux density above the canopy J_1 can be obtained first:

$$J_1 = \sum_{j=1}^n (A_j/A_0) b_j, \quad (5.5)$$

where A_n is defined as unity and the determinant A_j ($j=0$ to $n-1$) is calculated by the following recurrent formulae:

$$A_i = A_{i+1} + R_{i+1} \sum_{j=i+1}^n (A_j/r_j). \quad (5.6)$$

Here R_i is the turbulent resistance between layers $i-1$ and i (the reference height refers to $i=0$). The resistance r_i is defined as:

$$r_i = r_{H,i} + \alpha r_{s,i}, \quad (5.7)$$

in which $r_{H,i}$ is the leaf boundary-layer resistance of layer i to heat transfer, $r_{s,i}$ the stomatal resistance of layer i . The parameter b_j in Eq.(5.5) is defined as:

$$b_j = (\alpha_{s,j} H_j' - \rho c_p D_0 / \Delta) / r_j. \quad (5.8)$$

Here ρc_p is the volumetric heat capacity of air, and D_0 the vapour pressure deficit at the reference height.

The source from layer i , J_i' is

$$J_i' = (\alpha_{s,i} H_i' - \rho c_p D_i / \Delta) / r_i, \quad (5.9)$$

where D_i is the vapour pressure deficit of the air in layer i , and can be calculated from D_0 and $R_j J_j$ by using Ohm's law in the vertical direction. Eq.(5.9) can therefore be rewritten in terms of b_i as

$$J_i' = b_i - \left(\sum_{j=1}^i R_j J_j \right) / r_i \quad (i=1 \text{ to } n-1). \quad (5.10)$$

Then the cumulative flux density above layer $j+1$ can be obtained:

$$J_{i+1} = J_i - J_i' \quad (i=1 \text{ to } n-1). \quad (5.11)$$

Eqs. (5.1) to (5.9) were derived in Chapter 4.

(c) C and λE profiles

It follows from Eqs.(5.2) that C_i and λE_i are readily obtained from H_i and J_i :

$$C_i = \alpha H_i + (1 - \alpha) J_i, \quad \lambda E_i = (1 - \alpha) (H_i - J_i) \quad (i=1 \text{ to } n-1). \quad (5.12)$$

(d) T and e profiles

The profiles of vapour pressure deficit D , air temperature T and air vapour pressure e are obtained by:

$$D_i = D_{i-1} + J_i R_i / (\rho c_p / \Delta) \quad (i=1 \text{ to } n), \quad (5.13)$$

$$T_i = T_{i-1} + C_i R_i / \rho c_p \quad (i=1 \text{ to } n), \quad (5.14)$$

$$e_i = e_{i-1} + \lambda E_i R_i / (\rho c_p / \gamma) \quad (i=1 \text{ to } n), \quad (5.15)$$

where D_0 , T_0 and e_0 specify the vapour pressure deficit, temperature and vapour pressure, respectively, of air at the reference height.

(e) T_L profile

The profile of leaf temperature T_L (including the temperature of the soil surface) is obtained by:

$$T_{L,i} = T_i + (C_i - C_{i+1})r_{H,i}/\rho c_p \quad (i=1 \text{ to } n), \quad (5.16)$$

where C_{n+1} is defined as zero.

5.2.2 Distinguishing sunlit and shaded leaves

So far, the model considers only the average radiation intensity in each layer. This is acceptable for an overcast sky, but on sunny days, sunlit and shaded leaves should be distinguished, because they have different stomatal resistance per leaf area. Thus, in each layer, leaves with different irradiation levels have to be distinguished. This is equivalent to splitting each layer into several sublayers, the turbulent resistances between these sublayers being equal to zero. In Figs.5.2(a) and 5.2(b), the corresponding electrical analogues for H and J are shown. Each of the three canopy layers is split here into only two sublayers for illustration. If 6 canopy layers and 6 irradiation levels are assumed, the total number of layers becomes 37, including the soil surface. It is fairly time-consuming to invert matrices of such a large size, even on mainframe computers. This is one of the main difficulties of the coupled electrical analogue. With the uncoupled models shown in Figs.5.2(a) and 5.2(b), however, this problem does not exist. If the layer index is denoted by i as before, and the irradiation index by k , then for the canopy the resistances $r_{H,i}$, $r_{s,i}$ and r_i are denoted by $r_{H,i,k}$, $r_{s,i,k}$ and $r_{i,k}$, radiation absorbed by $S_{i,k}$ and the parameters b_i by $b_{i,k}$. For the H profile, it is clear from inspection of Fig.5.2(a) that Eq.(5.4) can be modified to:

$$H_i = \sum_{j=n}^i \sum_{k=0}^m H_{j,k}, \quad (5.17)$$

where m denotes the total number of irradiation levels for sunlit leaves, and $k=0$ refers to shaded leaves. Since the turbulent resistances between the sublayers are zero, Eqs.(5.5), (5.6), (5.10) and (5.11) for the J profile are still valid if b_i and r_i are defined as:

$$b_i = \sum_{k=0}^m b_{i,k}, \quad 1/r_i = \sum_{k=0}^m (1/r_{i,k}), \quad (5.18)$$

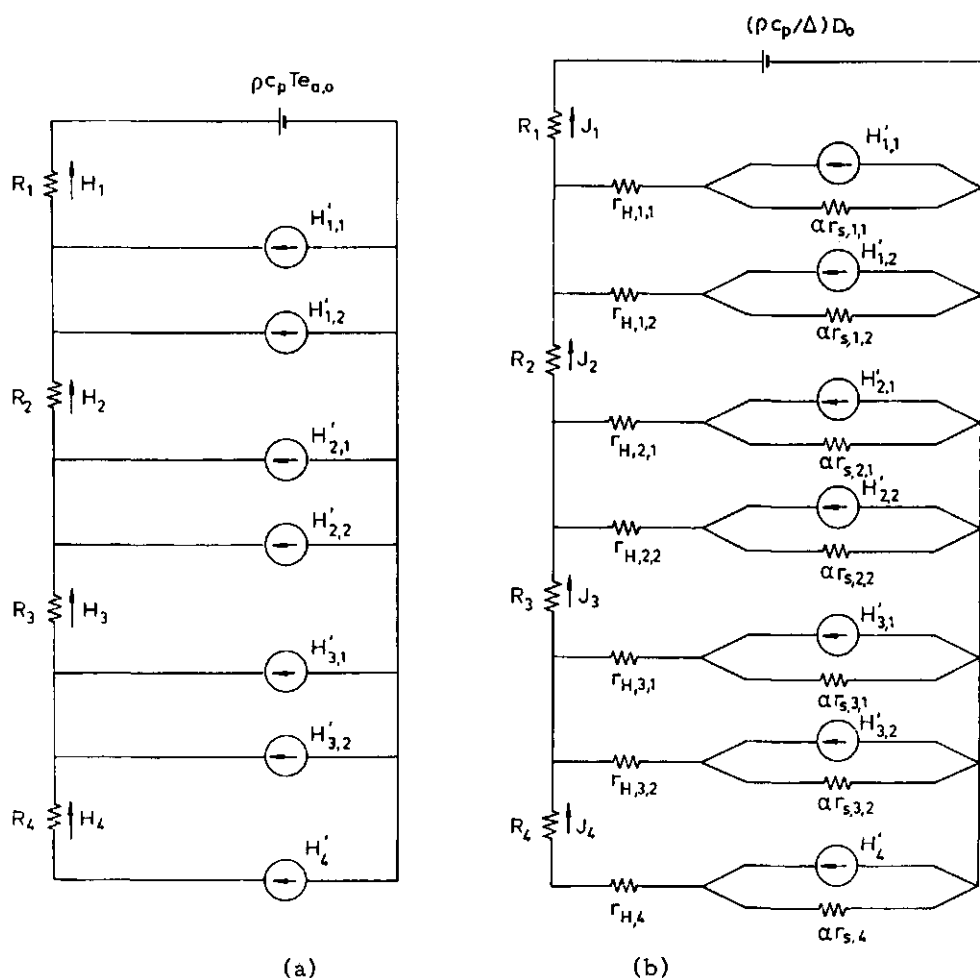


Fig.5.2. Electrical analogues when sunlit and shaded leaves are distinguished: (a) for enthalpy and (b) for saturation heat.

where $b_{i,k}$ is defined as:

$$b_{i,k} = (\alpha r_{s,i,k} H'_{i,k} - \rho c_p D_0 / \Delta) / r_{i,k}. \quad (5.19)$$

The J profile is, therefore, still readily obtainable. The profiles of sensible and latent heat flux densities, temperature, vapour pressure, vapour pressure deficit of air and averaged leaf temperature are obtained in the same way.

5.2.3 Heat flux density into the soil surface

Unfortunately, the uncoupling procedure is invalid in soil because of different vertical transfer coefficients for sensible and latent heat. The heat flux density into the soil surface G has to be known in the uncoupled electrical analogues shown in Figs. 5.2(a) and 5.2(b). In some cases G is not available and has to be simulated; in other cases the value measured by heat plate or derived from measured soil temperature profile is not reliable, so, in spite of these measurements, G should still be simulated. On the other hand, when the time course of the soil temperature profile is included in a complete program simulating crop micrometeorology, then G is no longer an input but an output variable.

Because the above-ground and below-ground parts are coupled with each other through G , an iteration method may be applied even if the soil temperature profile is known. A value for G is first guessed; a more accurate value of G is determined as follows.

The soil-surface temperature can be obtained from the above-ground part as $T_{s,a}$ by the method described above (Eq. (5.16)). But it can also be found from the below-ground part as $T_{s,u}$:

$$T_{s,u} = T_{s,1} + (d_1/k')G^0, \quad (5.20)$$

where G^0 is the guessed heat flux density, d_1 the distance between the soil surface and the center of the top soil layer, k' the conductivity for heat in the soil, and $T_{s,1}$ the temperature of the first soil layer. This temperature is simulated by dividing the soil into layers using G as an input (de Wit and van Keulen, 1972). The temperatures $T_{s,a}$ and $T_{s,u}$ are now different, of course. The problem is to find an increment of G , denoted as G' , to make $T_{s,a}$ and $T_{s,u}$ about equal to each other, within a tolerable error. Denoting the corresponding soil temperature as T_s^* , the following equation can be obtained:

$$T_s^* = T_{s,a} + (dT_{s,a}/dG)G', \quad T_s^* = T_{s,u} + (dT_{s,u}/dG)G', \quad (5.21)$$

and eliminating T_s^* yields:

$$G' = (T_{s,a} - T_{s,u}) / (dT_{s,u}/dG - dT_{s,a}/dG). \quad (5.22)$$

$dT_{s,u}/dG$ can be found from Eq. (5.20):

$$dT_{s,u}/dG = d_1/k'. \quad (5.23)$$

The value of $dT_{s,a}/dG$ requires more consideration. It can be proven by using Eqs.(5.9), (5.12), (5.13), and (5.14) that $dT_{s,a}/dG$ is approximately:

$$\begin{aligned}dT_{s,a}/dG &= - (\alpha/\rho c_p)(R_t + r_{H,n}) && \text{(for a wet soil surface)} \\ &= - (1/\rho c_p)(R_t + r_{H,n}) && \text{(for a dry soil surface),} \quad (5.24)\end{aligned}$$

where R_t is the turbulent resistance between the reference height and the soil surface. The subsequent estimate of G is then:

$$G^1 = G^0 + G', \quad (5.25)$$

With this method the convergence is very fast. Calculation shows that for a requirement of the relative error in $T_{s,a}$ and $T_{s,u}$ smaller than 1 percent, one iteration is enough for a wet soil surface and three or four for a dry soil surface.

5.2.4 Parameter evaluation

Before the relevant profiles can be calculated, the characteristics of S , R , r_H and r_s have to be determined. Goudriaan's (1977) study is one of the most detailed, so the relevant formulas used in this simulation program are taken mainly from his book. No attempt is made here to explain these formulas, readers being referred to the original book for more detailed information.

Because the present steady-state approach is different from the dynamic approach used by Goudriaan, some changes are necessary. The maximum CO_2 assimilation rate and the dark respiration rate of leaves were given as known functions of leaf temperatures; Goudriaan could obtain these by using previous temperature values, since his model used a small time interval of about one second. In the steady-state approach unnecessary iterations are avoided by replacing the leaf temperatures by the air temperature at the reference height. This leads to only small errors. Moreover, the thermal radiation is assumed to be extinguished exponentially with depth into the canopy, with a coefficient that is different for day and night.

The stomatal resistance, r_s , is defined as the difference between r_v and r_H , the former is the leaf resistance to vapour transfer and composed of the real stomatal resistance, r_s^* , and the boundary-layer resistance to

vapour, $r_{b,V}$. Strictly speaking, $r_{b,V} = 0.93r_H$ (Goudriaan, 1977, Eq.(3.6)), so the relationship between r_s and r_s^* is:

$$r_s = r_V - r_H = r_s^* - 0.07r_H. \quad (5.26)$$

This difference is significant only when the wind speed is low.

5.3 Simulation program

5.3.1 Some remarks

(a) Stability correction

The stability correction of the profiles of wind speed and turbulent resistance is included only above the canopy under stable condition, because calculations show that this is the only case in which this correction is significant. The correction function is the same as that used by Goudriaan, but the Monin-Obukhov length L is taken as the criterion parameter rather than the Richardson number Ri . L is calculated directly from a so-called equivalent heat flux density above the canopy, defined as $C+0.1\gamma\lambda E$. The minimum value of L is set equal to 10^{-3} rather than 10^{-20} as in MICRO-WEATHER. This value is related to the maximum turbulent resistance between the reference height and the top of the canopy. According to Hiramatsu (1984), this value must be carefully chosen, and 10^{-3} is perhaps still too low.

(b) Initialization

There is no need of initialization for steady-state approach, because at any time equilibrium is assumed. But the temperature in the soil is never in equilibrium, integration has to be carried out to trace its variation in time. The temperature profile in the soil must therefore be initialized. This is done also for the heat flux density into the soil surface G , the Monin-Obukhov length L and the water content of the canopy.

(c) Size of the program and the execution time

The program contains about 300 statements, occupying 10K memories. Because the soil temperature profile is simulated, the time step of integration is determined by the thickness of the thinnest soil layer. In this program it is 2 cm, so a time step of 1/8 hour is used. The execution time

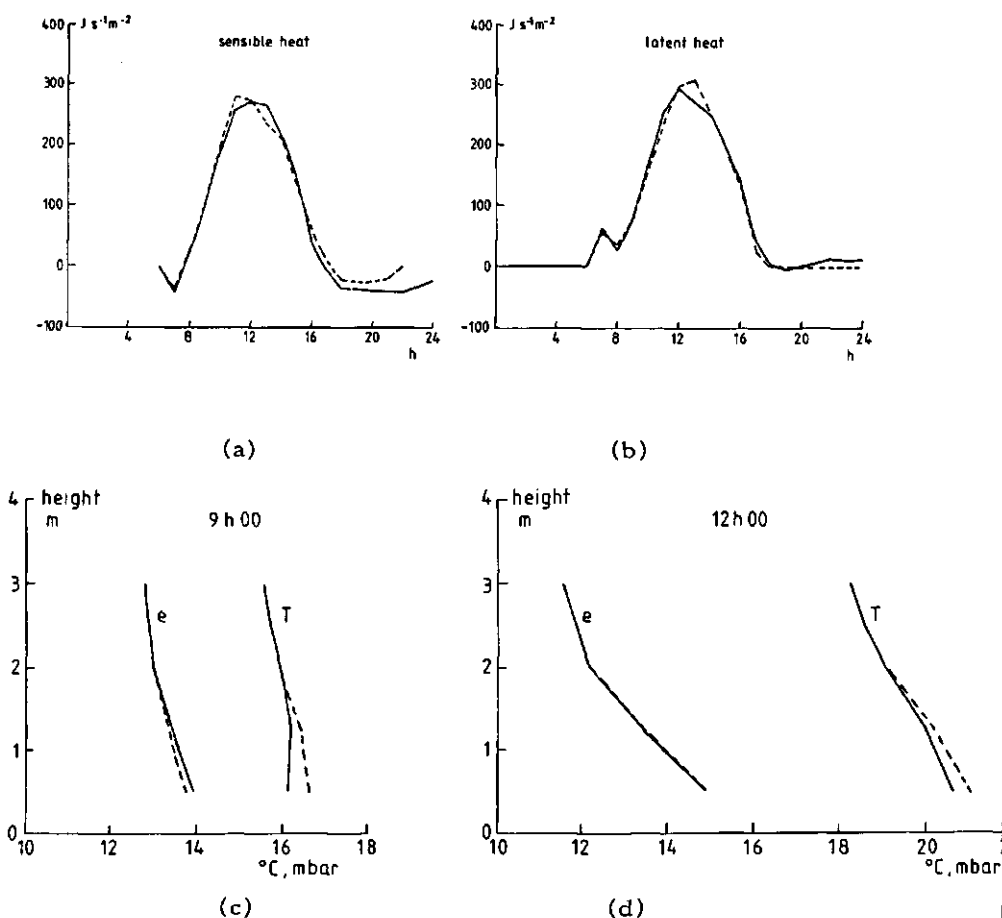


Fig.5.3. Comparison with MICROWEATHER. The solid lines represent the outputs of MICROWEATHER, and the broken lines those of the present program: (a) total sensible heat flux density and (b) total latent heat flux density above the canopy; and temperature (T) and vapour pressure (e) profiles at 9h00 (c) and at 12h00 (d).

for one time step is 6 seconds for night time and 12 seconds for day time (on a microcomputer Apple II), so that it takes about 30 minutes to simulate a day. A list of the program and the symbols used in the program is given in Appendix A-1 and A-2, respectively.

5.3.2 Results

The comparison is made between the outputs of the present program and MICROWEATHER, using the data for a case study. The time course of the simulated total sensible and latent heat flux densities from the two programs are given in Figs.5.3(a) and 5.3(b). The profiles of air temperature and vapour pressure at 9h00 and 12h00 are presented in Figs.5.3(c) and 5.3(d). The agreement is very good, demonstrating the feasibility of the steady-state approach based on the uncoupled electrical analogues for enthalpy and saturation heat.

No attempt is made here to test the model against independent experimental data, this will be left for later work; but MICROWEATHER has been tested for Indian Corn (*Zea mays* L.) by Stigter et al. (1977) and for a rice crop by Hiramatsu et al. (1984). This gives indirect support to the present simulation program.

5.4 Discussion

The uncoupled electrical analogues shown in Figs.5.1(a) and 5.1(b) not only simplify calculations but also provide a clear picture of the transfer of sensible and latent heat between atmosphere and a multi-layer canopy. Enthalpy flux is influenced only by the energy supply, the resistances have no effect. To study the role of the relevant resistances we need only to examine the electrical analogue for saturation heat; this is certainly an advantage. It was shown in Chapter 4 that the relationship between the Bowen ratio β and H and J is:

$$\beta = ((\gamma/\Delta)H + J)/(H - J), \quad (5.27)$$

or, better expressed, as:

$$\beta = (\gamma/\Delta + J/H)/(1 - J/H). \quad (5.28)$$

Eq.(5.28) means that the Bowen ratio is uniquely determined by the ratio J/H . For illustration it will be shown now the influence of the relevant resistances on the total flux density J above the canopy.

(a) Stomatal resistance

From Fig.5.1(b) it can be seen that the stomatal resistance $r_{s,i}$, more precisely $\alpha r_{s,i}$, is a shunt resistance to the current source H_i' . This means the smaller the $r_{s,i}$, the smaller the contribution of the H_i' to the total flux density J will be. Since this contribution is positive (upward) during day time, J will decline as $r_{s,i}$ decreases. The other part of J , caused by the potential source $\rho c_p D_0 / \Delta$ is negative (downward). The absolute value of this part will increase as $r_{s,i}$ decreases, as can be seen from Fig.5.1(b). Therefore when $r_{s,i}$ decreases both parts of J will decrease. We can expect therefore that the stomatal resistance has a strong influence on J/H , and thus on the Bowen ratio.

(b) Surface boundary-layer resistance

Fig.5.1(b) shows that if $r_{s,i}$ is not equal to zero, the contribution of the current source H_i' to J is also influenced by $r_{H,i}$. The smaller the $r_{H,i}$, the larger the fraction of the current source flowing through $r_{H,i}$. This effect is opposite to that of $r_{s,i}$. Since the downward part caused by the potential source will also increase as $r_{H,i}$ decreases, these two effects will partly compensate. We can expect that the influence of the surface boundary-layer resistance will not be as strong as that of the stomatal resistance.

(c) Turbulent resistance

Each layer is separated by a turbulent resistance R_i (Fig.5.1(a)). When R_i decreases, the downward part as well as the upward part of J will increase. Furthermore, R_i is usually smaller than $r_{H,i}$ and is much smaller than $r_{s,i}$. Thus the net effect can be expected to be rather small.

In Fig.5.4(a) is presented the dependence of the ratio J/H and the Bowen ratio β on stomatal, surface boundary-layer and turbulent resistances within the canopy obtained from the simulation model at 9h00. These results confirm those of the qualitative analysis; in particular, the dependence of J/H on the turbulent resistance is remarkably small. This result can be used for obtaining a simplified model in which only the total flux densities above the canopy are of interest.

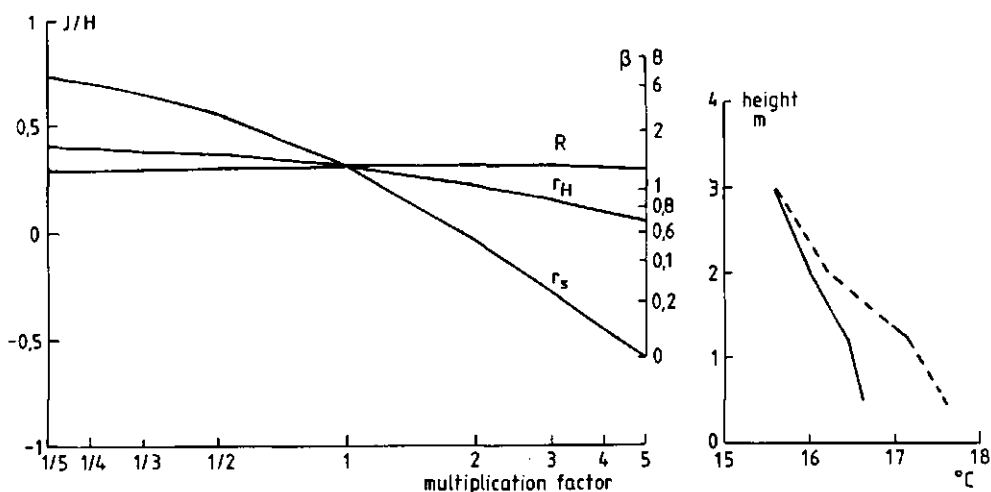


Fig.5.4. (a) Dependence of J/H and the Bowen ratio on the variations of the stomatal resistance r_s , surface boundary-layer resistance r_H and turbulent resistance R within the canopy. The abscissa is the multiplication factor for the resistances. (b) Temperature profile for unchanged (solid line) and doubled turbulent resistance (broken line).

Although the turbulent resistance within the canopy has little effect on the total flux density above the canopy, the profiles of the potentials such as temperature and humidity, and in particular, the amplitudes of variations, are strongly influenced by the value of R_1 . This is because they are determined by the product of the relevant flux density and the turbulent resistance. In Fig.5.4(b) the temperature profiles are given for unchanged and doubled turbulent resistances within the canopy.

The purpose of including the detailed description of the required parameters in this simulation program is to show the ability of a microcomputer to treat the complex crop micrometeorological problems, and also to provide a program for practical use rather than only for illustration. Based on this detailed program some simplification can be made on later development, and the validity of the simplification can be checked by comparing the output from the simplified program with that from this detailed one.

6 A Graphical Extrapolation Method to Determine Canopy Resistance (submitted to Agricultural Meteorology)

Abstract

The profile of vapour pressure in Monteith's extrapolation method is replaced by the profile of dew-point temperature. The canopy resistance can then be obtained directly by a graphical extrapolation method. The effect of choosing different excess resistances on the canopy resistance thus obtained is discussed.

6.1 Introduction

For studying the transfer of sensible and latent heat from a crop canopy, single-layer models are still widely used because of their simplicity. In these models a crop canopy is treated as a surface equivalent to a big leaf at a certain level above the ground. Analogous to the stomatal resistance for a single leaf, Monteith (1963) introduced a bulk resistance r_c , which is often called canopy resistance, and proposed an extrapolation method to obtain the surface values of temperature and vapour pressure. The value of the canopy resistance then can be calculated. Since then, there has been some discussion (Thom, 1972, 1975; Monteith, 1973) about the discrepancy between the locations of the equivalent surfaces for momentum absorption and for the transfer of sensible and latent heat. This discrepancy is due to a so-called excess resistance to the sensible and latent heat transfer (Thom, 1972). The extrapolation method is improved by including the excess resistance, but the canopy resistance is still obtained by calculation rather than by extrapolation itself. The reason is that, in Monteith's extrapolation method humidity is specified by the water vapour pressure e , so that two different abscissas for the vapour pressure e and the temperature T are required; and the horizontal distance between T and e profiles has no physical meaning.

In this Chapter, the water vapour pressure e is replaced by the dew-point temperature T_d , so that one abscissa can be used for both temperature and humidity, the horizontal distance between T and T_d profiles now being proportional to the vapour pressure deficit of the air. Moreover, T and T_d profiles can be further extrapolated downward, so the canopy resistance can be obtained directly from the graph. Based on this

graphical representation, the effect of choosing different values of the excess resistance on the canopy resistance thus obtained can be clearly demonstrated.

6.2 Monteith's extrapolation method

Above a crop canopy the wind speed u , air temperature T and water vapour pressure e are measured at several heights. These profiles are regarded as logarithmic, so they are represented by straight lines in a graph with $\ln(z-d)$ as ordinate. The parameter d is called zero plane displacement.

First, the wind profile is extrapolated downward to intersect the ordinate. The intersection point is $\ln(z_0)$ (Fig.6.1), where z_0 is called roughness length. This level at the height $d+z_0$ is regarded as the location of the equivalent momentum sink of the crop canopy, because wind speed and momentum vanish there. Similarly the profiles of temperature and vapour pressure can be extrapolated to obtain the values of temperature and vapour pressure at some equivalent surface. The problem is: to which height should these profiles be extrapolated?

Monteith (1963) extrapolated these profiles down to the level $\ln(z_0)$, which implies that the location of the equivalent surface for sensible and latent heat sources is assumed the same as that for momentum absorption. The surface values of temperature and vapour pressure thus obtained are denoted by $T(0)_1$ and $e(0)_1$ in Fig.6.1.

There are, however, systematic vertical differences within a crop canopy in the distribution of sources and sinks for heat, water vapour and momentum. It is unlikely that the equivalent surface for sensible and latent heat sources is at the same height as that for momentum. Roughly speaking, compared with the heat and vapour transfer the absorption of momentum is enhanced by pressure forces normal to the leaf surfaces, so the resistance to heat and vapour transfer is higher than that to momentum transfer. The difference between them is called excess resistance, denoted as r_{ex} (Thom, 1972).

According to the aerodynamic method (Monteith, 1973), the turbulent resistance between two levels z_1 and z_2 , r , is:

$$r = (1/k u_*) (\ln(z_2-d) - \ln(z_1-d)), \quad (6.1)$$

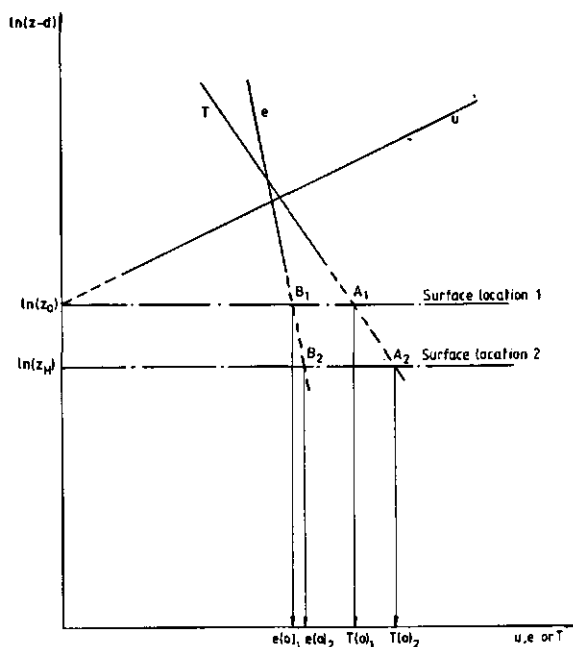


Fig.6.1. Monteith's extrapolation method.

where k is the von Karman's constant, and u_* the friction velocity. The parameters d , z_0 and u_* can be obtained from the wind profile (Thom, 1975). Eq.(6.1) means that, in a graph with $\ln(z-d)$ as ordinate, such as Fig.6.1, the vertical distance in the figure is in fact a measure of turbulent resistances between relevant levels. The fact that heat and vapour experience an excess resistance compared with momentum means that the equivalent surface for heat and water vapour is below that for momentum, say at $\ln(z_H)$ shown in Fig.6.1, $\ln(z_H)$ being determined by, following Eq.(6.1), the value of the excess resistance:

$$\ln(z_0) - \ln(z_H) = k u_* r_{ex}. \quad (6.2)$$

To obtain representative surface values of temperature and vapour pressure, the profiles of temperature and vapour pressure should be extrapolated to the level $\ln(z_H)$ as shown in Fig.6.1. The intersection points A_2 and B_2 represent the surface temperature $T(0)_2$ and vapour pressure $e(0)_2$, respectively.

When $T(0)$ and $e(0)$ are obtained by extrapolation (either as $T(0)_1$ and $e(0)_1$ or as $T(0)_2$ and $e(0)_2$), the canopy resistance is calculated by:

$$r_c = (\rho c_p / \gamma) (e_s(T(0)) - e(0)) / \lambda E, \quad (6.3)$$

where ρc_p is the volumetric heat capacity of air, γ the psychrometric constant and λE the latent heat flux density above the canopy.

6.3 Graphical extrapolation method to determine r_c

Besides the water vapour pressure e the dew-point temperature T_d can also be used to specify the humidity of the air.

The saturated vapour pressure versus temperature curve is more or less exponential in nature, but as a first approximation, a segment of the curve can be replaced by a straight line with a slope Δ , evaluated at a selected temperature T_p . Thus,

$$T - T_d = (e_s(T) - e) / \Delta, \quad (6.4)$$

$$e_s(T) = e_s(T_p) + \Delta(T - T_p), \quad (6.5)$$

and it follows from these two equations that

$$T_d = e / \Delta + \text{const}, \quad (6.6)$$

where the constant is equal to $T_p - e_s(T_p) / \Delta$. Thus, the profile of T_d is also logarithmic. The procedure for obtaining the locations of the equivalent surfaces for momentum and heat, $\ln(z_0)$ and $\ln(z_H)$, and the representative surface value of temperature is the same as in the Monteith's method. For illustration, the surface location 2 in Fig.6.2 is taken as the location for the equivalent surface for heat and vapour. The surface temperature obtained by extrapolation is then determined by the intersection point A_2 as $T(0)_2$. Now extrapolate the profile of dew-point temperature T_d , to intersect the surface location 2. The intersection point is B_2 (Fig.6.2), which gives the surface value of the dew-point temperature $T_d(0)_2$.

The difference between this method and Monteith's method is that the T_d profile can be extrapolated further downward to reach the surface temperature $T(0)_2$. The intersection point is denoted by C_2 , and the level is represented by $\ln(z_s)$. The length of A_2C_2 in the graph is proportional to the canopy resistance, which can be proven as follows.

Because the resistances involved have dimension $s\ m^{-1}$, they can be made dimensionless by multiplying with a velocity. The characteristic velocity scale here is obviously u_* , so that a dimensionless excess resistance r_{ex}^* , which is often denoted as B^{-1} , and a dimensionless canopy resistance r_c^* are defined as:

$$r_{ex}^* = B^{-1} = u_* r_{ex}, \quad (6.7)$$

$$r_c^* = u_* r_c. \quad (6.8)$$

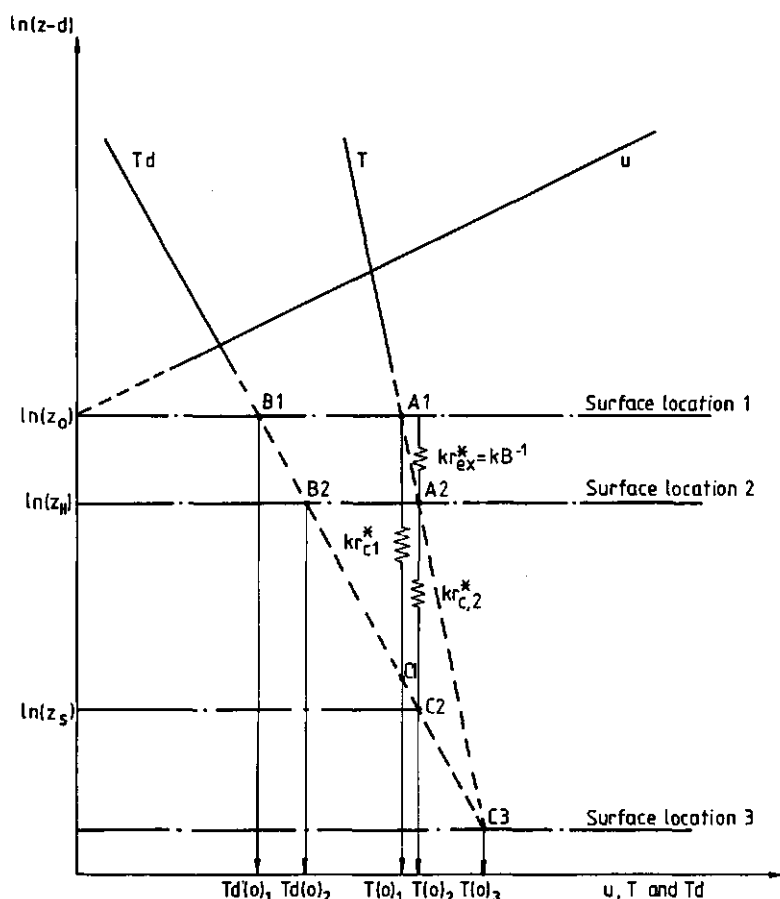


Fig.6.2. Extrapolation method determining canopy resistance graphically.

It follows from Eqs.(6.2) and (6.7) that the distance between the surface locations 1 and 2 equals kB^{-1} , as shown in Fig.6.2.

According to the aerodynamic method, the latent heat flux density is calculated by:

$$\lambda E = -(\rho c_p / \gamma) k u_* (z-d) de/dz = -(\rho c_p / \gamma) k u_* de/d\ln(z-d). \quad (6.9)$$

Eq.(6.9) shows that the latent heat flux density is proportional to the slope of the e line in a coordinate system with $\ln(z-d)$ as ordinate. This slope can be replaced, following Eq.(6.6), by that of T_d line, denoted as s_{Td} . Then Eq.(6.9) can be written as:

$$\lambda E = -k u_* \Delta(\rho c_p / \gamma) s_{Td}. \quad (6.10)$$

The canopy resistance r_c , following Eqs.(6.3), (6.6) and (6.10), is now:

$$r_c = -(1/k u_*) (T(0) - T_d(0)) / s_{Td}. \quad (6.11)$$

From Fig.6.2 it can be seen that $T(0)-T_d(0)$ is the length of B_2A_2 , and $-(T(0)-T_d(0))/s_{Td}$ is the length of A_2C_2 . Hence, it has been proven that the length of A_2C_2 , which is obtained by extrapolation is really proportional to the canopy resistance r_c , or more precisely, it equals kr_c^* , as shown in Fig.6.2.

6.4 The effect of choosing different r_{ex} on r_c

It can be seen from the above presented argument that discarding Monteith's assumption about the coincidence between the equivalent surfaces for heat and momentum introduced an uncertainty about how to choose the appropriate surface location. Although the excess resistance r_{ex} and its dimensionless counterpart B^{-1} were introduced, they cannot be determined a priori, or by the profiles of wind speed, temperature and vapour pressure above the canopy. In fact, B^{-1} is related to distributions of sinks and sources for momentum, heat and water vapour, so that it can only be simulated by a multi-layer model (Chapter 5), or measured experimentally (Chamberlain, 1966). Thom (1972) estimated that B^{-1} is approximately 4 for several crops. This subject will not be discussed here, since the aim is to examine the effect of choosing different values of excess resistance on the value of the canopy resistance obtained by extrapolation. In fact, this

effect can be clearly shown in the graph using the dew-point temperature extrapolation method.

Because the air humidity is specified now by dew-point temperature T_d rather than by vapour pressure e , the same abscissa for both T and T_d can be used. Furthermore, the saturation temperature deficit, $T - T_d$, which is proportional to the water vapour deficit, is immediately visible as the horizontal distance between the two lines for T and T_d .

When the Bowen ratio $(C/\lambda E)$ equals a critical value, λ/Δ the saturation heat flux density $J = C - (\gamma/\Delta) \lambda E$ equals zero. The driving force for J , the gradient of the vapour pressure deficit (Chapter 4) is then also zero. In this case, the T_d line becomes parallel to that of T . It can be clearly seen from Fig.6.2 that the length of A_2C_2 will be independent of the surface location for heat and vapour when T and T_d lines are parallel. In other words, the canopy resistance r_c obtained by extrapolation is independent of the value chosen for the excess resistance, as mentioned by Thom (1975).

When the T_d line deviates from the parallel-to- T -line position to the right, as shown in Fig.6.2, i.e. J is smaller than zero or the evaporation rate is larger than the so-called equilibrium evaporation rate (Priestley and Taylor, 1972), as the chosen value of the excess resistance increases, the value of the canopy resistance declines. The minimum is zero, shown in Fig.6.2 as the surface location 3. This is the location of an equivalent wet surface giving the same sensible and latent heat flux densities as those above the real canopy. When the T_d line deviates to left, increasing the chosen value of the excess resistance, increases the canopy resistance. In this case, equivalent wet surface is not below, but above the measured profiles.

It can also be seen from this approach that the larger the deviation of the Bowen ratio from its critical value, the larger the effect of the different values of the excess resistance on the value of the obtained canopy resistance will be. Only in these cases is it important to know the value of B^{-1} in order to obtain a correct value of the canopy resistance.

6.5 Discussion

The linearization of the saturated vapour pressure curve is an approximation, it is feasible only when the linearized region is not too large. This region is determined by the lowest dew-point temperature of the air and the surface temperature (Chapter 4). In this Chapter the saturation vapour pressure curve in the whole region is replaced by a single straight line with a slope determined at a selected temperature, usually the mid-point temperature in the region. Because the surface temperature is unknown before extrapolation, iteration is needed. A ten-degree temperature difference is acceptable (Chapter 4). When the temperature difference is too large, the temperature interval to be linearized can be split into two parts in order to reduce the error. One represents the region between the lowest dew-point temperature of the air and the dew-point temperature of the surface; the other represents that between the dew-point temperature of the surface and the surface temperature. Then, two slopes Δ_1 and Δ_2 are introduced, evaluated at the mid-point temperatures of these two regions. It can be shown that Eq.(6.11) for the canopy resistance r_c is modified by a multiplication factor Δ_2/Δ_1 , while the essential features of the graph do not change.

7 Canopy Resistance and Excess Resistance Derived from a Multi-Layer Micrometeorological Model

(submitted to Boundary-Layer Meteorology)

Abstract

The equivalent Penman's formulas for enthalpy and saturation heat, unified for single- and multi-layer models (Chapter 4), are used to express the canopy resistance r_c and the excess resistance r_{ex} (or its dimensionless counterpart B^{-1} defined as $r_{ex} u_*$) of a single-layer model in terms of the parameters of a multi-layer model. Some approximation methods are developed to simplify the expressions. It is shown that under the condition of a dense canopy with a dry soil surface, r_c is a good representative of the bulk stomatal resistance of the canopy calculated as all the stomatal resistances of the leaves acting in parallel, and B^{-1} equals $c_1 + c_2 u_*^{1/2}$ with c_1 and c_2 being two constants obtainable from the parameters of the multi-layer model. For a sparse canopy with a wet soil surface, however, these conclusions cannot be drawn. The numerical results for r_c and B^{-1} obtained from a simulation program (Chapter 5) were also given.

7.1 Introduction

Since direct measurement of evapo-transpiration rate in the field is difficult, various estimation methods have been developed during the past three decades, as reviewed by Stewart (1983). A widely used formula is Penman's formula, which is fairly successful in estimating evaporation rate above a free water surface. Penman's formula has also been employed to estimate transpiration rate above vegetation. The canopy-soil surface system, which is essentially not a single source plane, is then treated as a big leaf located at a certain height above the ground. The physiological control of transpiration is characterized by a so-called canopy resistance r_c (Monteith, 1963, 1965); and the location of the leaf was thought initially to be at the same level as the equivalent sink for momentum (Monteith, 1963), but has since been considered to be at a lower level, characterized by a so-called excess resistance r_{ex} (Thom, 1972, 1975).

It was argued (Cowen, 1968; Thom, 1975) that the canopy resistance contains both physiological and aerodynamic components. Measurements on

a range of crops such as barley, sorghum, soybean and sugar beet have shown, however, that the aerodynamic component of the canopy resistance is negligible (Monteith, 1981) and that r_c is close to a the 'bulk stomatal resistance' of a canopy r_{ST} , defined with all the component leaves treated as parallel resistors. Although the theoretical justification for regarding r_c as r_{ST} has been examined (Thom, 1975; Shuttleworth, 1976), a satisfactory explanation is still lacking. The second parameter is the excess resistance, or its dimensionless counterpart B^{-1} defined as $r_{ex} u_*$ in which u_* is the friction velocity. This has been measured using radioactive gases both in a wind tunnel (Chamberlain, 1966), and in the field (Chamberlain and Chadwick, 1965). B^{-1} was found proportional to $u_*^{1/n}$ with n varying between 2 and 3. Chamberlain (1966) and Thom (1972) employed an electrical analogue (essentially a single-layer model for a wet canopy), and derived the formula $B^{-1} = c_2 u_*^{1/2}$, where c_2 is a constant that has to be determined by field experiments. Thom (1972) further argued that if the mean drag coefficient of a canopy is taken as a function of u_* , to account for the so-called shelter effect, B^{-1} should be proportional to $u_*^{1/3}$.

During the past two decades, along with the rapid developments in computer science, sophisticated multi-layer micrometeorological simulation models have been developed. The behaviour of a crop canopy is simulated based on the physical and physiological properties of the canopy components, mainly leaves, which can be measured under controlled conditions in laboratories. Compared with Penman's approach, which is often referred to as single-layer model, the multi-layer model is more realistic, and more easily adaptable to various circumstances.

It can be seen that the two parameters r_c and r_{ex} of the single-layer model can be, in principle, derived from the parameters of the multi-layer model. Unfortunately, however, most of the micrometeorological models are too complicated to yield an analytical solution to the total transpiration rate above the canopy. Although a so-called combination equation for the total latent heat density above a canopy was derived by Shuttleworth (1976, Eq.(56)), it contains unknown temperature and vapour pressure profiles within the canopy in the definitions of the equivalent resistance to heat, r_H , and to vapour, r_v , so that it is not, strictly speaking, a real analytical solution.

In Chapter 4, two uncoupled electrical analogues for enthalpy and saturation heat were developed to replace the coupled one for sensible and

latent heat. Equivalent Penman's formulas were also found, which are applicable to both single- and multi-layer models, so a derivation of r_c and r_{ex} from the multi-layer model can now be given.

7.2 Formulas linking r_c and r_{ex} to the parameters in multi-layer models

In terms of the enthalpy flux density, $H=C+\lambda E$, and saturation heat flux density, $J=C-(\gamma/\Delta)\lambda E$ (where C is the sensible and λE the latent heat flux density, γ the psychrometric constant, and Δ the slope of the vapour saturation curve) Penman's formulas for a single-layer model can also be expressed as (Chapter 4):

$$H = S - G, \quad (7.1)$$

$$J = (\alpha r_s (S-G) - \rho_c D_0 / \Delta) / (R + r_H + \alpha r_s). \quad (7.2)$$

Here, S is the net radiation absorbed by the canopy-soil surface system, G the heat flux density into the soil surface, D_0 the vapour pressure deficit of the air at the reference height, ρ_c the volumetric heat capacity of air, R the turbulent resistance for heat transfer between the reference height and the equivalent surface for heat and vapour, r_H the surface boundary-layer resistance to heat transfer, r_s the difference between the surface resistance to vapour transfer and r_H , and α is defined as $\gamma/(\gamma+\Delta)$. The electrical analogue for J is shown in Fig.7.1(a).

In Monteith's approach, however, r_s is denoted by the canopy resistance r_c , and $R+r_H$ by R_m+r_{ex} , where R_m is the turbulent resistance to momentum transfer between the reference height and the equivalent surface for momentum absorption, which is higher in position than that for heat and vapour. Eq.(7.2) can now be rewritten to include r_c and r_{ex} explicitly:

$$J = (S-G)(\alpha r_c / (R_m + r_{ex} + \alpha r_c)) - (\rho_c D_0 / \Delta) / (R_m + r_{ex} + \alpha r_c). \quad (7.3)$$

The unified Penman's formulas for single- and multi-layer models are (Chapter 4):

$$H = \sum_{j=1}^n H_j = S - G, \quad (7.4)$$

$$J = \sum_{j=1}^n (A_j/A_0) b_j = \sum_{j=1}^n (A_j/A_0) (\alpha r_{s,j} H_j' - \rho c_p D_0 / \Delta) / r_j, \quad (7.5)$$

where H_j' is the enthalpy source from layer j , which is the net radiation absorbed in the layer S_j for the canopy (neglecting the energy consumption in photosynthesis), and $S_n - G$ for the soil surface; $r_{s,j}$ is the stomatal resistance of layer j , n the total number of layers including the soil surface, and r_j and A_j are calculated as:

$$r_j = r_{H,j} + \alpha r_{s,j}, \quad (7.6)$$

$$A_j = A_{j+1} + R_{j+1} \sum_{k=j}^n (A_k / r_k), \quad (7.7)$$

in which R_j is the turbulent resistance between layer $j-1$ and j (the reference height refers to $j=0$), and A_n is defined as unity. The electrical analogue is shown in Fig.7.1(b).

It follows from Eq.(7.1) and (7.4) that the enthalpy flux density for single- and multi-layer models are equal, provided S and G are the same for both models. This is always true if both models refer to the same canopy-soil surface system under the same weather conditions. Thus, to study the relationship between the parameters used in these two models

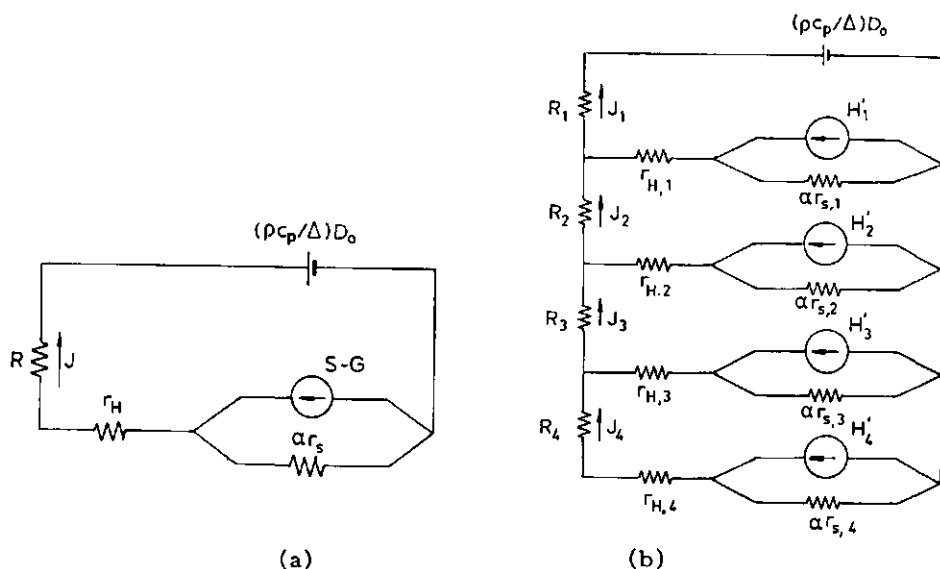


Fig.7.1. Electrical analogues of saturation heat: (a) for a single-layer model; and (b) for a multi-layer model.

only the saturation heat flux density above the canopy needs to be considered.

Defining the fraction of the energy gain in layer j , p_j , as:

$$p_j = H_j' / (S - G), \quad (7.8)$$

Eq.(7.5) can be rewritten as:

$$J = (S-G) \sum_{j=1}^n ((A_j/A_0)(\alpha r_{s,j} p_j / r_j)) - (\rho c_p D_0 / \Delta) \sum_{j=1}^n ((A_j/A_0)(1/r_j)). \quad (7.9)$$

Both Eq.(7.3) and Eq.(7.9) contain two driving forces on the right-hand side: the current source $S-G$ and the potential source $\rho c_p D_0 / \Delta$. As a first approximation, $r_{s,j}$ can be considered independent of D_0 , so if J is to be the same under any values of D_0 for both models, the following two equations should hold:

$$r_c / (R_m + r_{ex} + \alpha r_c) = \sum_{j=1}^n ((A_j/A_0) r_{s,j} p_j / r_j), \quad (7.10)$$

$$1 / (R_m + r_{ex} + \alpha r_c) = \sum_{j=1}^n ((A_j/A_0) / r_j). \quad (7.11)$$

These two equations form the required relationship between the canopy resistance r_c , the excess resistance r_{ex} and the parameters used in the multi-layer models.

7.3 Behaviour of the canopy resistance r_c

Eliminating $R_m + r_{ex} + \alpha r_c$ from Eqs.(7.10) and (7.11) yields:

$$r_c = \sum_{j=1}^n (p_j r_{s,j} A_j / r_j) / \sum_{j=1}^n (A_j / r_j). \quad (7.12)$$

Since the summation in Eq.(7.12) is carried out over all layers including the soil surface, r_c is influenced by both the canopy and the soil surface. Because the behaviours of r_s for the canopy and the soil surface are different, the numerator and the denominator of Eq.(7.12) are better split into two parts related to the canopy and the soil surface, respectively:

$$r_c = \left(\sum_{j=1}^{n-1} (p_j r_{s,j} A_j / r_j) + p_n r_{s,n} / r_n \right) / \left(\sum_{j=1}^{n-1} (A_j / r_j) + 1 / r_n \right), \quad (7.13)$$

where the subscript n refers to the soil surface. The canopy resistance is likely to be a good representation of the bulk stomatal resistance of the canopy only when the influence of the soil surface is rather small, i.e. the second terms in both numerator and denominator should be negligible. For a dry soil surface, the 'stomatal' resistance of the soil surface $r_{s,n}$ is very large, according to Eq.(7.6), $1/r_n$ in the denominator can be neglected, and $r_{s,n}/r_n$ in the numerator approaches unity. If the canopy is dense, the net radiation absorbed by the soil surface S_n is small compared with $S-G$, and of comparable size to G , so p_n is rather small and the second term in the numerator can be neglected. Under these two conditions Eq.(7.13) becomes:

$$r_c = \sum_{j=1}^{n-1} (p_j r_{s,j} A_j / r_j) / \sum_{j=1}^{n-1} (A_j / r_j). \quad (7.14)$$

Now a number of situations will be discussed where r_c is indeed equal to the bulk stomatal resistance r_{ST} .

(a) When there is no water stress, the stomatal resistance of the leaves is approximately inversely proportional to the visible radiation absorbed, the product $p_j r_{s,j}$ is then unlikely to change much from layer to layer. The following equations then hold approximately:

$$p_1 / (1/r_{s,1}) = \dots = p_{n-1} / (1/r_{s,n-1}) = \sum_{j=1}^{n-1} p_j / \sum_{j=1}^{n-1} (1/r_{s,j}) = p_c r_{ST}, \quad (7.15)$$

where r_{ST} is, following the usage of Thom (1975), the bulk stomatal resistance of the canopy, and $p_c = 1 - p_n$. If $p_j r_{s,j}$ in Eq.(7.14) is replaced by $p_c r_{ST}$, this term can be moved out of the summation operation, so Eq.(7.14) becomes:

$$r_c = p_c r_{ST}. \quad (7.16)$$

(b) When there exists a severe water stress, the openings of the stomata are small, $r_{s,j}$ becomes very large compared with $r_{H,j}$ and R_j , so

r_j is approximately equal to $\alpha r_{s,j}$ (Eq.(7.6)) and A_j ($j=1$ to n) approach $A_n=1$ (Eq.(7.7)). In this case Eq.(7.14) becomes:

$$r_c = \left(\sum_{j=1}^{n-1} p_j \right) / \sum_{j=1}^{n-1} (1/r_{s,j}) = p_c r_{ST}. \quad (7.17)$$

(c) When the canopy is completely wet, all $r_{s,j}$'s equal zero, Eq.(7.14) becomes:

$$r_c = 0 = p_c r_{ST}. \quad (7.18)$$

For a dense canopy p_c is about equal to unity, so that in all these cases the canopy resistance r_c is approximately equal to the bulk stomatal resistance of the canopy r_{ST} . This explains the experimental results mentioned above. Furthermore, the analysis also reveals the conditions under which this conclusion can be drawn: a dry soil surface and a dense canopy. The analysis also shows that even under these two conditions, r_c is only approximately equal to r_{ST} . For practical purpose, however, this difference is not important. When the soil surface is wet, particularly under a sparse canopy, the influence of the soil surface can not be neglected. It follows from Eq.(7.13) that r_c then consists of four resistances connected as shown in Fig.7.2:

$$r_c = 1 / (1/(p_c r_{ST}) + 1/r_a) + 1 / (1/(p_n r_{s,n}) + 1/r_b), \quad (7.19)$$

where

$$r_a = \sum_{j=1}^{n-1} (p_j r_{s,j} A_j / r_j) / (1/r_n), \quad (7.20)$$

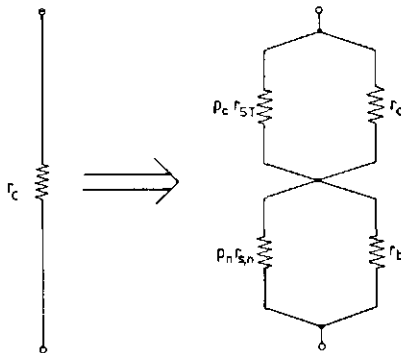


Fig.7.2. Four components of the canopy resistance r_c .

$$r_b = (p_n r_{s,n} / r_n) / \sum_{j=1}^{n-1} (\Lambda_j / r_j). \quad (7.21)$$

If the soil surface is dry, $p_n r_{s,n}$ and r_a are very large compared with r_b and $p_c r_{ST}$, respectively, so these can be neglected, r_c then equals a resistance with $p_c r_{ST}$ and r_b in series. For a dense canopy p_n is about zero, then r_b is negligible, this is the case discussed above ($r_c = r_{ST}$). For a sparse canopy, however, r_b could be large, so r_c may be larger than r_{ST} . If the soil surface is wet, $r_{s,n} = 0$, r_c equals a resistance as with $p_c r_{ST}$ and r_a in parallel, so r_c will always be smaller than r_{ST} , and the sparser the canopy, the more significant the discrepancy will be.

The daily course of r_c (calculated by Eq.(7.12)) and r_{ST} obtained from a simulation program (Chapter 5) using the data for a case study to a maize canopy (Goudriaan, 1977) are shown in Fig.7.3. Fig.7.3(a) is for a dense canopy (LAI=3.73) with a dry soil surface (dotted line) or a wet soil surface (broken line), r_{ST} being given also (solid line). Fig.7.3(b) is for a sparse canopy (LAI=0.5). The salient features discussed above can be seen clearly in the figures.

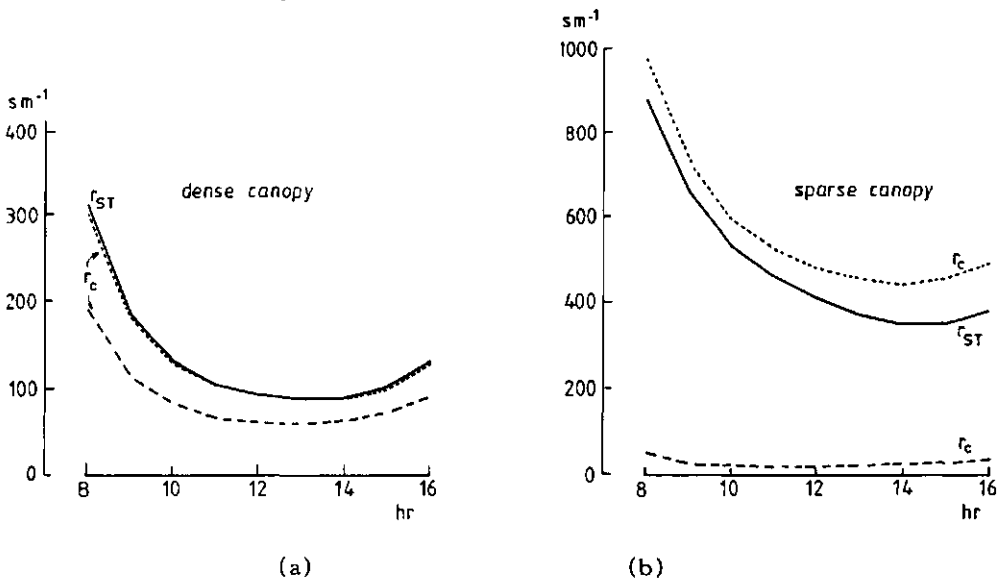


Fig.7.3. Daily course of the canopy resistance r_c and the bulk stomatal resistance r_{ST} obtained from the numerical simulation program. The dotted lines refers to a dry soil surface, and the broken lines to a wet one: (a) for a dense canopy (LAI=3.73), and (b) for a sparse canopy (LAI=0.5)

7.4 Behaviour of the excess resistance r_{ex}

It follows from Eq.(7.11) that

$$r_{ex} = R_g - R_m - \alpha r_c, \quad (7.22)$$

where

$$R_g = 1 / \sum_{j=1}^n ((A_j / A_0) / r_j). \quad (7.23)$$

The physical significance of the resistance R_g can be explained as follows. Let $H_j' (j=1 \text{ to } n)$ in Eq.(7.5) all equal zero, Eq.(7.5) then becomes:

$$J = - (\rho_c D_0 / \Delta) / R_g. \quad (7.24)$$

Since $\rho_c D_0 / \Delta$ is the potential source at the reference height as shown in Fig.7.1(b), and setting $H_j'=0$ is equivalent to removing all the current sources in the figure, the physical meaning of R_g is clearly the actual load resistance seen by the potential source.

The diagram in Fig.7.1(b) after removing all the current sources is shown in Fig.7.4(a). R_g is the resistance seen from the two top terminals

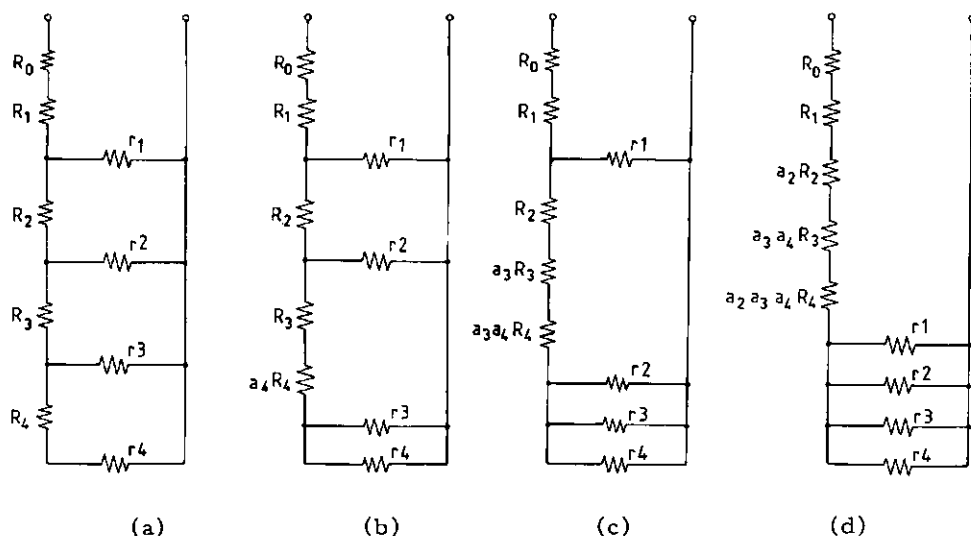


Fig.7.4. Simplification of the resistance scheme shown in Fig.7.1(b) after removing all the current sources.

in the figure. R_1 shown in Fig.7.1(b) has been split into two parts, R_0 and R_1 , the former denotes now the turbulent resistance between the reference height and the top of the canopy, and the latter that between the top and the centre of the first layer. It follows from Eqs.(7.6), (7.7), and (7.23) that R_g depends on R_j , $r_{H,j}$ and $r_{s,j}$ in a complicated way. This can be seen also from Fig.7.4(a), because the resistance scheme contains many networks which are difficult to handle. Therefore, the behaviour of the excess resistance r_{ex} is also complicated. It can be shown, however, that under certain conditions B^{-1} is approximately equal to $c_1 + c_2 u_*^{1/2}$, and the two constants c_1 and c_2 can be determined by the parameters of the multi-layer model. It is required then to obtain a simplified expression for the resistance R_g .

7.4.1 Estimation of R_g

The standard method of transforming a resistance scheme from one type to another does not help here to simplify the scheme shown in Fig.7.4(a). An approximate method must therefore be developed. The idea is to find a simpler resistance scheme without networks to replace the original one. Hence, the diagram in Fig.7.4(a) is transformed into that shown in Fig. 7.4(b). It can be seen that one network consisting of R_4 , r_3 and r_4 is replaced by $a_4 R_4$ in series with r_3 and r_4 , which are now in parallel; a_4 is a parameter. In order to keep R_g unchanged, the resistance of the new system of R_4 , r_3 and r_4 has to be the same as that of the original network, so

$$a_4 R_4 + r_3 r_4 / (r_3 + r_4) = r_3 (r_4 + R_4) / (r_3 + r_4 + R_4), \quad (7.25)$$

from which a_4 can be determined as:

$$a_4 = 1 / ((1 + r_4 / r_3) (1 + r_4 / r_3 + R_4 / r_3)). \quad (7.26)$$

Denoting $g_i = 1/r_i$ ($i=1$ to n), under the condition of R_4 being much smaller than r_3 , a_4 can be approximated as:

$$a_4 = g_4^2 / (g_3 + g_4)^2. \quad (7.27a)$$

By transforming the resistance scheme further to that shown in Fig. 7.4(c), and in Fig.7.4(d), the parameters a_3 and a_2 are introduced and determined by:

$$a_3 = (g_3 + g_4)^2 / (g_2 + g_3 + g_4)^2 \quad (\text{when } R_3 + a_4 R_4 < r_2) \quad (7.27b)$$

$$a_2 = (g_2 + g_3 + g_4)^2 / (g_1 + g_2 + g_3 + g_4)^2 \quad (\text{when } R_2 + a_3 R_3 + a_3 a_4 R_4 < r_1) \quad (7.27c)$$

and a_1 is defined as unity. By defining

$$q_1 = a_1 = 1 = G_1^2 / G_1^2, \quad q_2 = a_1 a_2 = G_2^2 / G_1^2, \quad (7.28a)$$

$$q_3 = a_1 a_2 a_3 = G_3^2 / G_1^2, \quad q_4 = a_1 a_2 a_3 a_4 = G_4^2 / G_1^2, \quad (7.28b)$$

where

$$G_i = \sum_{j=1}^n g_j \quad (i=1 \text{ to } n, \text{ and } n=4 \text{ here}), \quad (7.29)$$

R_g can be expressed as:

$$R_g = R_0 + R_a + 1/G_1, \text{ with} \quad (7.30)$$

$$R_a = \sum_{j=1}^n q_j R_j. \quad (7.31)$$

The physical meaning of the three components of R_g (Eq.(7.30)) must be explained. It can be seen from Fig.7.4(a) that if the turbulent resistances within the canopy are neglected by setting all R_j 's ($j=1$ to n) equal to zero, all r_j 's will be connected with each other in parallel resulting in a resistance $1/G_1$ (the third component of R_g), and R_g then equals $R_0 + 1/G_1$. When the R_j 's are not equal to zero, but are small compared with r_j 's, their contribution to R_g can be approximated by R_a , which is a weighted sum of the R_j 's.

The resistance scheme shown in Fig.7.4(d) appears similar to that used by Thom (1975, p.65), but he obtained his scheme by assuming ad arbitrium that the turbulent resistance must be calculated from the reference height to a certain level within the canopy: he did not explain why his scheme should replace the more realistic one shown in Fig.7.4(a). In contrast, the resistance scheme shown in Fig.7.4(d) is obtained through analysis, so the way how to calculate the resistance R_a is also determined (Eq.(7.31)).

As n tends to infinity, g_j , G_j , q_j , and R_j in Eqs.(7.27) through (7.31) become continuous functions of height z : $g(z)$, $G(z)$, $q(z)$, and $dz/K_H(z)$, where $K_H(z)$ is the turbulent exchange coefficient for heat transfer within

the canopy. Eq.(7.28) becomes $q(z)=G(z)^2/G(z_c)^2$, where z_c is the crop height. Eqs.(7.29) and (7.31) become an integration of, respectively, $g(z)dz$ and $(q(z)/K_H(z))dz$ from $z=0$ to z_c . Assuming that both $K_H(z)$ and $g(z)$ are independent of the height z and neglecting the influence of the soil surface, $q(z)$ becomes $(z/z_c)^2$ according to Eqs.(7.27) and (7.28), $K_H(z)$ becomes $K_H(z_c)$, and R_a can be found by integration:

$$R_a = (1/3)R_p. \quad (7.32)$$

Here, R_p is the total turbulent resistance between the top and the bottom of the canopy for the constant $K_H(z)$ profile:

$$R_p = z_c/K_H(z_c) = ((z_c/k)/(z_c-d))u_*^{-1}. \quad (7.33)$$

where k is the von Karman's constant, d the zero plane displacement, and u_* the friction velocity.

7.4.2 Behaviour of r_{ex} and B^{-1} for a wet canopy

In reality both $K_H(z)$ and $g(z)$ are functions of height z . The latter depends on the profiles of the surface boundary-layer resistance as well as on the stomatal resistance (Eq.(7.6)). For a wet canopy, however, the stomatal resistances are all zero: $g(z)$, R_g , and r_{ex} are determined merely by the aerodynamic resistances. In order to obtain an explicit expression of r_{ex} in terms of u_* , the profiles of the turbulent exchange coefficient and wind velocity within a canopy are needed.

There are two types of theoretical $K_H(z)$ profiles within a canopy: either constant and exponential. Because the turbulent resistance within the canopy has little effect on the total flux densities above the canopy (Chapter 5), the constant $K_H(z)$ profile is preferred here. Based on the assumption of a constant $K_H(z)$ profile, an analytical expression for the wind velocity within the canopy was derived by Landsberg and James (1971):

$$u(z) = u(z_c)(1 + m(1-z/z_c))^{-2}, \quad (7.34)$$

where $u(z_c)$ is the wind velocity at the top of the canopy, and m is the parameter determined by:

$$m = (1/k)(c_d z_c^{-1} \ln((z_c-d)/z_0)/(6(z_c-d)))^{1/2}. \quad (7.35)$$

Here, c_d is the mean drag coefficient of the leaves, l_c the leaf area index of the whole canopy, and z_0 the roughness length. The leaf and soil surface boundary-layer resistance $r_H(z)$ (per leaf area) and $r_{H,n}$ can be calculated as (Goudriaan, 1977):

$$r_H(z) = 90(w_L/u(z))^{1/2}, \quad (7.36)$$

$$r_{H,n} = 180(w_s/u(0))^{1/2} = 180(1+m)(kw_s/\ln((z_c-d)/z_0))^{1/2}u_*^{-1/2}, \quad (7.37)$$

where w_L is the mean leaf width, and w_s the mean diameter of the soil clods. For a wet canopy with a uniform leaf area density profile, the second component of R_g (Eq.(7.30)) defined by Eq.(7.31) can be obtained from Eqs.(7.29), (7.34) through (7.37) after some manipulations:

$$R_a = c'R_p, \text{ with} \quad (7.38a)$$

$$c' = (2+2b+2b^2 - (\ln^2(1+m)+2(1+b)\ln(1+m))/m) / (\ln(1+m)+b)^2, \text{ and} \quad (7.38b)$$

$$b = (90m/l_c)(w_L/u(z_c))^{1/2}/r_n. \quad (7.38c)$$

For a dry soil surface, b becomes zero, and as m tends to zero, wind velocity, and consequently $g(z)$, become constant within the canopy, c' tends to $1/3$ according to Eq.(7.38b). This is consistent with the result obtained above.

The third component of R_g (Eq.(7.30)), $1/G_i$, for a wet canopy is $r_{H,n}$ in parallel with r_{HT} , which is called, similar to r_{ST} , the bulk leaf surface boundary-layer resistance of the canopy (calculated with all the corresponding components acting in parallel). This resistance can be obtained in the same way as for R_a :

$$\begin{aligned} r_{HT} = 1/G(z_c) &= (90m/l_c)(w_L/u(z_c))^{1/2}/\ln(1+m) \\ &= (90m/(l_c \ln(1+m)))(kw_L/\ln((z_c-d)/z_0))^{1/2}u_*^{-1/2}, \end{aligned} \quad (7.39)$$

then Eq.(7.30) can be rewritten as:

$$R_g = R_0 + c'R_p + r_{HT}r_{H,n}/(r_{HT}+r_{H,n}). \quad (7.40)$$

From Eqs.(7.22) and (7.40), r_{ex} for a dense and wet canopy ($r_c=0$), with a wet soil surface can be obtained:

$$r_{ex} = R_0 + c'R_p - R_m + r_{HT}r_{H,n}/(r_{HT}+r_{H,n}). \quad (7.41)$$

The resistances R_0 and R_m can be determined by the aerodynamic method (Monteith, 1973):

$$R_0 = (0.74 \ln((z_r - d)/(z_c - d)) / k) u_*^{-1} \quad (7.42)$$

$$R_m = (\ln((z_r - d)/z_0) / k) u_*^{-1} \quad (7.43)$$

where z_r is the reference height. Examining the terms on the right-hand side of Eq.(7.41) shows that the first three terms, R_0 , $c'R_c$, and R_m are proportional to u_*^{-1} , and the last term is proportional to $u_*^{-1/2}$, so that the relationship between r_{ex} , B^{-1} , and u_* can be written as:

$$r_{ex} = c_1 u_*^{-1} + c_2 u_*^{-1/2}, \quad (7.44)$$

$$B^{-1} = c_1 + c_2 u_*^{1/2} \quad (7.45)$$

(c_1 and c_2 are two constants, the expression for c_1 can be found from Eqs.(7.42), (7.43), (7.38), and (7.33) and that for c_2 from Eqs.(7.37) and (7.39)). Therefore, c_1 and c_2 can be determined by the parameters used in the multi-layer model.

The dependence of B^{-1} on u_* for a wet canopy with a wet soil surface was also obtained by means of the numerical simulation program. The results are shown in Fig.7.5 marked by dots or crosses, together with the straight lines given by Eq.(7.45) for a dense canopy (LAI=3.73) and for a sparse canopy (LAI=0.5). The overestimation by Eq.(7.45) is caused by neglecting the terms such as R_4/r_3 in Eq.(7.26), but this error is small. It confirms the approximate method for estimating R_g developed in subsection 7.2.3(a).

The square root of u_* in Eq.(7.45) is related to the assumption that the drag coefficient c_d is independent of u_* . Thom (1972) pointed out that because of the shelter effect, c_d is proportional to $u_*^{-1/2}$, and then B^{-1} is proportional to $u_*^{1/3}$. This subject will not be discussed here.

7.4.3 Behaviour of r_{ex} and B^{-1} for a dry canopy

When the canopy is not wet, the stomatal resistance has to be taken into account. Eq.(7.41) now becomes:

$$r_{ex} = R_0 + c'R_p - R_m + 1/G_1 - \alpha r_c. \quad (7.46)$$

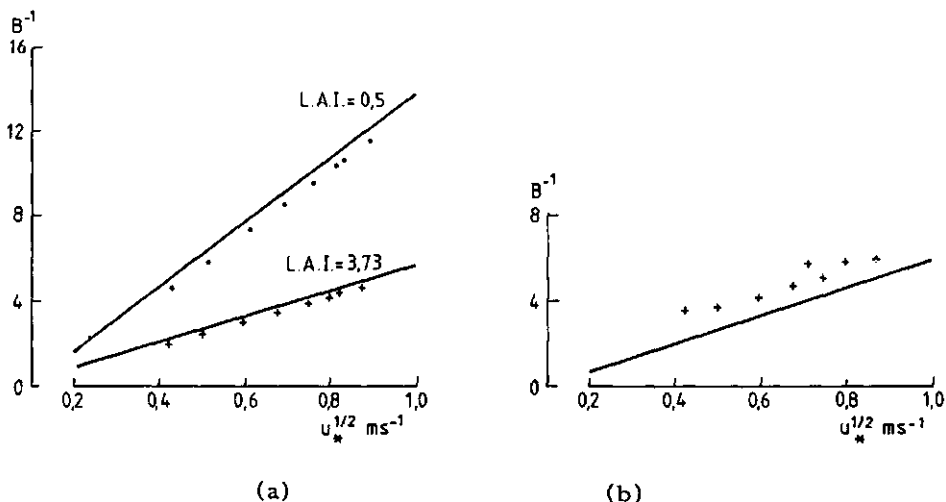


Fig.7.5. The relationship between B^{-1} and $u_*^{1/2}$ obtained from the numerical simulation programs is compared with the approximate analytical expressions (solid lines): (a) for a wet canopy with a wet soil surface; and (b) for a dry canopy with a dry soil surface.

As previously mentioned, because of Eq.(7.6), $g(z)$ now depends not only on the profile of the surface boundary-layer resistance $r_H(z)$, but also on that of the stomatal resistance $r_s(z)$. Thus, c' also depends on this. G_1 in Eq.(7.46) is composed of the contribution from the soil surface ($1/r_n$) and that from the canopy (the sum of $1/r_j$, $j=1$ to $n-1$). In reality, both $r_H(z)$ and $r_s(z)$ increase with the depth into the canopy, but usually at different rates. As a first approximation, the contribution of the canopy to G_1 can be estimated by the bulk leaf boundary-layer resistance r_{HT} and the bulk stomatal resistance r_{ST} of the canopy. $1/G_1$ is then:

$$1/G_1 = 1/(r_{HT} + \alpha r_{ST}) + 1/r_n. \quad (7.47)$$

For a dry soil surface, the second term can be neglected. Eq.(7.47) will be exactly true if $r_H(z)$ and $r_s(z)$ increase at identical rates.

In the same spirit, the profile of the weighting factor $q(z)$ (Eq.(7.28)) can still be approximated solely by $r_H(z)$, so Eqs.(7.38b and c) can still be used to estimate c' . Eq.(7.46) can then be written as:

$$r_{ex} = R_0 + c'R_p - R_m + r_{HT} + \alpha r_{ST} - \alpha r_c. \quad (7.48)$$

For a dense canopy with a dry soil surface, r_c is approximately equal to r_{ST} , so the last two terms in the right-hand side of Eq.(7.48) can be ignored. Eq.(7.48) is then equivalent to Eq.(7.41); thus, Eqs.(7.44) and (7.45) for r_{ex} and B^{-1} are still approximately valid.

In Fig.7.5(b) the result from the numerical simulation model is shown for a dense canopy with a dry soil surface (marked as crosses), together with the straight line from Eq.(7.45). It can be seen that they are still in fair agreement with each other, although not as good as in the case of a wet canopy shown in Fig.7.5(a).

When the canopy is sparse and the soil surface is wet, r_c is different from r_{ST} as discussed in Subsection 7.2.2, the last two terms in Eq.(7.48) do not cancel against each other, so the situation becomes complicated. No analytical expressions could be found for c_1 and c_2 .

The parameters used in the simulation program (Chapter 5) are typical for a maize stand. Fig.7.5(b) shows that the value of B^{-1} is around 4, which is consistent with the value suggested by Thom (1972) based mainly on experiments in the fields.

7.5 Discussion

The two important Eqs.(7.10) and (7.11), linking r_c and r_{ex} of the single-layer model with the parameters of the multi-layer model, were obtained under the assumption that the stomatal resistance is independent of the vapour pressure deficit at the reference height. There is, however, some evidence that the stomatal resistance does depend on the vapour pressure deficit. In this case, mathematically speaking, only one equation can be obtained by equalizing J' for both models, and r_c and r_{ex} cannot be derived separately. From the physical point of view, however, Eq.(7.11) means that the actual load resistance in contact with the potential source $\rho c_p D_0 / \Delta$ is identical for both single- and multi-layer models. The physical meaning of Eq.(7.10) is that the contribution of the current source S-G to J in both models is the same. Therefore, these two equations are still physically sound, and can thus be used in practice.

It has been shown in the present paper that both the canopy resistance r_c and the excess resistance r_{ex} contain physiological and aerodynamic components. Under the condition of a dense canopy with a dry soil surface,

however, r_c contains only, approximately, the physiological part, and r_{ex} the aerodynamic part. This result is striking, it justifies the applicability of the single-layer model under the condition stated above.

The separation of the physiological and aerodynamical parts is not possible for a sparse canopy with a wet soil surface. Since the influence of the soil surface cannot then be neglected, the single-layer model is no longer plausible. It is likely that a double-layer model - one layer representing the canopy and the other representing the soil surface - will give better results. By using a double-layer model, it will be possible to 'extract' the bulk stomatal resistance of the canopy from the value of the canopy resistance obtained from aerodynamic measurements above the canopy.

8 General discussion and suggestions

Mathematical analysis has long been used and is well developed in physics and engineering, but in agricultural science its application has been much limited, because of the complexity of the natural systems in agriculture. Various factors interact with each other so it is difficult to formulate a simple mathematical description and to find analytical solutions to these equations. At the beginning, therefore, only much simplified mathematical models were used. The emergence of high-speed computers and the rapid development in the software enable modellers to construct more realistic simulation models. More and more factors are taken into account, and more and more parameters are introduced, with the consequence that the complexity of the simulation model grows beyond the immediate grasp of the human mind. Simulation models may then become counterproductive because they block further communication between scientists. Therefore further theoretical research to find simplifying relationships on a higher level of understanding remains necessary, even though simulation models are available.

This study shows that it is possible to find simpler relationships for highly complex, multi-parameter systems which not only deepen the understanding, but also result in much more efficient and lucid computer algorithms. The vector-matrix representation of the radiation and its interaction with a crop canopy used in Chapters 2 and 3, made the equations for radiation transfer more lucid and resulted in a clearer picture about the physical process of the transfer of the radiation in crop canopies. Under the vector-matrix notation, the meaning of the reciprocity relation became clearer: it is equivalent to the symmetry of the matrix representing the interaction of the radiation with the whole canopy. The radiation-path approach developed in Chapter 2 further deepened the understanding of the reciprocity relation: it is closely related to the reversibility of the radiation paths. The differential equations developed in Chapter 3 simplified the mathematical expression of directional transfer of the radiation in crop canopies; they turned out to be in the same form as the simple Kubelka-Munk equations, only the scalar being replaced by corresponding vectors and matrices. This development encouraged to find the analytical solutions to the profiles of the radiation intensities from all directions. The computation of the reflectance pattern of various crop canopies is thus

greatly simplified, which resulted in a computer algorithm to account for the azimuthal variations of the reflectance. The introduction of the enthalpy and saturation heat in Chapter 4 provided a new look to the old problems of the sensible and latent heat transfer. Formerly, the sensible and latent heat flux densities were treated separately and described by separate equations, as they are driven by different driving forces and experience different resistances. To satisfy the energy balance, however, the sum of the sensible and latent heat must be equal to the net radiation absorbed. This causes the transfer processes of the sensible and latent heat to depend on each other. The advantage of using instead enthalpy and saturation heat flux, is that they can be independently calculated. The enthalpy flux density is the sum of the sensible and latent heat flux densities, driven by the net radiation absorbed; and the saturation heat flux density is the weighted sum of the sensible and latent heat flux densities, driven by the gradient of the vapour pressure deficit. The stomatal resistances of leaves have no influence on the enthalpy but only on the saturation heat. Based on this approach the computation of the profiles of temperature and humidity is simplified to such an extent that a crop micrometeorological simulation program executable on microcomputers could be written.

Because the time which was available to complete this dissertation is limited, the applications of the improvements to the crop micrometeorological modelling have not been fully worked out. The Kubelka-Munk equations in vector-matrix forms established in Chapter 3 can account for the azimuthal variations of reflectance. The analytical and approximate solutions for the canopy bidirectional reflectance provide a means to calculate the reflectance pattern of various crop canopies with an acceptable execution time. Moreover, the possibility of calculating the azimuthal distribution of radiation enables to discard the assumption of the Lambertian property of the leaves and to use the measured data of bidirectional reflectance and transmittance of the single leaves. It is desirable to quantify the effects of the non-Lambertian property of the leaves and the azimuthal variations. Several data sets of bidirectional canopy reflectance for soybean, corn and wheat have been assembled by the Laboratory for Remote Sensing at the Purdue University, West-Lafayette, Indiana, U.S.A. These data sets may then be used to determine to what extent the observations can be

explained by including the non-Lambertian property of the leaves and the azimuthal variations. This topic is definitely of interest for current research.

The simulation program in BASIC, executable on microcomputers developed in Chapter 5 is a generalized one for all kinds of crops. In particular, it can be applied to short grass, where Goudriaan's (1977) simulation model MICROWEATHER has difficulties with the small time coefficient. The program could also be further developed to simulate the evapo-transpiration from a partly wet canopy after a rainfall by treating the wet leaves as having zero stomatal resistances. The simulation model in BASIC can be also incorporated into a pest development and plant disease model to simulate the profile of the leaf wetness, which is important to the development of some pests and plant diseases. Moreover, with the decreasing price of microcomputers, it is becoming more and more common to equip measuring instruments in the field with a microcomputer. The program in BASIC provides the required software to treat the data instantaneously. Then, the simulated transpiration rate, for instance, can be obtained immediately and used in optimization of irrigation.

If only the total sensible and latent heat flux densities above a canopy are required, the multi-layer model for the sensible and latent heat transfer can be simplified to contain only two layers, one represents the whole canopy and the other represents the soil surface. The computation is then much easier. This version of the simulation program of crop micrometeorology can be included in a crop growth model such as BACROS (de Wit et al., 1978). It is likely to simplify the crop growth model to such an extent that it can also be executed on a microcomputer. It would then be possible to monitor the crop growth in the field, and thus to acquire information for control operations.

Because of the complexity of the atmosphere-vegetation-soil system, simplifications must be made in simulation of the transfer of energy momentum and mass in this system. One of the most frequently adopted simplifying assumptions is horizontal homogeneity. This assumption reduces a three-dimensional transfer problem to an one-dimensional problem: only vertical variations of the variables such as radiation intensity, wind velocity ect. are studied. In practice, the vegetation is seldom horizontally homogeneous, because crops are often planted in rows; and the soil is often horizontal heterogeneous. Including this horizontal heterogeneity,

however, makes the mathematical analysis so complicated, that it is worthy to do it only for a few special cases. In most cases, the assumption of the horizontal homogeneity works fairly well, so this assumption is adopted throughout the dissertation. Therefore, the transfer model studied in this dissertation is essentially one-dimensional. At transitions in surface properties such as roughness, crop resistances, albedo, etc., advection may be important. In this case, a two-dimensional model is needed. If measurements are done directly above the crop surface, the micrometeorological model can be used for small fields. Clearly, the influence of adjacent fields increases when measurements are done at higher altitudes. Then considerable problems of extrapolation remain when only standard meteorological data from a weather station are available. There is still a major gap between crop micrometeorology and the planetary boundary-layer meteorology, concerning horizontal area scales of hundreds of square kilometers, and vertical scales up to 100 meters.

This study confirms the validity of the concept of canopy resistance, and shows that it can be derived as the parallel circuiting of stomatal resistances for most practical purposes. Therefore the importance of the behaviour of stomatal resistance and its linkage with other processes such as photosynthesis, senescence, rooting is underlined. Further progress in understanding crop growth, and in optimization of the use of limited resources such as water and nutrients, will require an integration of more plant physiological knowledge in existing simulation models. Also the development of new concepts in this area is needed to straighten out and unify the vast but incoherent knowledge in the fields of environmental crop physiology.

Appendix

A-1 List of the program (executable on an Apple II)

```

1  REM CROP MICROMETEOROLOGY SIMULATION ON MICROCOMPUTERS (CMSM)
3  REM SPHERICAL LEAF ANGLE DISTRIBUTION IS ASSUMED
5  REM ABBREVIATIONS. G:GOUDRIAAN J.(1977),CROP MICROMETEOROLOGY.
6  REM P:PENNING DE VRIES F.W.T.& VAN LAAR H.H.(1982),
7  REM SIMULATION OF PLANT GROWTH AND CROP PRODUCTION.
8  REM C:PRESENT PAPER OF CHEN.
9  REM THE NUMBER FOLLOWED IS THE EQUATION INDEX.
20 DIM Z6(11),D6(11),T6(11),M4(13),S4(13),X(20),Y(20)
36 N=4:M=5:L=10:Z6(1)=0.02:REM STRATIFICATION
37 D6(1)=Z6(1)/2:FOR I=2 TO L+1:Z6(I)=1.2*Z6(I-1)
38 D6(I)=(Z6(I-1)+Z6(I))/2:NEXT:REM STRATIFICATION

39 REM INPUT KNOWN OR MEASURED DATA
40 READ P1,K5,G1,A1,A8,A9,L5,I3
44 DATA 3.1415926,0.41,0.67,1240,2.2672E-7,10.8E6,2.5E9,0.5
90 FOR I=1 TO 9:READ K1(I):NEXT:REM G:2.34
94 DATA 5.737,1.932,1.183,0.872,0.707,0.610,0.552,0.518,0.502
100 FOR I=1 TO 9:READ B1(I):NEXT:REM G:P.9,BU(1-9)
110 DATA 0.030,0.087,0.133,0.163,0.174,0.163,0.133,0.087,0.030
120 FOR I=1 TO 9:READ Q8(I):NEXT:REM P:P.105,(32)
124 DATA 0.90,0.54,0.38,0.29,0.25,0.22,0.20,0.19,0.18
126 FOR I=1 TO 9:READ Q9(I):NEXT:REM P:P.105,(32)
128 DATA 0.68,0.32,0.21,0.16,0.13,0.12,0.11,0.10,0.10
130 FOR I=0 TO M:READ Q1(I):NEXT
134 DATA 0,0.1,0.3,0.5,0.7,0.9
140 READ D3,L0,Z2:DATA 270,45,3:REM EXPERIMENT SPECIFICATION
150 READ W6,L6,V6,W7:DATA 0.05,1.3,2E6,-0.1:REM SOIL DATA
154 READ Z1,L1,W1,C0,S8,S9,E2,O2,R7,G6,R8:REM PLANT DATA
156 DATA 2.5,3.73,0.05,0.3,0.2,0.85,17.2E-9,120,2E3,3.5E-8,1E7
158 FOR I=0 TO 7:READ T3(I),W3(I):NEXT:REM G:P.87,FIG.17
160 DATA 0.5,-50,0.7,-17,0.8,-14,0.84,-12.5,0.88,-10,0.9,-8.1,1,0,1.5,40.5
162 FOR I=0 TO 5:READ T5(I),C5(I):NEXT:REM G:P.87,FIG.18
164 DATA 0,0.08,10,0.08,20,0.29,30,0.94,37,1,48,0.87
166 FOR I=0 TO 5:READ V6(I),R6(I):NEXT:REM G:P.87,FIG.17
168 DATA 0.5,1E4,0.6,3E3,0.7,800,0.8,600,0.9,130,1.5,130
170 FOR I=0 TO 5:READ T2(I),F2(I):NEXT:REM G:P.76,FIG.16
174 DATA 0,0,10,0,20,1.39E-6,25,1.67E-6,35,1.67E-6,40,0.56E-6
176 REM PARABOLIC LAI PROFILE IS ASSUMED FOR N=4 AS FOLLOWS:
177 Z(1)=0.387*Z1:Z(3)=Z(1):Z(2)=Z1-2*Z(1)
178 O1=330:A(N)=1:N1=N-1:E9=L1/N1
194 FOR I=1 TO L+1:READ T6(I):NEXT:REM INITIALIZATION
196 DATA 12.2,12.9,13.6,14.3,15,15.5,15.7,15.7,15.4,15.2,15.2

198 A2=A1/G1:L0=L0*P1/180:B6=D6(1)/L6
200 X=-0.13*P1*COS(P1*(D3+10)/182.5):REM G:2.106
204 S1=SIN(L0)*SIN(X):C1=COS(L0)*COS(X)
224 A7=1.83E-6*(O1-O2)/1.66:REM G:3.10
270 L3=SQR(4*W1*Z1/P1/L1)*I3:REM G:4.45
280 C4=SQR(CO*L1*Z1/2/L3):REM G:4.49
284 D0=Z1-SQR(L3*Z1/C4)/K5:X=Z1-D0:REM G:4.61
286 Y=Z2-D0:Z0=X*EXP(-Z1/C4/X):REM G:4.62

```



```

288 A4=LOG(X/Z0):A5=LOG(Y/Z0):A6=0.37/L3
290 V8=SQR(1-S8):V9=SQR(1-S9):REM G:2.20
294 X3=0:FOR I=1 TO 9:X3=X3+B1(I)*EXP(-K1(I)*L1)
296 NEXT K7=-LOG(X3)/L1
300 X1=V8:GOSUB 1010
330 K8=K9:FOR I=0 TO 9:P8(I)=P9(I):NEXT
350 X1=V9:GOSUB 1010:GOTO 1200
1000 REM SUBROUTINE EXTIN.& REFL.COEFF. OF DIFFUSE RADIATION
1010 X2=(1-X1)/(1+X1):REM G:2.21
1030 X=0:Y1=0.0353:Y2=0.94623*X1:FOR I=1 TO 9
1040 Y=Y1+Y2*K1(I):X=X+B1(I)*EXP(-Y*L1):NEXT
1060 K9=-LOG(X)/L1:REM G:2.41
1090 P9(0)=0:X=-0.0111544:Y=1.117:FOR I=1 TO 9
1100 X4=1-EXP(-2*X2*K1(I)/(1+K1(I))):REM G:2.45
1110 P9(I)=X+Y*X4:REM G:2.46
1130 P9(0)=P9(0)+B1(I)*P9(I):NEXT
1160 RETURN

1190 REM INPUT OBSERVED WEATHER DATA
1200 FOR I=0 TO 13:READ M4(I),S4(I):NEXT
1202 DATA 0,-40,6,-30,6.5,0,8.5,105,9.8,400,11.2,660,12.1,690,13.2,630,14.1,530
      15.1,380,16.1,200,17.1,14,18.1,-84,24,-40
1210 FOR I=0 TO 6:READ M7(I),T7(I):NEXT
1212 DATA 0,13.5,6,12.9,10,16.5,14,20,16,20.6,18,14.1,24,13.5
1220 FOR I=0 TO 5:READ M8(I),E8(I):NEXT
1222 DATA 0,13,6,12,8.5,13,13,11.2,18,15,24,13
1230 FOR I=0 TO 6:READ M9(I),U9(I):NEXT
1232 DATA 0,0.7,8,0.7,9,2,11,3,16,1,17,0.7,24,0.7
1240 R3(N)=0:N3=1

1280 D4=1/8:M4=D4*3600
1300 FOR D2=1 TO 1:REM ENDS 5574
1302 PRINT "DAY=";D2:PRINT
1306 C7=0:E7=0:F7=0
1307 L4=0.01:G=-30:W2=0.975:W0=2.5E-3*L1*W2
1308 FOR I=1 TO N1:D5(I)=0:W(I)=0:NEXT
1310 FOR M2=0 TO 24 STEP D4:REM ENDS 5540
1330 X=M2:FOR I=0 TO 13:X(I)=M4(I):Y(I)=S4(I):NEXT
1334 GOSUB 1370:S=Y
1340 FOR I=0 TO 6:X(I)=M7(I):Y(I)=T7(I):NEXT
1344 GOSUB 1370:T(0)=Y
1350 FOR I=0 TO 5:X(I)=M8(I):Y(I)=E8(I):NEXT
1354 GOSUB 1370:E0(0)=Y
1360 FOR I=0 TO 6:X(I)=M9(I):Y(I)=U9(I):NEXT
1364 GOSUB 1370:U(0)=Y:GOTO 1400
1370 REM SUBROUTINE INTERPOLATION
1372 IF X=0 THEN Y=Y(0):GOTO 1380
1374 FOR I=0 TO 20:IF X(I)>=X THEN K=I-1:GOTO 1378
1376 NEXT I
1378 Y=Y(K)+(Y(I)-Y(K))/(X(I)-X(K))*(X-X(K))
1380 RETURN
1400 X1=T(0)+239
1404 X2=6.11*EXP(17.4*T(0)/X1):REM G:3.21
1410 D1=X2*4158.6/X1/X1
1414 A0=G1/(G1+D1):B0=1-A0:REM C:(5)
1416 A3=A1/D1:D(0)=X2-E0(0):V0=A3*D(0)
1420 GOSUB 5600:REM AERODYNAMICS

```

```

1428 REM RADIATION REGIME, RS(I) AND B(I). UP TO L.5440.
1430 X1=T(0)+273.2:X2=1.2*T(0)-21:REM G:2.67
1434 Y2=T(0)-2:Y3=Y2+273.2:X3=X2+273.2
1440 X4=(X1+X3)/2:Y4=(X1+Y3)/2
1450 B2=A8*X4*X4*X4*(X1-X3):REM G:2.66
1460 B3=A8*Y4*Y4*Y4*(X1-Y3)
1470 R5=0.167E-6*EXP(0.07*(T(0)-30))
2000 H0=S1+C1*COS(P1*(M2+12)/12):REM G:2.107
2001 IF H0<1E-10 GOTO 5400:REM NIGHT
2002 X0=ATN(H0/SQR(1-H0*H0))*180/P1

2003 REM INTERPOLATION FOR SUN HEIGHT DEPENDENT PARAMETERS
2004 IF X0<=5 THEN X=1:H0=0.5/K1(1):GOTO 2018
2005 IF X0>=85 THEN X=9:H0=0.5/K1(9):GOTO 2018
2008 X=INT((X0+5)/10):X1=X+1
2009 Y1=(X0-X*10+5)/10:Y=1-Y1
2011 Q8=Q8(X)*Y+Q8(X1)*Y1:Q9=Q9(X)*Y+Q9(X1)*Y1
2013 P8=P8(X)*Y+P8(X1)*Y1:P9=P9(X)*Y+P9(X1)*Y1
2016 GOTO 2040
2018 Q8=Q8(X):Q9=Q9(X):P8=P8(X):P9=P9(X)

2040 REM FRACTION OVERCAST AND INCOMING RADIATION
2050 X1=1280*H0*EXP(-0.15/H0):REM P:P.103,(24)
2060 Y1=X1/5:K1=0.5/H0
2100 X2=Q8*P8(0)+(1-Q8)*P8:Y2=B2
2110 X3=Q9*P9(0)+(1-Q9)*P9:Y3=B3
2120 X4=1-(X2+X3)/2:Y4=1-0.6*P8(0)-0.4*P9(0)
2130 IF N3=0 THEN Y2=0:Y3=0:X4=1:Y4=1
2140 F3=(X4*X1-S-Y2)/(X4*X1-Y2-Y4*Y1+Y3)
2144 IF F3<0 THEN F3=0:X1=(S+Y2)/X4
2146 IF F3>1 THEN F3=1:Y1=(S+Y3)/Y4
2150 S6=X1*(1-F3)/2:S7=Y1*F3:X=0.0353:Y=0.94623
2160 K3=X+Y*V8*K1:K4=X+Y*V9*K1:REM G:2.42
2180 V4=S6*(1-Q8):V5=S6*Q8+S7*0.6
2190 N4=S6*(1-Q9):N5=S6*Q9+S7*0.4
2200 X7=V4*(1-P8):X8=V5*(1-P8(0)):V2=V4*(1-S8)
2210 Y7=N4*(1-P9):Y8=N5*(1-P9(0)):N2=N4*(1-S9)
2220 Y9=B2*(1-F3)+B3*F3

2350 X1=1:X2=1:X3=1:X4=1:X5=1:X6=1
2390 FOR I=1 TO N1:X0=E9*I
2400 Y1=EXP(-K3*X0):Y2=EXP(-K4*X0):REM G:3.36
2900 Y3=EXP(-K8*X0):Y4=EXP(-K9*X0):REM G:3.35
3000 Y5=EXP(-K7*X0):Y6=EXP(-K1*X0):REM G:3.37
3050 X9=X6-Y6:P(I)=X9/E9/K1:REM G:3.38
3060 X=X7*(X1-Y1)+X8*(X3-Y3)
3070 Y=Y7*(X2-Y2)+Y8*(X4-Y4)-Y9*(X5-Y5)
3080 V3(I)=(X-V2*X9)/E9:REM G:3.40
3090 S3(I)=(Y-N2*X9)/E9+V3(I):H(I)=X+Y
3110 X1=Y1:X2=Y2:X3=Y3:X4=Y4:X5=Y5:X6=Y6:NEXT I
3130 H9=X7*Y1+Y7*Y2+X8*Y3+Y8*Y4-Y9*Y5
3810 X=W2:FOR I=0 TO 5:X(I)=V6(I):Y(I)=R6(I):NEXT I
3814 GOSUB 1370:R6=Y
3870 X=T(0):FOR I=0 TO 5:X(I)=T2(I):Y(I)=F2(I):NEXT I
3874 GOSUB 1370:F5=Y+R5:E3=E2/Y
3940 V2=V2/H0:S2=V2+N2/H0

```

```

4070 FO=0:FOR I=1 TO N1:L2(0)=E9*(1-P(I))
4072 X=E9*P(I)/M:FOR K=1 TO M:L2(K)=X:NEXT
4120 X7=0:X8=0:X9=0:Y7=0:X=W(I):Y3=V3(I):Y4=S3(I)
4130 Y5=R3(I):Y2=1/Y5:Y8=R2(I)
4140 YO=1/(R6+Y5):Y9=1/(R7+Y5):Y1=0.795*Y8
4150 FOR K=0 TO M:Y=Q1(K):X1=Y3+Y*V2:REM G:3.34
4164 Y6=F5*(1-EXP(-X1*E3))-R5:REM G:3.8
4166 IF X<0 THEN X2=Y2:GOTO 4190
4170 IF Y6<=0 THEN X2=Y9:GOTO 4190
4180 X2=1/(A7/Y6-Y8):REM G:3.10&C:(32)
4184 IF X2>Y0 THEN X2=Y0:Y6=A7/(R6+Y1):REM G:3.9
4190 X5=L2(K):X9=X9+X2*X5:Y7=Y7+Y6*X5
4210 X6=(Y8+A0/X2)/X5:REM C:9
4214 X3=Y4+Y*S2-A9*Y6:REM C:(23)
4220 X7=X7+1/X6:REM C:(22)
4230 X8=X8+X3/X2/X6:NEXT K:REM C:(21)&(23)
4270 R3(I)=E9/X9:R4(I)=1/X7:REM C:(22)
4274 B(I)=A0*X8-V0*X7:REM C:(21)&(23)
4280 H(I)=H(I)-A9*Y7:FO=FO+Y7:NEXT I
4290 GOTO 5438
5400 FO=-R5*L1:IF N3=0 THEN S=-B3
5404 X1=1:FOR I=1 TO N1:Y1=EXP(-0.2*E9*I)
5408 H(I)=S*(X1-Y1)+A9*R5*E9:X1=Y1
5410 IF W(I)=0 THEN R3(I)=R7+R3(I):REM C:25B
5430 R4(I)=(R2(I)+A0*R3(I))/E9
5434 B(I)=(A0*H(I)*R3(I)/E9-V0)/R4(I):NEXT
5436 H9=S*X1

5438 K=0:B5=(A0+(1-A0)*R3(N)/1E9)/A1*(R9+R2(N))
5439 REM ITERATION FOR G(ENDS 5478)
5440 H(N)=H9-G:B(N)=(A0*R3(N)*H(N)-V0)/R4(N)
5450 GOSUB 6000
5472 K=K+1:X=T6(0)-T6(1)-B6*G:REM C:24&27
5474 Y=X/(B6+B5):IF ABS(X/T6(0))<0.01 GOTO 5479
5476 IF K>6 THEN PRINT "G=";G,"DG=";Y:GOTO 5479
5478 G=G+Y:GOTO 5440:REM C:(31)

5479 GOSUB 6400:IF M2-INT(M2)>0 GOTO 5530
5490 PRINT "WEATHER CONDITIONS AT TIME=";M2;" "
5492 PRINT "INCOM.RED.", "TEMPERATURE", "V.PRESSURE", "WIND"
5493 PRINT S,T(0),EO(0),U(0):PRINT
5495 PRINT "MON.LENGTH", "TUR.RES.R(0)", "U STAR", "PHO.RATE"
5496 PRINT L4,R(0),U0,F0:PRINT
5498 PRINT "TOT.ENTH.", "TOT.SA.HEAT", "TOT.SE.HEAT", "TOT.LA.HEAT"
5499 PRINT H,J,C,E:PRINT
5502 PRINT "SOIL NET RAD.", "G", "SOIL-SUR.TEMP.", "REL.CAN.W.C."
5503 PRINT H9,G,T6(0),W2:PRINT
5520 IF M2/3-INT(M2/3)<1E-5 THEN GOSUB 7000
5524 PRINT :PRINT "*****":PRINT
5530 C7=C7+C:E7=E7+E:F7=F7+F0
5540 NEXT M2
5550 C7=C7*M4:E7=E7*M4:F7=F7*M4
5551 PRINT "DAILY TOTALS"
5552 PRINT "SEN.HEAT", "LAT.HEAT", "WATER LOSS", "CO2 ASSIMIL."
5554 PRINT C7,E7,E7/L5,F7:PRINT:PRINT "DEW"
5556 FOR I=1 TO N1:PRINT D5(I)/L5:NEXT:PRINT

```

```

5570 PRINT "*****";PRINT
5574 NEXT D2
5580 END
5590 STOP

```

```

5600 REM SUBROUTINE AERODYNAMICS
5660 X=A5:X9=A4:Y=0.74*(A5-A4):IF L4<0 GOTO 5680
5664 X0=Z0/L4:X1=(Z1-D0)/L4:X2=(Z2-D0)/L4
5670 X=X+4.7*(X2-X0):REM G:4.33
5674 X9=X9+4.7*(X1-X0):Y=Y+4.7*(X2-X1)
5680 U0=K5*U(0)/X:REM G:4.33
5810 U(1)=U0/K5*X9:R(0)=Y/K5/U0:REM G:4.29
5840 X=Z(1):FOR I=2 TO N:U(I)=U(1)*EXP(-C4*X/Z1):X=X+Z(I):NEXT
5850 FOR I=2 TO N1:R(I)=A6*(Z(I-1)+Z(I))/U(I):NEXT
5870 R(1)=R(0)+A6*Z(1)/U(1):R(N)=A6*Z(N1)/U(N)
5890 R9=0:FOR I=1 TO N1:R9=R9+R(I)
5910 R2(I)=92.5*SQR(W1*2/(U(I)+U(I+1))):REM G:3.2
5920 R3(I)=-0.07*R2(I):NEXT:R9=R9+R(N)
5930 R2(N)=185*SQR(W6/U(N)):R4(N)=R2(N)+A0*R3(N)
5990 RETURN

```

```

6000 REM SUBROUTINE FLUXES, J SOURCES, AIR & SOIL TEMPERATURE
6010 X=0:H=0:J=0:FOR I=N TO 1 STEP -1
6030 X=X+A(I)/R4(I):A(I-1)=A(I)+R(I)*X:REM C:(8)
6050 J=J+B(I)*A(I):H=H+H(I):NEXT
6080 J=J/A(0):REM C:(7)
6090 C=A0*H+B0*J:E=B0*(H-J):REM C:(3)&(4)
6110 C2=C+0.1*G1*E:REM G:4.1
6120 L4=-27.85*A1*U0*U0*U0/K5/C2:REM G:4.19
6124 IF L4<1E-3 AND L4>0 THEN L4=1E-3
6210 X=H:Y=J:X3=0:FOR I=1 TO N:X3=X3+R(I)*Y
6220 X4=B(I)-X3/R4(I):J(I)=X4:REM C:(12)
6230 X1=A0*X+B0*Y:REM C:(14)
6240 T(I)=T(I-1)+X1*R(I)/A1:REM C:(17)
6250 X=X-H(I):Y=Y-X4:NEXT
6260 T6(0)=T(N)+X1*R2(N)/A1
6290 RETURN

```

```

6400 REM SUBROUTINE DEW AND SOIL TEMPERATURE INTEGRATION
6410 FOR I=1 TO N:X=B0*(H(I)-J(I)):REM C:(15)
6420 Y=X*M4:W(I)=W(I)+Y:IF W(I)>0 THEN W(I)=0
6430 IF X<0 THEN D5(I)=D5(I)-Y
6440 E(I)=X:NEXT I
6610 Y1=G:FOR I=1 TO L:X6=Z6(I)*V6
6620 Y2=(T6(I)-T6(I+1))*L6/D6(I+1)
6630 Y3=Y1-Y2:T6(I)=T6(I)+Y3*M4/X6:Y1=Y2
6640 NEXT:T6(L+1)=T6(L)
6644 W2=W0/L1/2.5E-3:IF E<0 GOTO 6800
6650 X=(T6(3)+T6(4)+T6(5))/3:FOR I=0 TO 5:X(I)=T5(I)
6654 Y(I)=C5(I):NEXT:GOSUB 1370:X5=1/Y/G6
6690 X=W2:FOR I=0 TO 7:X(I)=T3(I):Y(I)=W3(I):NEXT I
6694 GOSUB 1370:W0=W0+M4*((W7-Y)/(R8+X5)-E/L5)
6800 RETURN

```

```

7000 REM SUBROUTINE PROFILE PRINT
7130 PRINT "H SOURCE","J SOURCE","C SOURCE","E SOURCE"
7140 FOR I=1 TO N:C(I)=A0*H(I)+B0*J(I)
7150 PRINT H(I),J(I),C(I),E(I):NEXT:PRINT
7170 PRINT "TEMPERATURE","VAPOR PRESSURE","VPD","WIND VELOCITY"
7180 X=E:Y=J:FOR I=1 TO N
7190 E0(I)=E0(I-1)+X*R(I)/A2:X=X-E(I):REM C:(18)
7200 D(I)=D(I-1)+Y*R(I)/A3:Y=Y-J(I):REM C:(16)
7240 PRINT T(I)-T(0),E0(I)-E0(0),D(I)-D(0),U(I):NEXT:PRINT
7300 PRINT "SOIL TEMP.","LEAF TEMP.","DEW","WETNESS"
7310 X=E9*A1:FOR I=1 TO N1
7320 T1(I)=T(I)+C(I)*R2(I)/X:REM C:(19)
7330 PRINT T6(I),T1(I),D5(I),W(I):NEXT
7340 FOR I=N TO L:PRINT T6(I):NEXT:PRINT
7342 PRINT "TUR.RES.","BOUN.RES.","STOM.RES.","LAYER RES."
7344 FOR I=1 TO N:PRINT R(I),R2(I),R3(I),R4(I):NEXT:PRINT
7360 RETURN

```

A-2 List of the symbols in the program

(the superscript c denotes constant, i input, and o output. Symbols in MICROWEATHER are also included in the second column.)

Symbols in program	Symbols in text	Description	Dimension
A(0 to N)	A_i	determinants	-
A0	α_i	$G1/(G1+D1)$	-
c A1	ρ_c, RHOC	volumetric heat capacity of air	$J m^{-3} K^{-1}$
A2	$\rho_c p/\gamma$	$A1/G1$	$J m^{-3} mbar^{-1}$
A3	$\rho_c p/\Delta$	$A1/D1$	$J m^{-3} mbar^{-1}$
c A4	p	$LOG((Z1-D0)/Z0)$	-
c A5		$LOG((Z2-D0)/Z0)$	-
A6		$0.74/2/L3$	m^{-1}
A7		$1.82E-6*(O1-O2)/1.66$	-
A8		four times Stefan-Boltzman constant	$J m^{-2} s^{-1} K^{-4}$
c A9		10.8E6	$J (kgCO_2)^{-1}$
B(1 to N)	BI	coefficients for calculating J_i	$J m^{-2} s^{-1}$
B0		$1-A0$	-
c B1(1 to 9)	BU	zonal distribution of overcast sky radiation	-
B2	LWRCI	longwave radiation loss of the canopy under a clear sky	$J m^{-2} s^{-1}$
B3	LWROI	longwave radiation loss of the canopy under an overcast sky	$J m^{-2} s^{-1}$
B5		$(A0/A1)*(R9+R2(n))$	-
B6		$D6(1)/L6$	-
o C	SHFL1	sensible heat flux above the canopy	$J m^{-2} s^{-1}$
o C(1 to N)	C_i	sensible heat source	$J m^{-2} s^{-1}$
i C0	DRAG	mean drag coefficient of leaves	-
C1	CCOS	intermediate variable	-
C2		equivalent heat flux: $C+0.1*G1*E$	$J m^{-2} s^{-1}$
i C4	ALPHAK	extinction coefficient for wind	-
i C5(1 to 5)	TREDTE	known reduction factor for root conductance	-
o C7		daily total of sensible heat loss	$J m^{-2}$
D(0 to N)	D_i	vapour pressure deficit profile	mbar
D0	D_i	zero plane displacement	m
D1	SLOPE	slope of saturated vapour pressure versus temperature curve	$mbar K^{-1}$
i D2		loop index variable	-
i D3	DAY	number of the day in the year reckoned from 1 January	-
i D4		time step	hr
o D5(1 to N-1)		daily total of dew	mmH2O
D6(1 to L)	DIST	distance between the adjacent soil layers	m
o E	LHFL1	latent heat flux above the canopy	$J m^{-2} s^{-1}$
o E(1 to N)	λE_i	latent heat source	$J m^{-2} s^{-1}$
i E0(0)	e_0	vapour pressure at reference height	mbar
o E0(1 to N)	e_i	vapour pressure profile	mbar
c E2	EFF	slope of photosynthesis-light	$kgCO_2 J^{-1}$

		response curve at compensation point	
o	E3	intermediate variable	-
i	E7	daily total of latent heat loss	$J m^{-2}$
	E8(1 to 5)	VPATB for input vapour pressure	mbar
	E9	DL leaf area index per layer	-
i	F0	canopy CO_2 assimilation rate	$kgCO_2 m^{-2} s^{-1}$
	F2(0 to 5)	AMTB maximum net CO_2 -assimilation rate at given temperatures	$kgCO_2 m^{-2} s^{-1}$
o	F3	FOV assumed fraction overcast	-
	F7	daily total of CO_2 assimilation	$kgCO_2 m^{-2}$
i	G	G heat flux density into soil surface	$J m^{-2} s^{-1}$
c	G1	PSCH psychrometric constant	$mbar K^{-1}$
	G6	SCRS maximal root conductance	$m^{-1} H_2O m^{-1} s^{-1} bar^{-1}$
o	H	enthalpy flux above the canopy	$J m^{-2} s^{-1}$
o	H(1 to N)	H_i' enthalpy flux source	$J m^{-2} s^{-1}$
	H0	SNHSS sine of the sun elevation	-
i	I	loop index variable	-
	I3	i_w, IW turbulent intensity in the canopy	-
o	J	saturation heat flux above the canopy	$J m^{-2} s^{-1}$
o	J(1 to N)	J_i' saturation heat source	$J m^{-2} s^{-1}$
c	K	loop index variable	-
	K1(1 to 9)	KB extinction coefficient for direct radiation and black leaves with a spherical leaf angle distribution	-
	K1	as above but for sun height h	-
	K3	KDV extinction coefficient for visible sun radiation at sun height h	-
	k4	KDN the same as K3 but for near-infrared sun radiation	-
	K5	KARMAN von Karman's constant	-
	K7	KBDF extinction coefficient for thermal radiation	-
	K8	KDFV extinction coefficient for visible diffuse radiation	-
	K9	KDFN extinction coefficient for near-infrared diffuse radiation	-
i	L	total number of soil layers	-
i	L0	LAT latitude	degrees
i	L1	LAI total leaf area index of canopy	$m^2 m^{-2}$
	L2(0)	shaded leaf area index in layer i	$m^2 m^{-2}$
	L2(1 to M)	sunlit leaf area index in layer i for each group	$m^2 m^{-2}$
	L3	turbulent intensity times mixing length within the canopy	m
c	L4	MONOBL Monin-Obukhov length	m
	L5	LHVAP latent heat for water vaporization	$J (m^3 H_2O)^{-1}$
i	L6	$k', LAMBDA$ thermal conductivity of the soil	$J m^{-1} s^{-2}$
c	M	total number of groups of sunlit leaves	-

ⁱ	M2	HOUR	local time in hours	hr
	M4		time step in seconds	s
	M4(0 to 13)		for input radiation data	hr
	M7(0 to 6)		for input temperature data	hr
	M8(0 to 5)		for input vapour pressure data	hr
	M9(0 to 6)		for input wind speed data	hr
^c	N	n, NUML1	total number of layers	-
	N1	NUMLL	N-1	-
	N2		N4*(1-S9)	J m ⁻² s ⁻¹
	N3		N3=0, input radiation is global, and N3=1, net radiation	
	N4		incoming near-infrared sun radiation	J m ⁻² s ⁻¹
	N5		incoming near-infrared diffuse radiation	J m ⁻² s ⁻¹
^c	O1	ECO2C	averaged external CO ₂ concentration	vpm
ⁱ	O2	RCO2I	assumed regulatory internal CO ₂ concentration	vpm
	P(1 to N-1)		profile of the fraction of sunlit leaves	-
^c	P1	π	ratio of the circumference of a circle to its diameter	-
	P8(0)	RFOVV	reflection coefficient of the canopy to visible sky radiation	-
	P8(1 to 9)	RFV	reflection coefficient of the canopy to visible sun radiation	-
	P8		as above but for sun height h	-
	P9(0)	RFOVN	reflection coefficient of the canopy to near-infrared sky radiation	-
	P9(1 to 9)	RFN	reflection coefficient of the canopy to near-infrared sun radiation	-
	P9		as above but for sun height h	-
^c	Q1(1 to m)		discretized cosine of the incident angles	-
^c	Q8(1 to 9)		fraction diffuse in visible radiation	-
	Q8		as above but for sun height h	-
^c	Q9(1 to 9)		fraction diffuse in near-infrared radiation	-
	Q9		as above but for sun height h	-
	R(0)	ABTURR	turbulent resistance between the reference height and crop top	s m ⁻¹
	R(1 to N)	R _i	profiles of turbulent resistance	s m ⁻¹
	R2(1 to N)	r _{H,i}	profile of leaf boundary layer resistance per leaf area	s m ⁻¹
^o	R3(1 to N-1)	r _{s,i}	profile of stomatal resistance per leaf area	s m ⁻¹
ⁱ	R3(N)	RESS	"stomatal" resistance of the soil surface	s m ⁻¹
	R4(1 to N)	r _i	profile of layer resistance	s m ⁻¹
	R5		dark respiration rate of leaves	kgCO ₂ m ⁻² s ⁻¹
	R6		actual value of the resistance	s m ⁻¹

		checked by water status	
ⁱ	R6(1 to 5)	SRWTB	known R6 values
ⁱ	R7	RESCW	leaf cuticular resistance
ⁱ	R8	WRESPL	xylem resistance to water flow
	R9	R _t	total turbulent resistance
ⁱ	S	NRADM	recorded incoming radiation
	S1	SSIN	intermediate variable
	S2		(V4*(1-S8)+N4*(1-S9))/H0
	S3(1 to N)		profile of absorbed net radiation
			per leaf area
ⁱ	S4(1 to 13)	NRADTB	input radiation data
	S6		derived incoming direct radiation
	S7		derived incoming diffuse radiation
	S8	SCV	scattering coefficient of leaves
			to visible radiation
	S9	SCN	scattering coefficient of leaves
			to near-infrared radiation
ⁱ	T(0)	T ₀	air temperature at reference height
^o	T(1 to N)	T ₀	air temperature profile
^o	T1(1 to N)	T ₁ ⁱ	leaf temperature profile
ⁱ	T2(1 to 5)		for known F2(1 to 5) data
ⁱ	T3(1 to 7)		for known W3(1 to 7) data
ⁱ	T5(1 to 5)		for known C5(1 to 5) data
^o	T6(1 to 1+1)	TEMP	soil temperature profile
ⁱ	T7(1 to 6)	TATB	input temperature data
ⁱ	U(0)		wind velocity at reference height
^o	U(1 to N)		wind profile within the canopy
	U0	USTAR	friction velocity
ⁱ	U9(1 to 6)	WINDRB	for input wind speed data
	V0		A3*D(0)
	V2		V4*(1-S8) or V4*(1-S8)/H0
	V3(1 to N)		profile of absorbed visible diffuse
			radiation per leaf area
	V4		incoming visible sun radiation
	V5		incoming visible diffuse radiation
ⁱ	V6	VHCAP	soil volumetric heat capacity
	V6(1 to 5)		for known R6(1 to 5) data
	V8	SQV	square of (1-S8)
	V9	SQNI	square of (1-S9)
	W(1 to N-1)		leaf wetness
	W0	WCCP	canopy water content
ⁱ	W1	WIDTH	mean width of leaves
	W2	RWCP	canopy relative water content
ⁱ	W3(1 to 7)	WSTTB	known canopy water potential
ⁱ	W6	HRES	mean diameter of soil clods
ⁱ	W7	WSTSL	soil water potential
	X, X0 to X9		intermediate variable
	Y, Y0 to Y9		intermediate variable
ⁱ	Z(1 to N-1)	DIK	canopy layer thickness
ⁱ	Z0	ZNOT	roughness length
ⁱ	Z1	CROPHT	crop height

ⁱ	Z2	REFHT	reference height	m
ⁱ	Z6(1 to L)	TCOM	thickness of the soil layers	m

Summary

In crop micrometeorology the transfer of radiation, momentum, heat and mass to or from a crop canopy is studied. Simulation models for these processes do exist but are not easy to handle because of their complexity and the long computing time they need. Moreover, up to now such models can only be run on mainframe computers. This study aims at developing a more elegant mathematical analysis that both deepens the understanding of the processes involved, and enables the writing of more efficient computer programs.

To model the radiation regime, Goudriaan (1977) divided the crop canopy into several layers. The radiation at each layer was classified into downward and upward flux densities, assigned to nine contiguous zones in a hemisphere. Then a set of equations was derived for these radiation components and an efficient iteration method was developed to solve them. The solutions gave a detailed description of the distribution of the radiation in a canopy, from which the zonal reflectance from a canopy can also be obtained. In addition, by computer experimentation a so-called reciprocity relation was found between a direct light source and the reflected radiance from vegetation. This relation has potential applications in remote sensing techniques. Remaining problems are: (a) the computation of the radiation profiles in a canopy needs much execution time; (b) azimuthal variations of bidirectional reflectance from a canopy cannot be simulated; and (c) the mathematical proof of the reciprocity relation was not found.

In Chapters 2 and 3, the downward and upward radiation from all directions in a hemisphere are represented by radiation vectors and the interactions of the radiation with a horizontally homogeneous canopy layer are represented by reflectance and transmittance matrices. In Chapter 2, the physical process of the reflection and transmission of radiation by a multi-layer canopy is examined under vector-matrix notation. The radiation vector incident upon the top of a canopy, may be directly reflected from the first layer forming a component of the reflected radiation vector from the top of the canopy; or it may, for instance, be transmitted through the first layer, reflected from the second layer, and transmitted again through the first layer, forming another component of the reflected radiation vector. Not every reflection-transmission series, called a radiation path, results in a component of the reflected radiation vector but there is an

infinite number of such paths. It is proven in Chapter 2 that the reciprocity relation holds if each radiation path contributing to the reflection vector can be reversed and also result in a component of the reflected radiation vector. It is shown that this reversibility of the radiation paths is generally true for reflection whereas for transmission a vertically uniform canopy and a black soil surface are required.

In Chapter 3, the radiation equations are rewritten as a set of difference equations with vectors as variables and matrices as coefficients. Then two differential equations for downward and upward radiation vectors are derived, where the coefficients are interception, backward and forward scattering matrices, which are the three basic matrices characterizing the interactions of a horizontally homogeneous canopy with radiation vectors. These two differential equations are, in fact, the vector-matrix version of the Kubelka-Munk equations, which are two scalar differential equations for total downward and upward radiation intensities in a canopy with horizontal Lambertian leaves. The extended Kubelka-Munk equations can describe the directional transfer of radiation in a canopy with non-Lambertian leaves and any leaf inclination distribution. This is more realistic than Suits' (1972) model containing, principally, only vertical and horizontal leaves. The azimuthal variations are included by extending the corresponding vectors and matrices. The analytical solutions for profiles of the downward and upward radiation vectors are found by means of a standard matrix method and also the bidirectional reflectance from a canopy is thus obtained. In spite of the availability of the analytical solution to the bidirectional reflectance from a canopy, however, the azimuthal resolution is still restricted by the execution time. Thus, for leaf canopies without azimuthal preference a special method reducing the dimensions of the relevant matrices, and an approximate method based on the radiation path method presented in Chapter 2 are developed. The approximate method allows the resolution of 10 degrees in azimuth as well as in inclination, and calculates the bidirectional reflectance from a canopy within an acceptable execution time.

In Chapters 4 to 7, profiles of temperature, humidity, sensible and latent heat flux densities in a canopy are studied in detail. Because the derived equations for sensible and latent heat flux densities are coupled with each other, they must be solved simultaneously. This leads to the following problems: (a) it costs much execution time and space so the

program cannot be executed on a microcomputer; (b) distinction of sunlit and shaded leaves within each layer would require to split each layer into several sublayers according to different irradiation levels and thus increase further the execution time and space; (c) the analytical expressions for total sensible and latent heat flux densities above a canopy are not available so that it is not possible to find relationships between the parameters used in the multi-layer model and those used in the single-layer model (Penman-Monteith approach), viz. the canopy resistance and the excess resistance.

In Chapter 4, the sensible and latent heat flux densities are replaced by the enthalpy flux density H , which is the sum of the sensible and latent heat flux densities, and by the saturation heat flux density J , which is a weighted difference between the sensible heat flux density and the latent heat flux density. This weight is done in such a way that the resulting equations for H and J are now mutually independent, so that the computation of the relevant profiles is greatly simplified. Two uncoupled electrical analogues for H and J , respectively, are designed, which are the counterparts of the coupled electrical analogue for the sensible and latent heat. The computation of the J profile is further simplified by recurrent formulas. Moreover, in terms of H and J , the well known Penman's formulas are expressed in a unified form applicable to both single- and multi-layer models, which provides a bridge between these two models.

In Chapter 5, a method to distinguish sunlit and shaded leaves is developed based on the two uncoupled electrical analogues for H and J and on the recurrent formulas developed in Chapter 4. Goudriaan's (1977) simulation program MICROWEATHER is then rewritten in BASIC. A complete list of the program and the symbols used in the program is given in the Appendix. This program in BASIC gives the same detailed description of the crop micrometeorology as MICROWEATHER does, while it can be executed on a microcomputer. The agreement between the results of these two programs is good.

In Chapter 6, Monteith's (1963) extrapolation method to obtain representative surface values of temperature and vapour pressure is extended by replacing the vapour pressure profile by the dew-point temperature profile. Thus, the canopy resistance can be obtained directly by graphical means. Two basic parameters of the single-layer model, the canopy resistance and the excess resistance, are clearly presented in this way.

In Chapter 7, the canopy resistance and the excess resistance are calculated from the parameters used in the multi-layer model by means of the unified Penman's formulas developed in Chapter 4. The formulas derived for these two resistances show that both of them contain aerodynamic and physiological components. It is shown that ,however, for a dense canopy with a dry soil surface, the canopy resistance contains mainly physiological components and is approximately equal to the resistance value calculated as all stomatal resistances of the leaves connected in parallel; the excess resistance contains mainly aerodynamic components and is a simple function of the friction velocity. In this case, therefore, the canopy resistance and the excess resistance can be estimated easily in terms of the parameters used in the multi-layer model.

In the discussion in Chapter 8, it is emphasized that the method to calculate bidirectional reflectance from a canopy developed in Chapter 3 can have important applications in remote sensing of vegetation, because it allows to study the effects of different leaf inclination distributions and non-Lambertian leaves. The results should be compared with data sets on the bidirectional reflectance from various vegetation canopies to see the practical significance of these two factors. The simulation program for crop micrometeorology developed for microcomputers (Chapter 5) can be used for short grass, where Goudriaan's MICROWEATHER has difficulties with the execution time caused by the small time coefficient of the model. The model can be further developed to simulate the evapo-transpiration from a canopy wetted by rainfall, and it could be incorporated into a pest and plant disease model. The results obtained on the canopy resistance and excess resistance (Chapter 7) justify the applicability of the single-layer model for a dense canopy. But for a sparse canopy the influence of the soil surface cannot be neglected, and the double-layer model - one represents the canopy and the other represents the soil surface - should be used. This version of the micrometeorological simulation program may be included in a crop growth model such as BACROS (de Wit et al., 1978).

Samenvatting

In de mikrometeorologie van gewassen wordt de overdracht van straling, moment, warmte en massa van en naar een gewasdek bestudeerd. Simulatie modellen voor deze processen bestaan reeds maar zijn slecht te hanteren door hun complexiteit en de lange rekentijd die zij vergen. Bovendien kunnen deze modellen tot nu toe alleen op een mainframe computer gedraaid worden. Deze studie tracht elegantere wiskundige analyses te ontwikkelen om enerzijds het inzicht in de betrokken processen te verdiepen, en anderzijds meer efficiënte computerprogramma's mogelijk te maken, die ook op mikrocomputers gedraaid kunnen worden.

Om straling te modelleren verdeelde Goudriaan (1977) het gewas in verscheidene lagen. In iedere laag werd de straling in negen neerwaartse en negen opwaartse fluxdichtheden verdeeld, die aan negen aansluitende zones van elke hemisfeer werden toegekend. Vervolgens werd een stelsel vergelijkingen voor deze stralingscomponenten afgeleid, en een efficiënte iteratie methode om ze op te lossen ontwikkeld. De oplossingen verschaften een gedetailleerde beschrijving van de verdeling van de straling in een gewas, waaruit ook de zonale bidirektionele reflectie van een gewas verkregen kan worden. Bovendien werd door computer-experimenten een zogenaamde reciprociteitsrelatie gevonden tussen een directe lichtbron en gereflekteerde straling van een gewas. Deze relatie heeft potentiële toepassingen in remote sensingtechnieken. Resterende problemen zijn: (a) de berekening van de stralingsprofielen in een gewas kost veel rekentijd; (b) de azimuthale variatie van de bidirektionele reflectie van een gewas kan niet gesimuleerd worden; (c) het wiskundige bewijs van de reciprociteitsrelatie was niet gevonden.

In Hoofdstuk 2 en 3 wordt de neerwaartse en opwaartse straling uit alle richtingen in een hemisfeer voorgesteld door stralingsvectoren en de interacties van de straling met een horizontaal homogeen gewaslaag door reflectie en transmissiematrices. In Hoofdstuk 2 wordt het fysische proces van reflectie en transmissie van straling door een meerlagengewas onder vektor-matrix notatie beschouwd. De stralingsvektor die op een gewas valt kan rechtstreeks vanaf de eerste laag gereflekteerd worden en zo een komponent van de gereflekteerde stralingsvektor van de top van het gewas vormen; of hij kan bijvoorbeeld door de eerste laag worden doorgelaten, door de tweede gereflekteerd, en weer door de eerste worden doorgelaten

en zo nog eens tot de gereflekteerde stralingsvektor bijdragen. Niet elke reflectie-transmissiereeks, een zogenaamd stralingspad, resulteert in een komponent van de gereflekteerde stralingsvektor, maar er is een oneindig aantal van zulke paden. In Hoofdstuk 2 wordt bewezen dat de reciprociteitsrelatie geldt indien elk tot de reflectie bijdragend stralingspad ook omgekeerd bewandeld kan worden en kan resulteren in een komponent van de gereflekteerde stralingsvektor. Aangetoond wordt dat deze omkeerbaarheid van de stralingspaden algemeen geldt voor reflectie, terwijl voor transmissie een vertikaal uniform gewas en een zwart bodemoppervlak vereist is.

In Hoofdstuk 3 worden de stralingsvergelijkingen herschreven als een stelsel differentiaal-vergelijkingen met vectoren als variabelen en matrices en coëfficiënten. Dan worden twee differentiaal-vergelijkingen voor neerwaartse en opwaartse stralingsvectoren afgeleid met als coëfficiënten de interceptie-, de terugwaartse en de voorwaartse verstrooiingsmatrices die de drie basismatrices vormen voor de interacties van een horizontaal homogeen gewas met de stralingsvectoren. Deze twee differentiaal-vergelijkingen zijn in feite de vektor-matrix versie van de Kubelka-Munk vergelijkingen, die twee scalaire differentiaal-vergelijkingen zijn voor totale neerwaartse en opwaartse stralingsintensiteiten in een gewas met horizontale Lambertiaanse bladeren. De uitgebreide Kubelka-Munk vergelijkingen kunnen de richtingsgewijze stralingsoverdracht in een gewas met niet-Lambertiaanse bladeren en elke bladhoekverdeling beschrijven. Dit is realistischer dan het modelgewas van Suits (1972) dat in principe alleen verticale en horizontale bladeren bevat. De azimuthale variaties worden in acht genomen door de overeenkomstige vectoren en matrices uit te breiden. De analytische oplossingen voor de profielen van neerwaartse en opwaartse stralingsvectoren worden gevonden door middel van een standaard matrix methode en zo wordt ook de bidirektionele reflectie van een gewas verkregen. Ondanks de beschikbaarheid van de analytische oplossing voor de bidirektionele reflectie van een gewas is de azimuthale resolutie nog beperkt door de rekentijd. Daarom is voor een bladerdek zonder azimuthale voorkeur een speciale methode ontwikkeld die de dimensies van de betrokken matrices reduceert en ook een benaderingsmethode die gebaseerd is op de stralingspadmethode uit Hoofdstuk 2. De benaderingsmethode staat een resolutie toe van 10 graden zowel in azimuth als in inclinatie, en berekent de bidirektionele reflectie van een gewas binnen aanvaardbare rekentijd.

In de Hoofdstukken 4 tot en met 7 worden de profielen van temperatuur, vocht, voelbare en latente warmtestroom-dichtheden in een gewas in detail bestudeerd. Omdat de afgeleide vergelijkingen voor voelbare en latente warmtestroom dichtheden met elkaar gekoppeld zijn, moeten ze simultaan worden opgelost. Dit leidt tot de volgende problemen: (a) het kost veel rekentijd zodat het programma niet op een microcomputer uitgevoerd kan worden; (b) onderscheid van zonverlichte en beschaduwde bladeren binnen elke laag zou de opsplitsing van elke laag in verscheidene sublagen volgens verschillende instralingsnivo's eisen; (c) de analytische uitdrukkingen voor de totale voelbare en latente warmtestroom-dichtheden boven een gewas zijn niet beschikbaar, zodat het niet mogelijk is relaties te vinden tussen de parameters van meerlagenmodellen en de parameters die in het éénlaag model gebruikt worden (Penman-Monteith benadering), zoals de gewasweerstand en de excessweerstand.

In Hoofdstuk 4 worden de voelbare en latente warmteflux-dichtheden zelf vervangen door de enthalpiestroomdichtheid H , die de som is van de voelbare en latente warmtestroom-dichtheden, en de verzadigingswarmteflux-dichtheid J , die het verschil is tussen de voelbare warmteflux-dichtheid en de latente warmteflux-dichtheid maal een konstante. Deze konstante wordt zo gekozen dat de resulterende vergelijkingen voor H en J onderling onafhankelijk zijn, en de berekening van de relevante profielen veel eenvoudiger is geworden. Twee ontkoppelde elektrische analogonschema's voor resp. H en J zijn ontworpen, die de tegenhangers zijn van het ene gekoppelde schema voor de voelbare en latente warmte. De berekening van het J profiel is verder vereenvoudigd door recursieve formules. Bovendien worden de bekende Penman vergelijkingen in termen van H en J in een gemeenschappelijke vorm gebracht die toepasbaar is voor zowel één- als meerlagenmodellen en als brug tussen deze beide modellen fungeert.

In Hoofdstuk 5 wordt een methode ontwikkeld om zonverlichte en beschaduwde bladeren te onderscheiden, gebaseerd op de twee ontkoppelde elektrische analogonschema's voor H en J en op de recursieve formules die in Hoofdstuk 4 ontwikkeld waren. Goudriaan's (1977) simulatieprogramma MICROWEATHER is daarna in BASIC herschreven. Een volledige listing van het programma en de symbolen die in het programma gebruikt zijn, zijn in de Appendix gegeven. Dit programma in BASIC geeft dezelfde gedetailleerde beschrijving van de gewasmikrometeorologie als MICROWEATHER, terwijl

het op een microcomputer uitgevoerd kan worden. De overeenstemming tussen de resultaten van beide programma's is goed.

In Hoofdstuk 6 wordt Monteith's (1963) extrapolatiemethode om representatieve oppervlaktewaarden van temperatuur en dampdruk te verkrijgen uitgebreid door het dampdrukprofiel door het profiel van de dauwpuntstemperatuur te vervangen. Zo kan de gewasweerstand rechtstreeks grafisch verkregen worden. Twee basisparameters van het éénlaagmodel, de gewasweerstand en de excessweerstand, worden op deze manier duidelijk voorgesteld.

In Hoofdstuk 7 worden de gewasweerstand en de excessweerstand berekend uit de parameters van het meerlagenmodel in termen van de gemeenschappelijke Penmanformules uit Hoofdstuk 4. De formules die voor deze twee weerstanden zijn afgeleid vertonen beide zowel aerodynamische als fysiologische componenten. Aangetoond wordt echter dat voor een dicht gewas met een droog bodemoppervlak de gewasweerstand voornamelijk fysiologische componenten bevat en ongeveer gelijk is aan de weerstandswaarde berekend als de parallelschakeling van alle stomataire weerstanden van de bladeren; de excessweerstand bevat voornamelijk aerodynamische componenten en is een eenvoudige functie van de wrijvingssnelheid. Daarom kunnen in dit geval de gewasweerstand en de excessweerstand gemakkelijk worden geschat in termen van parameters die in het meerlagenmodel zijn gebruikt.

In de discussie in Hoofdstuk 8 wordt benadrukt dat de methode om bidirektionele reflectie van een gewas te berekenen zoals die in Hoofdstuk 3 ontwikkeld is belangrijke toepassingen in remote sensing van vegetatie kan hebben, omdat het in staat stelt de effecten van verschillende bladhoekverdelingen en niet-Lambertiaanse bladeren te bestuderen. De resultaten zouden vergeleken moeten worden met data sets voor de bidirektionele reflectie van verschillende gewasdekken om de praktische betekenis van deze twee factoren te zien. Het simulatieprogramma voor gewasmikrometeorologie ontwikkeld voor microcomputers (Hoofdstuk 5) kan voor kort gras gebruikt worden, waar Goudriaan's MICROWEATHER problemen heeft met de rekentijd wegens de kleine tijdcoëfficiënt in het model. Het model kan verder ontwikkeld worden om de evapo-transpiratie van een bladerdek nat geworden door een regenbui te simuleren, en het zou ook in een ziekte- en plagenmodel ingebouwd kunnen worden. De resultaten verkregen over de gewasweerstand en de excessweerstand (Hoofdstuk 7) rechtvaardigen de toepasbaarheid van een éénlaagmodel voor een dicht bladerdek. Maar voor

een open gewas kan de invloed van het bodemoppervlak niet verwaarloosd worden, en moet het tweelagenmodel - één stelt het gewas voor en de ander het bodemoppervlak - gebruikt worden. Deze versie van het mikro-meteorologische simulatiemodel kan in een model voor gewasgroei als BACROS (de Wit et al., 1978) ingebouwd worden.

Acknowledgements

This work was supported by the Ministry of Education and Science of the Netherlands. The cost of printing of the dissertation was partly covered by the 'Stichting Landbouwhogeschool Fonds'. I gratefully acknowledge their support.

I am very much indebted to Prof. C.T. de Wit, Prof. L. Wartena, and Dr. J. Goudriaan for their support and inspiration to the production of the present report. Their critical reading and many helpful suggestions are most gratefully acknowledged. I am grateful to Dr. R. Rabbinge for his kind support in many respects and for his comments on the manuscript.

Many thanks are due to Mrs. H. H. van Laar for her excellent editing work. The manuscript was prepared with typing assistance of Mr. B. H. J. van Amersfoort. The drawings were carefully prepared by Mr. G. C. Beekhof. The photography was done by Mr. P. R. Stad. The English was corrected by Dr. P. Cortes and Dr. S. A. Ward. The cover was designed by Mrs. Xu Peiwen. Their help is greatly acknowledged.

References

- Allen, W.A., and Richardson, A.J. (1968), Interaction of light with a plant canopy. *J. Opt. Soc. Am.*, 58(8):1023-1028.
- Allen, W.A., Gayle, T.V., and Richardson, A.J. (1970), Plant canopy irradiance specified by the Duntley equations. *J. Opt. Soc. Am.* 60(3):372-376.
- Begg, J.E., Bierhuizen, J.F., Lemon, E.R., Misra, D., Slatyer, R.O., and Stern, W.R. (1964), Diurnal energy and water exchanges in bulrush millet. *Agric. Meteorol.* 1:294-312.
- Breece, H.T., and Holmes, R.A. (1971), Bidirectional scattering characteristics of healthy green soybean and corn leaves in vivo. *Appl. Opt.* 10(1):119-127.
- Brown, K.W., and Covey, T.V. (1966), The energy budget evaluation of the micrometeorological transfer processes within a corn field. *Agric. Meteorol.* 3:73-96.
- Bunnik, N.J.J. (1978), The multispectral reflectance of shortwave radiation by agricultural crops in relation with their morphological and optical properties. Mededelingen Landbouwhogeschool Wageningen, Nederland 78-1.
- Chamberlain, A.C. (1966), Transport of gasses to and from grass and grass-like surfaces. *Proc. Roy. Soc. A*, 290:236-265.
- Chamberlain, A.C., and Chadwick, R.C. (1965), Transfer of iodine from atmosphere to ground. Report AERE-R4870, United Kindom Atomic Energy Authority.
- Chance, J.E., and Cantu, J.M. (1975), A study of plant canopy reflectance model. Final Report on Faculty Research Grant, Pan American University.
- Chance, J.E., and LeMaster, E.W. (1977), Suits reflectance model for wheat and cotton: theoretical and experimental tests. *Appl. Opt.* 16(2):407-412.
- Chandrasekhar, S. (1950), Radiative transfer. Clarendon Press, Oxford, 393pp.
- Cooper, K., Smith, J.A., and Pitts, D. (1982), Reflectance of a vegetation canopy using the adding method. *Appl. Opt.* 21(22):4112-4118.
- Cowen, I.R. (1968), Mass, heat and momentum exchange between stands of plants and their atmospheric environment. *Quart. J. Roy. Met. Soc.*, 94:523-544.
- Denmead, O.T. (1969), Comparative micrometeorology of a wheat field and a forest of *Pinus radiata*. *Agric. Meteorol.*, 6:357-371.

- Goudriaan, J. (1977), Crop micrometeorology: a simulation Study. Simulation Monographs, Pudoc, Wageningen, 249pp.
- Goudriaan, J., and Waggoner, P.E. (1972), Simulating both aerial microclimate and soil temperature from observation above the foliar canopy. *Neth. J. agric. Sci.* 20:104-124.
- Hiramatsu, Y., Takuro, S., and Maitani, T. (1984), Goudriaan's model of crop micrometeorology applied to rice crop. Okayama Univ. Kurashihi, Japan (in prep.).
- Hulst, H. C. van de (1963), A new look at multiple scattering. New York, NASA Goddard Space Flight Center, 81pp.
- Inoue, E. (1963), On the turbulent structure of airflow within crop canopies. *J. Meteor. Soc. Japan*, 41:319-326.
- Kubelka, P., and Munk, F. (1931), Ein Beitrag zur Optik der Farbanstriche. *A. Techn. Physik*, 11:593-601.
- Laar, H.H. van, Kremer, D., and Wit, C.T. de (1977), Maize. In: Crop photosynthesis: methods and compilation of data obtained with a mobile field equipment, (Th. Alberda, Ed.), *Agric. Res. Rep.* 865, Pudoc, Wageningen, 12-22.
- Landsberg, J.J., and James, G.B. (1971), Wind Profiles in plant canopies: studies on an analytical model. *J. appl. Ecol.* 8:729-741.
- Lemon, E.R. (1960), Photosynthesis under field conditions. II. An aerodynamic method for determining the turbulent carbon dioxide exchange between the atmosphere and a corn field. *Agron. J.*, 52:697-703.
- Lemon, E.R. (1963), Energy and water balance of plant communities. In: Environmental control of plant growth, (L. T. Evans, Ed.), New York and London, 55-78.
- Lemon, E.R., and Wright, J.L. (1969), Photosynthesis under field conditions. X.A. Assessing sources and sinks of carbon dioxide in a corn crop using a momentum balance approach. *Agron. J.*, 61:405-411.
- Long, I.F., Monteith, J.L., Penman, H.L., and Szeicz, G. (1964), The plant and its environment. *Meteor. Rundsch.*, 17:97-101.
- McNaughton, K.G. (1976), Evaporation and advection I: evaporation from extensive homogeneous surfaces. *Quart. J. Roy. Met. Soc.*, 102:181-191.
- Monsi, M., and Saeki, T. (1953), Uber den Lichtfactor in den Pflanzengesellschaft und seine Bedeutung fur die Stoffproduktion. *Jap. Journ. Bot.*, 14:22-52.
- Monteith, J.L. (1963), Gas exchange in plant communities. In: Environmental

- control of plant growth, (L.T. Evans, Ed.), Academic press, New York, 95-112.
- Monteith, J.L. (1965), Evaporation and environment. Symp. Soc. Expl. Biol. XIX, 205-234.
- Monteith, J.L. (1973), Principles of environmental physics. Edward Arnold, London, 241 pp.
- Monteith, J.L. (1981), Evaporation and surface temperature. Quart. J. Roy. Met. Soc., 107:1-27.
- Paltridge, G.W., and Platt C.M.R. (1976), Radiative processes in meteorology and climatology. Elsevier, New York, 393pp.
- Penman, H.L. (1948), Natural evaporation from open water, bare soil and grass. Proc. Roy. Soc. A., 193:120-146.
- Perrier, A. (1976), Etude et essai de modelisation des echanges de masse et d'energie au niveau des couverts vegetaux. -- These de Doctorat d'Etat -- Universite de Paris VI -- avril 1976, Paris, 240pp.
- Priestley, C.H.B., and Taylor, R.J. (1972), On the assessment of surface heat flux and evaporation using large-scale parameters. Mon. Weather Rev., 106:81-92.
- Ross, J. (1981), The radiation regime and architecture of plant stands. Dr. W. Junk Publishers, The Hague, 391pp.
- Shuttleworth, W.J. (1976), A One-dimensional Theoretical Description of the Vegetation-Atmosphere Interaction. Boundary-Layer Meteorol. 10:273-302.
- Stewart, J.B. (1983), A discussion of the relationships between the principal forms of the combination equation for estimating crop evaporation. Agric. Meteorol., 30:111-127.
- Stigter, C.J., Goudriaan, J., Bottemanne, F.A., Birnie, J., Lengkeek, J.C., and Sibma, L. (1977), Experimental evaluation of a crop climate simulation model for Indian corn (*Zea mays* L.). Agric. Meteorol. 18:163-186.
- Suits, G.H. (1972), The calculation of the directional reflectance of a vegetative canopy. Remote Sensing of Environment, 2:117-125.
- Thom, A.S. (1972), Momentum mass and heat exchange of vegetation. Quart. J. Roy. Met. Soc., 98:124-134.
- Thom, A.S. (1975), Momentum, mass and heat exchange of plant communities. In: Vegetation and the atmosphere. V.1 (J.L. Monteith, Ed.), Academic Press, London, 57-109.
- Waggoner, P.E., and Reifsnyder, W.E. (1968), Simulation of the temperature, humidity and evaporation profiles in a leaf canopy. J. appl. Meteorol.

7:400-409.

Waggoner, P.E., Furnival, G.M., and Reifsnyder, W.E. (1969), Simulation of the microclimate in a forest. Forest Sci. 15:37-45.

Wit, C.T. de (1965), Photosynthesis of leaf canopies. Agric. Res. Rep.

No 663. Pudoc, Wageningen, 57pp.

Wit, C.T. de, and Keulen, H. van (1972), Simulation of transport processes in soils. Simulation Monographs, Pudoc, Wageningen, 109pp.

Wit, C.T. de, et al. (1978), Simulation of assimilation, respiration and transpiration of crops. Simulation Monographs, Pudoc, Wageningen, 167pp.

Curriculum vitae

Chen Jialin was born on 19 January 1947 in Shanghai, China. In 1965 he graduated from the 51-st secondary school, Shanghai. He obtained his diploma in Physics in 1970 from Fu-Dan University, China. From 1970 to 1978 he worked with an electrical company in the province Guangxi, China. From October 1978 to September 1980 he studied as a graduate student at the Institute of Plant Physiology, Academia Sinica. Since September 1980 he worked as a guest researcher at the Department of Theoretical Production Ecology of the Agricultural University, Wageningen, the Netherlands. The main work of his Ph. D. studies was carried out in the period of September 1980 to October 1982. From November 1982 to June 1983 he studied at the faculty of Mathematics and Physics of the University of Utrecht, the Netherlands and graduated cum laude in Meteorology. This dissertation was written in the period of October 1983 to June 1984.